Approved for public release; distribution is unlimited.

PhilSea10 APL-UW Cruise Report: 5–29 May 2010

by Rex K. Andrew, James A. Mercer, Bradley M. Bell, Andrew A. Ganse,
Linda Buck, Timothy Wen, and Timothy M. McGinnis

Technical Report

APL-UW TR 1001
October 2010

Applied Physics Laboratory University of Washington
1013 NE 40th Street Seattle, Washington 98105-6698

Grants N00014-08-1-0843, N00014-07-1-0743, N00014-03-1-0181
N00014-08-1-0800, N00014-08-1-0797, and N00014-08-1-0200

ACKNOWLEDGMENTS

The research cruise reported here was funded under ONR Grants N00014-08-1-0843 (North Pacific Acoustic Laboratory) and N00014-07-1-0743 (Acoustic Source Deployment Instrumentation). Funding for the Philippine Sea experiment design and planning came from an earlier North Pacific Acoustic Laboratory grant N00014-03-1-0181.

Funding for hardware and hardware development came from three DURIP awards: 1) N00014-07-1-0743 (Source Deployment), 2) N00014-08-1-0800 (TCTD), and 3) N00014-08-1-0797 (Philippine Sea Instrumentation).

Andrew White was funded under ONR student support grant N00014-08-1-0200.

ABSTRACT

A team from the Applied Physics Laboratory of the University of Washington (APL-UW) conducted underwater sound propagation exercises from 5 to 29 May 2010 aboard the R/V *Roger Revelle* in the Philippine Sea. This research cruise was part of a larger multi-cruise, multi-institution effort, the PhilSea10 Experiment, sponsored by the Office of Naval Research, to investigate the deterministic and stochastic properties of long-range deep ocean sound propagation in a region of energetic oceanographic processes. The primary objective of the APL-UW cruise was to transmit acoustic signals from electro-acoustic transducers suspended from the R/V *Roger Revelle* to an autonomous distributed vertical line array (DVLA) deployed in March by a team from the Scripps Institution of Oceanography (SIO.) The DVLA will be recovered in March 2011. Two transmission events took place from a location designated SS500, approximately 509 km to the southeast of the DVLA: a 54-hr event using the HX554 transducer at 1000 m depth, and a 55-hr event using the MP200/TR1446 "multiport" transducer at 1000 m depth. A third event took place towing the HX554 at a depth of 150 m at roughly 1–2 kt for 10 hr on a radial line 25–43 km away from the DVLA. All acoustic events broadcasted low-frequency (61–300 Hz) m-sequences continuously except for a short gap each hour to synchronize transmitter computer files. An auxiliary cruise objective was to obtain high temporal and spatial resolution measurements of the sound speed field between SS500 and the DVLA. Two methods were used: tows of an experimental "CTD chain" (TCTD) and periodic casts of the ship's CTD. The TCTD consisted of 88 CTD sensors on an inductive seacable 800 m long, and was designed to sample the water column to 500 m depth from all sensors every few seconds. Two tows were conducted, both starting near SS500 and following the path from SS500 towards the DVLA, for distances of 93 km and 124 km. Only several dozen sensors responded during sampling. While the temperature data appear reasonable, only about one-half the conductivity measurements and none of the pressure measurements can be used. Ship CTD casts were made to 1500 m depth every 10 km, with every fifth cast to full ocean depth.

Contents

List of Figures

List of Tables

This page is blank intentionally.

EXECUTIVE SUMMARY

A team from the Applied Physics Laboratory, University of Washington (APL-UW; Chief Scientist Jim Mercer) conducted underwater sound propagation exercises in the Philippine Sea from 5 to 29 May 2010 aboard the R/V *Roger Revelle*. This cruise was part of a larger multi-cruise, multi-institution effort, the PhilSea10 Experiment, to investigate the deterministic and stochastic properties of long-range deep ocean sound propagation in a region of energetic oceanographic processes.

The principal assets involved are shown in Fig. 1. T1 through T6 were moored autonomous acoustic transceivers deployed in March 2010 by Scripps Institution of Oceanography (SIO.) SIO also deployed an experimental autonomous "full water column" distributed vertical line array (DVLA) near T6. The primary objective of the APL-UW cruise was to transmit acoustic signals from electro-acoustic transducers suspended from the R/V *Roger Revelle* to the DVLA. The DVLA will be recovered in March 2011.

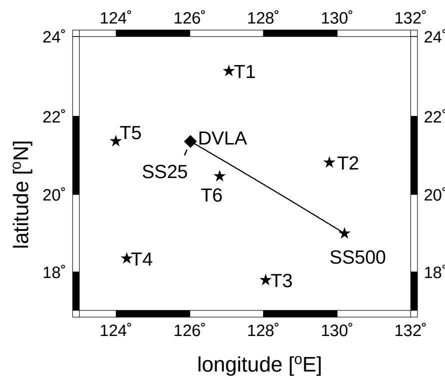

Figure 1: APL-UW and SIO assets, PhilSea10 Experiment.

Three transmission events were conducted:

1. 54-hr event using the HX554 transducer at 1000 m depth
2. 55-hr event using the MP200/TR1446 "multiport" transducer at 1000 m depth
3. 10-hr tow of the HX554 at a depth of 150 m at $\sim 1-2$ kt

The first two transmission events took place from location SS500, approximately 509 km to the southeast of the DVLA. The tow, denoted SS25 in Fig. 1, followed a radial line 25 to 43 km away to the south-southwest from the DVLA.

All acoustic events broadcasted signals continuously except for a short gap each hour to synchronize transmitter computer files. Standard m-sequences with carrier frequencies of 61 Hz (shallow tow) or 82 Hz (deep) were used with the HX554, which was cautiously operated at reduced capacity following serious damage sustained during the PhilSea09 cruise and subsequent repairs during the summer of 2009. An experimental signal consisting of two superimposed m-sequences (with different laws and different carrier frequencies of 200 Hz and 300 Hz) was broadcast from the MP200/TR1446.

An auxiliary cruise objective was to obtain high temporal and spatial resolution measurements of the sound speed field between SS500 and the DVLA. Two methods were used: tows of an experimental "CTD chain" (TCTD) and periodic casts of the ship's CTD.

The TCTD consisted of 88 sensors, each measuring conductivity, temperature and pressure, on an inductive seacable 800 m long, and was designed to sample the water column to 500 m depth from all sensors every few seconds. Two tows were conducted, both starting near SS500 and following the path from SS500 towards the DVLA. The first tow covered 93 km in 39 hr, and the second 124 km in 30 hr. The number of sensors responding in each tow was roughly three dozen initially, then gradually decreased to about one dozen. The temperature measurements provide a map of the upper ocean temperature field that is consistent with ship CTD measurements. About one-half of the conductivity measurements appear usable, but the pressure readings are largely unusable. Sensor depth can, nevertheless, be inferred from the pressure data recorded by the SeaBird CTDs mounted on the cable.

The sensors were removed from the original seacable after the cruise and put on a new 800-m seacable in Kao-Hsiung for the following R/V *Roger Revelle* cruise (Chief Scientist R.-C. Lien), which happened in June 2010.

In addition to several ship CTD casts made at SS500 and at the DVLA, 51 casts were made at regular sampling intervals (10 km) along the DVLA to SS500 path. The casts were to 1500 m depth, with every fifth cast to full ocean depth, $\sim 5000 - 6000$m.

1 Introduction – PhilSea10 Experiment

For several decades, the Office of Naval Research has sponsored an international consortium of scientists to investigate deterministic and stochastic acoustic propagation at low frequencies over long ranges in the deep ocean. Most of these "blue water" experiments have been conducted in the central North Pacific, where oceanographic processes are relatively benign. The natural progression for these studies is to determine whether and to what extent the models and predictions developed during these efforts apply in a region with more vigorous oceanic processes.

To this end, the scientific consortium identified the Philippine Sea to be a reasonable venue for study. This region is bounded to the south by the North Equatorial Current and to the west by the Kuroshio. Mesoscale structures propagate westward into the basin and collide with eddies spun off from the Kuroshio, creating energetic and complicated oceanography.

For the purposes of this report, the PhilSea10 Experiment consists of several cruises:

1. Scripps Institution of Oceanography (SIO), under Chief Scientist Dr. Peter Worcester, deployed a tomographic array of autonomous moored transceivers and a distributed vertical line array (DVLA) from 6 to 28 April 2010 from the R/V *Roger Revelle*.

2. The Applied Physics Laboratory, University of Washington (APL-UW), under Chief Scientist Dr. James Mercer, conducted the ship-suspended and towed environmental and acoustic operations from the R/V *Roger Revelle* from 5 to 29 May 2010.

3. The Massachusetts Institution of Technology (MIT), under Chief Scientist Dr. Arthur Baggeroer, towed an acoustic source from the R/V *Roger Revelle* from 7 to 20 July 2010.

4. The University of Hawaii (UH), under Chief Scientist Dr. Bruce Howe, will deploy acoustic Seagliders in the region from the R/V *Roger Revelle* in approximately November 2010.

5. SIO (Worcester) will recover the autonomous moored transceivers and the DVLA in March 2011 with the R/V *Roger Revelle*.

6. Woods Hole Oceanographic Institution, under Chief Scientist Dr. Ralph Stephen, will deploy ocean bottom seismometers and tow an over-the-side acoustic projector from the R/V *Roger Revelle* in the DVLA region in April 2011.

This report summarizes the principal efforts of the 2010 APL-UW cruise.

2 Experiment Site

The principal assets involved in the PhilSea10 Experiment (Fig. 2) were:

1. The DVLA — a "full water column" array (in 5000 m of water) consisting of five segments each containing 30 hydrophones.

2. Six autonomous transceiver moorings (T1–T6).

3. Ship-suspended stationary transmissions from "ship stop" SS500. Stationary operations at SS500 included standard environmental measurements and acoustic transmissions from the repaired HX554 pressurized bender bar projector and the MP200 double-ported free-flooded resonator.

4. Transect measurements and towed operations along some or all of the path between SS500 and the DVLA. This included several tows of a newly developed high-resolution TCTD and a CTD transect (using the ship's Seabird CTD) made approximately every 10 km.

5. A towed transmitter exercise through a reliable acoustic path ("RAP") zone from roughly 25 km from the DVLA for about 18 km. This exercise used the repaired HX554, and is (inappropriately) called "ship stop" SS25.

Target locations of the transceiver moorings and SS500 are shown in Table 1. The location for the DVLA is the surveyed location provided by P. Worcester in an email dated 27 April 2010.

3 Acoustic Exercises

The primary goal of this cruise was to transmit signals from two different projectors from stationary location SS500 for many hours each, and to transmit from a shallow depth for about 10 hr along a drifting track called "ship stop" SS25 from about 25 km from the DVLA through a RAP range.

The transmission events are summarized here in chronological order. There were two transmission events from SS500, the first involving the MP200/TR1446 system (section 3.1), the second the HX554 system, (section 3.3). The drifting exercise used the HX554 system (section 3.2.)

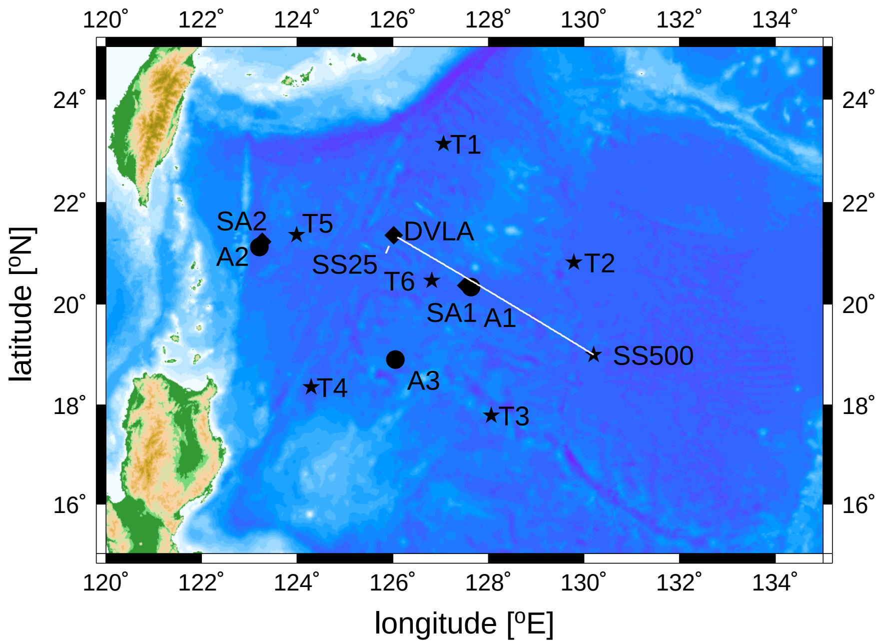

Figure 2: Principal assets, PhilSea10 Experiment. T1–T6 are moored autonomous transceivers. The DVLA is an autonomous vertical line array. APL-UW transmitted to the DVLA from SS500, and along the very short white line labeled SS25. The long white line indicates the propagation path from SS500 to the DVLA; TCTD tows and the periodic CTD casts covered some or all of this path. A1–A3 are moorings with surface buoys deployed by R.-C. Lien (APL-UW) during the ITOP (Impact of Typhoons on the Ocean in the Pacific) Experiment. Moorings SA1 and SA2 are subsurface moorings, also deployed by Lien.

3.1 Location SS500 — MP200/TR1446 System

The MP200/TR1446 system was lowered to approximately 1000 m. There is a mark on the suspension cable a few meters shy of this depth, at about 300 revolutions of the drum. The drum is dogged at one rotation angle, so available depths are quantized by the drum circumference. Using the pressure readings from the underwater package telemetry bottle, the underwater package was repositioned so that the telemetry GUI reported 998 m. (This is the depth of the pressure sensor.)

asset	location
SS500	19.0°N, 130.2°E (19° 00.00′N, 130° 12.00′E)
T1	23.138°N, 127.063°E (23° 08.28′N, 127° 03.78′E)
T2	20.823°N, 129.789°E (20° 49.38′N, 129° 47.34′E)
T3	17.788°N, 128.058°E (17° 47.28′N, 128° 03.48′E)
T4	18.351°N, 124.290°E (18° 21.06′N, 124° 17.40′E)
T5	21.366°N, 123.992°E (21° 21.96′N, 123° 59.52′E)
T6	20.468°N, 126.812°E (20° 28.08′N, 126° 48.72′E)
DVLA	21.36240°N, 126.01315°E (21° 21.7440′N, 126° 0.7889′E)

Table 1: Locations of assets.

3.1.1 Multiport Signal

An experimental signal was used with the MP200/TR1446 system. Because this transducer has a doubly resonant response, input signals generally need to be pre-equalized to yield useful in-water radiated signals. Prior efforts to transmit wideband signals placed the carrier frequency midway between the two resonance frequencies, but this results in driving most of the spectral energy into a band of relatively poor response, and therefore the attainable source levels were limited (and compromised) by the output power capacity of the amplifier.

It is always more advantageous to drive a transducer at its resonance frequency. Because the MP200/TR1446 has two resonance frequencies, and the device is nearly linear, it is possible to construct a drive signal containing the superposition of a signal with a carrier at the lower resonance and a second signal with a carrier at the upper resonance. However, because the two transducer resonances are quite sharp (high-Q), there is no advantage to using a Q = 2 signal, as in past practice, at either resonance. Such a wideband signal would extend in frequency far beyond the local resonance, with substantial extension into frequency regions where the system response is poor. This would simply be a return to the problems encountered with the prior efforts. Therefore, each of the two signals would require a higher Q. There is, however, another trade-off: increasing signal Q (decreasing signal bandwidth) results in poorer time resolution. This was not an option in previous short range experiments because the arrival times of different branches of the timefront were so close that broadened pulses would smear the timefronts together, rendering analysis difficult.

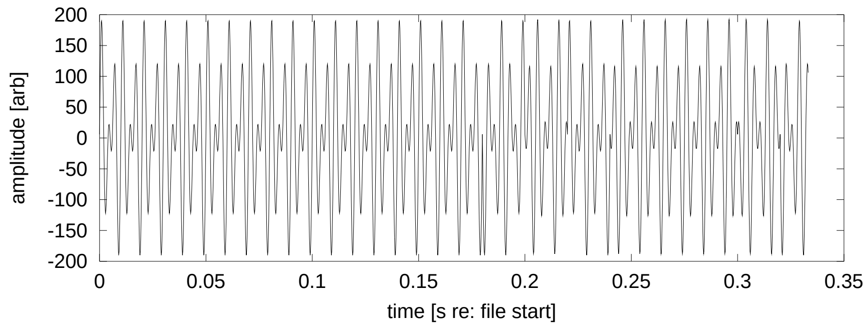

Figure 3: Dual m-sequence signal raw waveform from the file `mdual01.wav`.

However, the overall duration of the signal expands with increasing source–receiver range, and broadened pulses can be acceptable at a range of 500 km. Additionally, signals with higher carrier frequencies will have better time resolution, even if the signal bandwidth is decreased.

To build a composite two-frequency drive signal that would be easily incorporated into the transmitter software, the two signals were required to be of equal length over a single signal period. This was accomplished by setting one carrier at 200 Hz and the other at 300 Hz, and adjusting the signal Q's to have a 2:3 ratio, respectively. This latter adjustment directly defines the number of carrier periods per chip in the respective m-sequences.

Two frequency signals were used in long-range ocean acoustics in the AST (Alternate Source Test) Experiment, which used carriers around 28 and 84 Hz. In that experiment, the 84-Hz m-sequence was an upper harmonic of, and hence linearly related to, the 28-Hz drive signal and was generated through nonlinearities in the transducer. Two-frequency signals have also been used in wave propagation in random media measurements of the atmosphere, where they are sometimes called two-color or even bichromatic signals.

The two m-sequences in the drive signal designed here are not harmonically related, but rather simply summed, so there was additional latitude in choosing signal parameters. Therefore, the laws for the two signals were chosen to be different. This allows the timefronts of the two signals to be measured independently. One advantage of this scheme, as shown below, is that a mediocre response for one of the m-sequences need not interfere with a good response for the other m-sequence.

This bichromatic signal was designed with the parameters given in Table 2. The signal was constructed using a special-purpose C program `makedualmseq`. A section of the raw waveform is shown in Fig. 3.

No marine mammal mitigation efforts were required, but each full power transmission began with a short ramp up from zero to full power to minimize turn-on transients.

parameter	red signal	violet signal
carrier	200 Hz	300 Hz
law	2033	3471
sequence length	1023	1023
cycles per digit	4	6
digit length	20.00 ms	20.00 ms
bandwidth	50.00 Hz	50.00 Hz
phase mod angle	88.209°	88.209°
sequence length	20.46 s	20.46 s
sequences per hour	175.95	175.95
shaping	none	none

Table 2: Parameters for the experimental dual m-sequence signal for the MP200/TR1446 system at location SS500.

Autospectra for the drive signal and the monitor channel signal are shown in Fig. 4. Both autospectra were estimated in Octave using the `pwelch` function with a blocksize of 8192 and a hanning window and no overlap. The sharp response of the MP200/TR1446 near 210 Hz clearly provides unfavorable "sharpening" of the "red" component.

Pulse compressed waveforms for both the drive and monitor hydrophone channels are shown in Fig. 5. Both "red" and "violet" pulses in the drive waveform have been shifted by 1.0 s; both pulses in the hydrophone channel have been shifted by -1.0 s. The pulse response of the violet component is comparable to that in the drive signal — this can be inferred from Fig. 4 because the spectral shape around 300 Hz in the radiated spectrum has a shape comparable to that in the drive signal. The pulse response of the red component is considerably broadened compared to that in the drive signal, and this can also be inferred from Fig. 4 because the spectral shape around 200 Hz in the radiated spectrum is much narrower than that in the drive signal.

These results suggest that post-processing for the MP200/TR1446 signal may be required to equalize the spectral shaping induced by the transducer to improve the timing resolution and/or decrease the trailing sidelobe energy in the red component, and perhaps in the violet component as well.

3.1.2 Multiport Calibration

The monitor hydrophone was used to calibrate the source level. For reference here and later, the signal conditioning in this channel is given in Fig. 6.

Several signal files were constructed, each file involving an increase in amplitude. At each stage, several transmissions were made and the resulting source level calculated from the acoustic signal recorded on the monitor channel. The source level calculation is simple: the

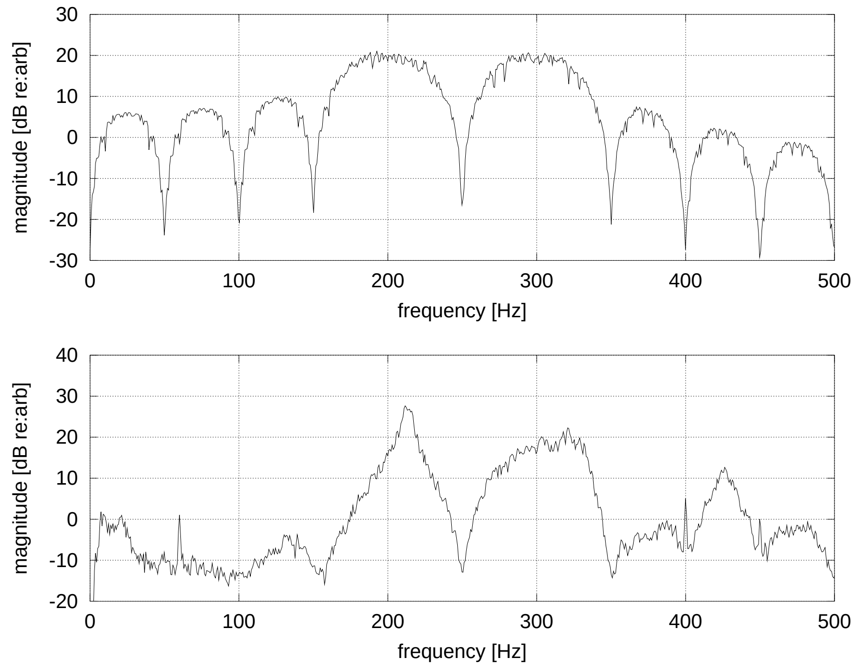

Figure 4: Dual m-sequence signal autospectra. Top: drive signal, estimated from the drive waveform file. Bottom: monitor hydrophone signal, estimated from 30 s of data from file `mdual04.A.sam`.

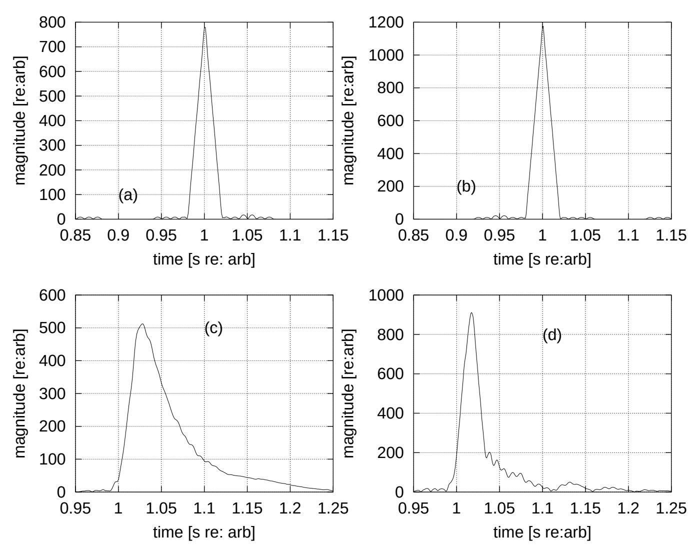

Figure 5: Dual m-sequence pulses after pulse compression. (a) Red component, drive signal, (b) violet component, drive signal, (c) red component, radiated signal, and (d) violet component, radiated signal.

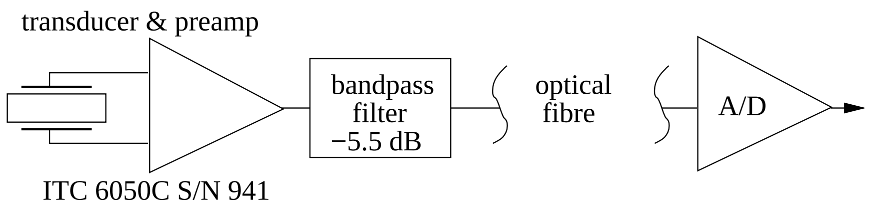

Figure 6: Monitor hydrophone channel schematic. The transfer function of the hydrophone plus its preamplifier is −159.0 dB re: 1 V/μPa dB from 100 Hz to 1 kHz. The fibre optic system contributes a loss of 5.5 dB over a passband of about 11 Hz to 4 kHz, all of which is due to conditioning within the telemetry bottle. The A/D has variable "gain."

source level is defined as

$$\mathrm{SL} = 20 \log_{10} p_{\mathrm{rms}} + 38.6, \tag{1}$$

where p_{rms} is the RMS pressure measured in the monitor hydrophone channel, and 38.6 dB is the correction from face-of-phone level at the monitor hydrophone to broadside radiated level corrected to 1 m.

The MP200/TR1446 takes more current for a given source level than the HX554 (primarily because some of the spectral energy is driven into regions of the transfer function away from resonance). The maximum source level at the highest tap setting of the Instruments, Inc., L50 was too restrictive in current: when the tap setting was moved to 848V/7.7A, additional source level became available. (These are RMS levels.) The file `mdual04.wav` was ultimately chosen for transmission. This file contains a dual signal constructed with an amplitude of 800. (Both components are given the same amplitude.) The computed source level for this signal (using file `mdual04.A.sam`) was roughly 191 dB re: 1 μPa @ 1 m. Unfortunately, all the files recorded during the calibration exercise had clipped cable drive voltage and current. Accurate measures of drive current and voltage can be recovered from the regular transmission files for this site. As an example, using file `1273337290.sam`, skipping the 40-s ramp, yields a cable drive voltage of 549 V RMS and a drive current of 5.5 A RMS.

3.1.3 Multiport Transmissions

There were 54 transmissions, each approximately 55 min long. The resulting transmission files are given in Appendix A.1.

parameter	value
law	2033
sequence length	1023
carrier	61.38 Hz
cycles per digit	2
digit length	32.58 ms
bandwidth	30.69 Hz
phase mod angle	88.209°
sequence period	33.33... s
sequences per hour	108
shaping	HPF20.nc

Table 3: Parameters for the full-power HX554 source for the drifting exercise, 150 m depth.

3.2 Location SS25 — HX554 System

3.2.1 Drift Exercise: Signal

The HX554 is expected to be resonant around 57 Hz at 150 m. The best transfer of energy into the radiated field occurs for a carrier about 5 Hz above the resonant frequency. The reduction (by half) of the total number of bars in the device likely reduces the radiated source level by up to 6 dB; for this reason, a longer m-sequence is used to recover via post-processing some of the lost SNR. Parameters for this signal are shown in Table 3.

Note that the maximum stress in the ceramic bars increases with decreasing depth (greater bar mobility with decreasing hydrostatic pressure) and this may be the limiting factor in source level at shallow depths.

3.2.2 Drift Exercise: Impedance

The standard preparatory procedure for the HX554 involves opening the gas pressurization valve to fill the transducer interior cavity with air. During this cruise, the valve was actuated electronically via control signals sent from the surface through the telemetry bottle. While air fills the transducer cavity, low-level "impedance" measurements of the transducer are conducted. Historically, the impedance measurements, in particular the admittance curve, show the gradual development of a resonance loop. When the loop is fully formed, the transducer is deemed fully filled, and the valve can be commanded closed.

The HX554 impedance measurements were conducted with the signal file `m61.LW.HPF20.wav`, which consists of an m-sequence with carrier frequency 61.38 Hz, sample rate 3069 Hz, law 2033, sequence length 1023, Q of 2, with all spectral content below 20 Hz filtered out. This signal has a low-level amplitude and a carrier frequency designed for a resonance around

filename	size	time	duration
`ss25-B.sam`	1119744 bytes	12:06:07	60 s
`ss25-C.sam`	11066836 bytes	12:17:52	600 s
`ss25-D.sam`	3702036 bytes	12:30:58	200 s

Table 4: Impedance files collected at SS25 for the HX554.

50 Hz; this signal was used in a previous Lake Washington engineering exercise [2]. Note that the transducer is expected to have a resonance around 57 Hz at 150 m depth.

The operation involves simultaneous output of the impedance signal and acquisition of multiple diagnostic channels. A custom circuit in the amplifier scales the cable voltage down by 1000, and scales the cable current by 100 mV/A. The data were acquired with gains of "4" on each of the cable voltage and current monitor channels. The files recorded are given in Table 4.

It was discovered in the Lake Washington exercises [1,2] that cross-talk from clock channels can introduce noise into the admittance curves, causing a "ratty" appearance. Therefore, only the cable voltage, cable current, and amplifier drive signal were recorded during this impedance exercise (i.e., no clocks were recorded).

Admittance is the complex ratio of current to voltage. Let $v(t)$ be the cable voltage and $i(t)$ the cable current, with Fourier transforms $V(f)$ and $I(f)$, respectively. Then the admittance is calculated as

$$Y(f) = I(f)/V(f). \tag{2}$$

The Fourier transforms are computed with discrete Fourier transforms. Practice has shown that the cleanest curves utilize discrete Fourier transforms equal in size to the m-sequence waveform itself.

After the valve was opened, the admittance loop quickly appeared; over subsequent minutes, it seemed to shrink a little, then not much at all. We eventually deemed the transducer "fully inflated" although perhaps it reached this state much sooner than realized. A typical chronological sequence of admittance loops for this operation is reproduced in Fig. 7. This sequence used the first 102300 points in each of the files listed in Table 6. The plot for file `ss25-D.sam` is characteristic of the admittance appearance during roughly the last 10 min of the operation: no further change was observed, and therefore this plot represents the admittance of the transducer when it was deemed fully filled. There is a single loop with a resonance at about 55 Hz.

Various algorithms have been used in an attempt to smooth the appearance of the admittance loop. Fig. 7b has a particularly ratty appearance (cause unknown.) Metzger used a running median in the `proc` program. Fig. 8f shows an output from the R program's "lowess" smoother that also provides a reasonably smoothed appearance and may be con-

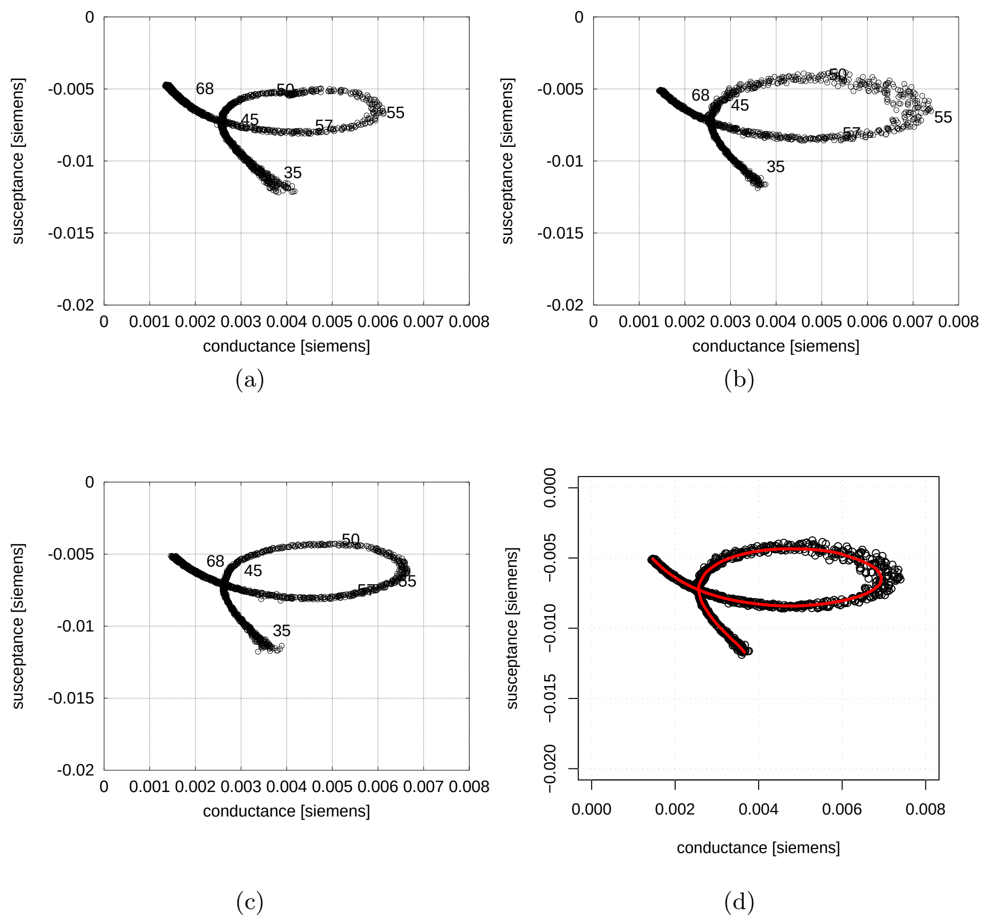

Figure 7: HX554 admittance plots at SS25. Depth is 150 m. 7a: `ss25-B.sam`. 7b: `ss25-C.sam`. This figure uses data starting 30 s into the file; earlier data were very "ratty" for unknown reasons. 7c: `ss25-D.sam`. 7d: Same as 7b, but using lowess smoothing. Lowess smoothing shown in red. For these data, the algorithm starts at high frequencies and smooths towards the lower frequencies.

sidered for future use.

3.2.3 Drift Exercise: Calibration

Because the HX554 had undergone significant repairs and modifications prior to this experiment, we had no confidence in the ability of any model to predict the transducer source level. So output level was adjusted manually.

Several signal files were constructed, each file involving an increase in amplitude. At each stage, several transmissions were made and the resulting source level calculated from the acoustic signal recorded on the monitor channel. The source level was calculated as described in section 3.1.2, except that the source level equation used an omnidirectional model for range dependence,

$$\mathrm{SL} = 20\log_{10} p_{\mathrm{rms}} + 20\log_{10} R, \tag{3}$$

where R is the range from the monitor hydrophone to the acoustic center of the transducer. The range for all deployments was 21 m.

We ultimately chose a transmission file amplitude of 400, which gave a computed source level of roughly 185 dB re 1 $\mu\mathrm{Pa}^2$ @ 1 m. There were three reasons for choosing this level and not a level closer to the original specification of 195 dB: 1) This exercise has a relatively short range of 25–40 km from the DVLA; 2) calculations suggest that the bender bars may come out of compression if driven at maximum voltage at shallow depths, and 3) this is an aging transducer with a history of problems and repairs, and may not be as robust as it was initially.

3.2.4 Drift Exercise: Transmissions

A list of all transmissions and associated diagnostic files for the HX554 during the drifting exercise is provided in Appendix A.2.

3.3 Location SS500 — HX554 System

The HX554 system was deployed 23 May. The system was lowered in a manner similar to that for the MP200/TR1446 and the winch dogged at a pressure sensor reading of 998 m. We first performed the pressurization sequence, followed by source level calibration efforts. We have not had this transducer at this depth since it was repaired, so we did not know what to expect. Following pressurization and calibration, we had a 55-hr transmission window.

3.3.1 HX554 Full Depth Signal

The HX554 was expected to be resonant around 75 Hz at a depth of 1000 m. The best transfer of energy into the radiated field occurs for a carrier about 5 Hz above the resonant frequency. The reduction (by half) of the total number of bars in the device likely reduces the radiated source level by up to 6 dB; for this reason, an m-sequence with a bit sequence longer than previously used was chosen so as to recover via post-processing some of the lost SNR. Parameters for this signal are shown in Table 5.

parameter	value
law	4533
sequence length	2047
carrier	81.88 Hz
cycles per digit	2
digit length	24.43 ms
bandwidth	40.94 Hz
phase mod angle	88.734°
sequence period	50.00 s
sequences per hour	72
shaping	HPF20.nc

Table 5: Parameters for the full power HX554 source, 1000 m depth.

filename	size	duration
`ss500impA.sam`	1497423 bytes	60 s
`ss500impB.sam`	1497423 bytes	60 s
`ss500impC.sam`	14748684 bytes	600 s
`ss500impD.sam`	14748684 bytes	600 s
`ss500impE.sam`	14748684 bytes	600 s
`ss500impF.sam`	14748684 bytes	600 s
`ss500impG.sam`	14748684 bytes	600 s

Table 6: Impedance files collected at SS500 for the HX554.

3.3.2 HX554 Impedance Measurements

The HX554 impedance measurements were conducted with the signal file `m81.LW.HPF20.wav`, which consists of an m-sequence with carrier frequency 81.76 Hz, sample rate 4088 Hz, law 1333, sequence length 511, Q of 2, with all spectral content below 20 Hz filtered out. This signal has a low-level amplitude and a carrier frequency designed for a resonance around 75 Hz; this signal was used in a Lake Washington engineering exercise [1]. Note that the transducer is expected to have a resonance around 75 Hz at 1000 m depth.

The files recorded are given in Table 6. The data were acquired with gains of “1” on each of the cable voltage and current monitor channels. (In retrospect, this was not enough gain. More would have decreased the “ratty” appearance of the admittance plots.)

A typical chronological sequence of admittance loops for this operation is reproduced in Fig. 8. This sequence used the first 51100 points in each of the files listed in Table 6. The plot for file `ss500impG.sam` is characteristic of the admittance appearance during roughly the last 30 min of the operation: no further change was observed, and therefore this plot represents the admittance of the transducer when it was deemed fully filled. Note that a resonance appears to be forming around 75 Hz in Fig. 8d, but it never fully matures into the primary (or sole) loop. The loop at 50 Hz remains the largest loop throughout.

It appears that the damage and repair to the transducer has seriously affected its designed performance at resonance, particularly at deeper depths (i.e., see section 3.2.2 for a comparison with the admittance loops measured at 150 m).

3.3.3 HX554 Calibration Measurements

The output level was adjusted manually (section 3.2.3). In addition, the weakness of the resonance loop at about 75 Hz in the admittance curves, and the unexpected dominance of the 50-Hz loop in the admittance curves, suggested that the best transfer of power into the water might be around 50 Hz. This made no sense. We therefore chose to use the signal designed for a transducer resonance near 75 Hz. (The parameters are given in Table 5.) The source level was calculated as described in section 3.1.2.

Because disabling half the bender bars in the HX554 may result in a 6-dB decrease in transmit voltage response, and recognizing that the HX554 is an aging device that has been prone to damage, we settled on an amplitude of 600. This produced a source level of about 186 dB re: 1 μPa @ 1 m. The longer m-sequence used here added an additional 3 dB, providing a source level with effectively 189 dB.

3.3.4 HX554 Full Depth Transmissions

A list of all transmissions and associated diagnostic files for the HX554 at SS500 is provided in Appendix A.3.

4 Tracking Instrumentation

A block diagram of the over-the-side system is shown in Fig. 9. Considerable new monitoring and control instrumentation was developed for this cruise, utilizing the optical fiber in the suspension cable for bi-directional communication between the surface and the underwater package. Some of the new capabilities (pressure sensor, Benthos acoustic modem, etc.) were elements of a tracking subsystem; other capabilities (battery voltage, gas valve, etc.) were for monitoring and controlling the state of the underwater package. Additional assets included the C-Nav GPS system, the Benthos DS7000 deck unit, and the InterOcean S4 current meter.

Most of this information was routed to the hydro lab's laptop computer running one or more LabView "virtual instruments" (VIs) for monitoring and control. An RS232 "sniffer" was used to send this input simultaneously to a logging computer where post-processing

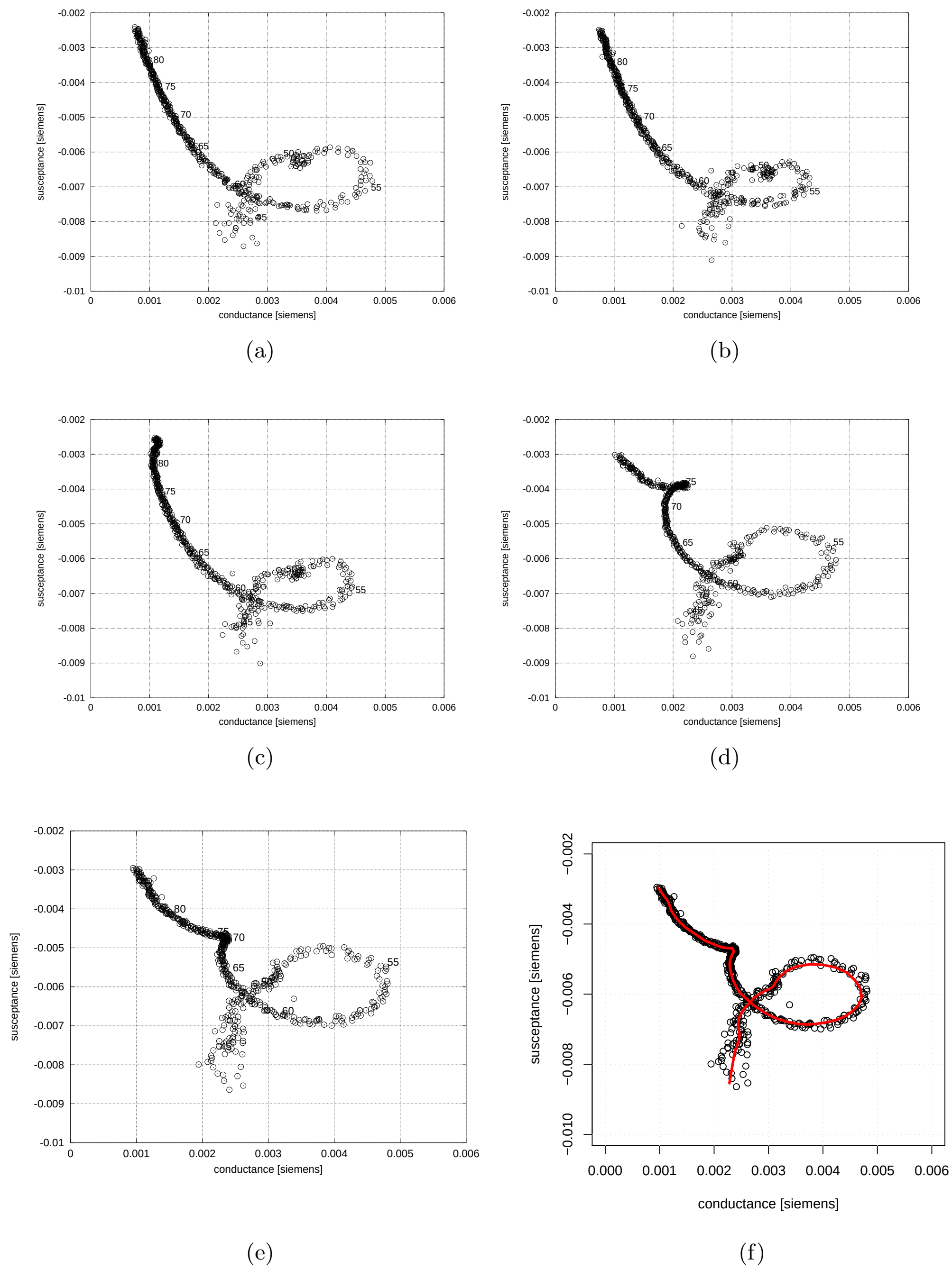

Figure 8: HX554 admittance plots at SS500. Depth is 998 m. 8a: `ss500impA.sam`, 09:48:45. 8b: `ss500impB.sam`, 10:51:44. 8c: `ss500impC.sam`, 11:01:04. 8d: `ss500impD.sam`, 11:12:44. 8e: `ss500impG.sam`, 12:01:58. 8f: Same as 8e, but using lowess smoothing. Lowess smoothing shown in red. For these data, the algorithm starts at high frequencies and smooths towards the lower frequencies.

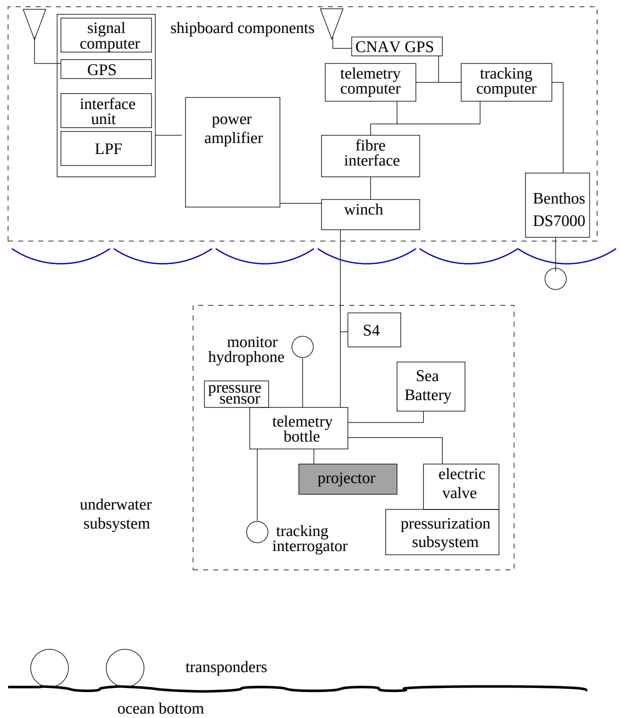

Figure 9: Block diagram of over-the-side system, PhilSea10, R/V *Roger Revelle*.

and analysis of the (largely acoustic) tracking data were performed. Example screenshots of the VIs are shown in Figs. 10, 11, and 12.

4.1 Underwater Package Telemetry

The software specification [3] for the telemetry system lists the data formats and conversions.

Analog-to-digital circuitry inside the telemetry bottle converted up to 8 channels of sensor data into 12-bit words and multiplexed them onto the optical fiber on command. Only four channels were used:

- **channel 0**: SeaBattery 1 (12 V)
- **channel 1**: Temperature Sensor 1
- **channel 2**: Temperature Sensor 2
- **channel 3**: SeaBattery 2 (24 V)

System state was logged by programs running on the topside tracking computers. These

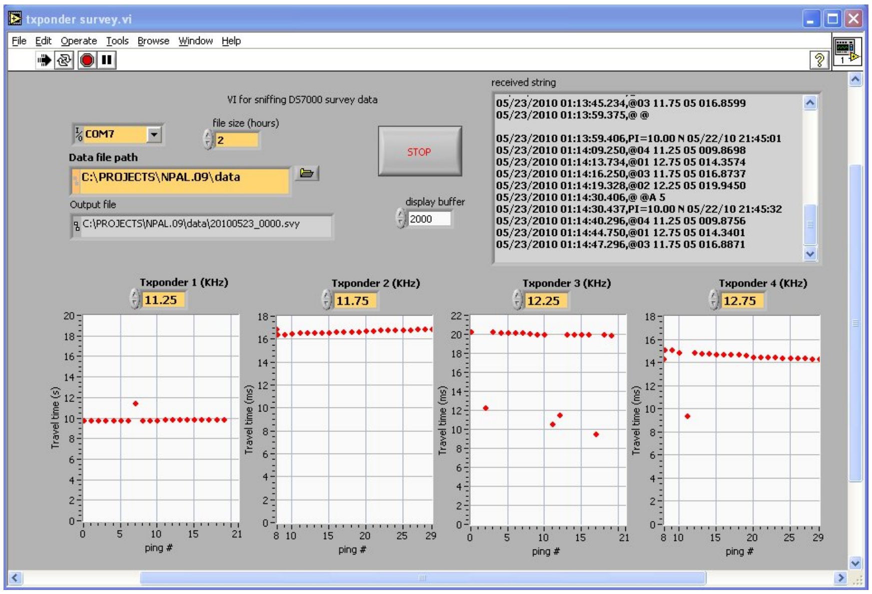

Figure 10: Screenshot of survey VI.

Figure 11: Screenshot of tracking VI.

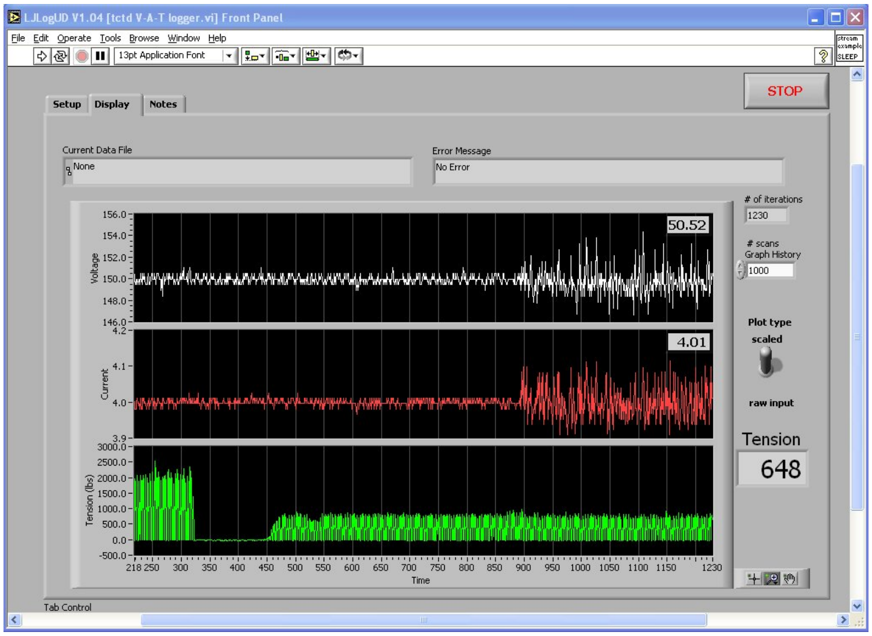

Figure 12: Screenshot of TCTD monitoring VI.

programs periodically queried the telemetry hardware for status, logging the time of the query, the response, and the time of the response. Both the command and the response were written to the log files.

4.1.1 Pressure

The ambient pressure at the underwater package is measured with a Mensor series 6000 digital pressure transducer. This device returns the pressure in bars. The device was queried once per second. The queries and responses were logged to files with names `pre-YYMMDD.HH`, with the same naming convention as described in Appendix C.

The pressure data were used initially to set the depth of the underwater package during lowering, and subsequently to measure the vertical motion of the package during transmissions.

4.1.2 Batteries

The voltages of the two SeaBatteries are found in the files `a2d-YYMMDD.HH`. (Appendix C describes file name conventions.) The conversion between data word and battery voltage is given in the specification [3]. Plots of the 12 V battery voltage versus time for both deployments at SS500 are shown in Fig. 13. The SeaBatteries were expected to deliver power

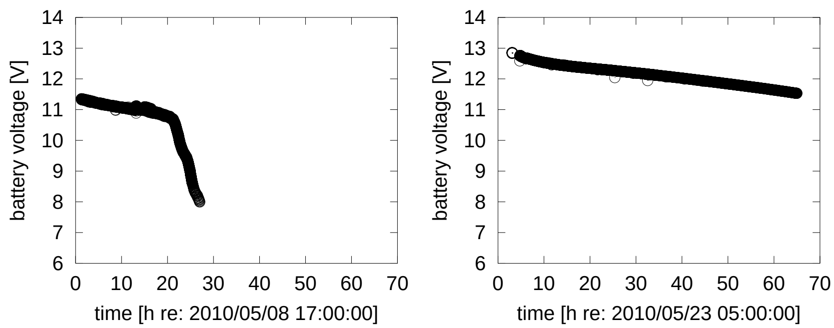

Figure 13: SeaBattery voltages on the 12 V battery for both deployments at SS500. Left: first deployment at SS500. Right: second deployment at SS500.

to the telemetry system for about 48 hr. The SeaBattery used for the first deployment at SS500 was not as healthy, and was unable to hold charge for the full deployment (approximately 55 hr). The SeaBattery used for the second deployment at SS500 was much better, and provided power for the entire deployment.

4.1.3 Tuner Temperature

Two thermistors were embedded in the MP200/TR1446 tuner during winding to monitor the core temperature during operation. Similar thermistors were embedded in the HX554 tuner. It was not known how much heat would build up inside the tuner during full power operation. Both thermistors were measured using custom circuitry in the telemetry bottle; the corresponding voltages were routed to the A/D and hence were logged at the surface. The voltages corresponding to these two thermistors are found in the files `a2d-YYMMDD.HH`.

The correction functions for the thermistors in the tuners were not known precisely. Calibration curves for similar thermistors were measured, and third-order polynomials fit to these curves. Using these polynomial corrections, Fig. 14 shows the temperatures for the first thermistor in the two long deployments, SS500-A and SS500-B. Although the temperature readings have some bias, these curves show that the tuners did not experience noticeable heating during either deployment.

4.1.4 Pressurization Valve

The InterOcean acoustic valve used to open and close the gas pressurization system was modified to open and close via commands from the topside controller, through the telemetry bottle. This system functioned properly.

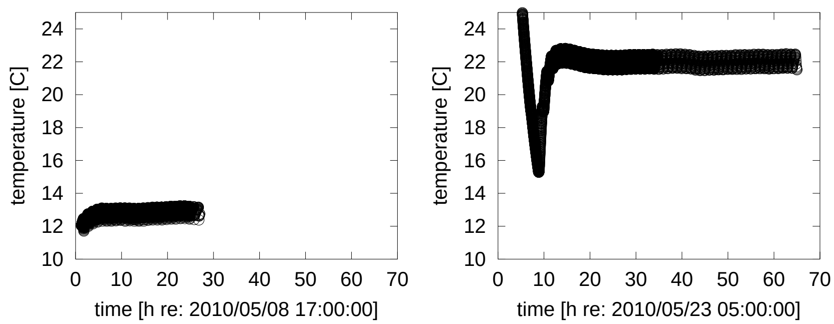

Figure 14: Tuner internal temperatures both for deployments at SS500. Left: the MP200/TR1446; right: the HX554.

4.2 C-Nav

As on the LOAPEX [4] cruise, our intention was to mount the C-Nav GPS antenna directly over the suspension cable. This was more difficult with the R/V *Roger Revelle* because the structure of the center span of the ship's A-frame had no attachment points.

The workaround was to construct an "arm" out of steel pipe and attach the arm to one of the service cages (Fig. 15). The vertical section of the arm was rotated so that the GPS antenna on top of the arm would be above the suspension cable when the A-frame was fully deployed. The arm was attached to a safety bar on the service cage using bolt plates (Fig. 16).

The C-Nav receiver was configured to output NMEA strings once per second. These were captured by the logging software and written to files with filenames `cnav-YYMMDD.HH`. (Appendix C describes file name conventions.)

The wiring configuration used on the R/V *Roger Revelle* is shown in Fig. 17.

4.3 S4

The acoustic tracking system for this experiment was backed up and validated by an alternate tracking system. During the LOAPEX cruise in 2004, we developed a (non-acoustic) tracking solution using the location of the C-Nav antenna, the current at the depth of the transmitter, and a dynamic cable model [4, 5]. In that experiment, the current at the transmitter depth of 800 m was measured using the ship's ADCP. This depth was the ADCP limit. On this cruise, the R/V *Roger Revelle* was outfitted with two ADCPs: an RD Instruments Ocean Surveyor, which again had a maximum depth limit of about 800 m, and an experimental "HDSS" Doppler shear profiler. Under ideal conditions, the HDSS system could recover measurements from 1000 m, but according to Jules Hummon [6], the HDSS current measurements were much less reliable than the HDSS shear measurements.

Figure 15: The GPS antenna mount on the service cage on the A-frame. Left: aft view, showing the position of the antenna and the main block. Right: side view aligned with the stern, with the A-frame in approximately the position required for the survey. During the survey, the over-the-side transducer hangs off the transom, and therefore this position of the A-frame puts the antenna directly over the cable anchor point at the edge.

A different solution was required for this cruise, where the expected deployment depth was 1000 m.

Following our experience in 2004, we appropriated the InterOcean Systems S4 current meter from the APL-UW Ocean Engineering equipment pool. There was some discussion regarding how to mount the S4. From a deployment perspective, the easiest solution was to mount the instrument from the suspension cable about 5–6 m (precise distance not significant) above the monitor hydrophone. The ship's Chief Engineer had a mounting bracket designed and constructed (Fig. 18). Although this was the easiest solution from a deployment perspective, there remains a concern that the proximity of the S4 to the steel bracket and the suspension cable may bias the measurements.

In all cases, the collection protocol was to measure the two components of the vector current at 2 Hz and average every four readings to produce an output sample every 2 s. The resulting files are listed in Table 7. The ".tab" files are tab-delimited ASCII text files. There were no data collected during the first deployment at SS500. The S4 was programmed to start several hours after programming, and when it awoke, it triggered a "watchdog timeout" that immediately shut it down again. InterOcean thinks this is a hardware malfunction

Figure 16: Mounting plates for the antenna arm. One mount consisted of one top and one bottom plate, and three cross bolts. Two mounts were used, one on each side of the service cage. One mount is shown in the picture.

station	raw file	exported file	start time	end time
SS500-A	N/A	N/A		
SS25	`ss25.s4b`	`ss25.tab`	2010/05/14 11:00:00	2010/05/15 10:22:18
SS500-B	`ss500bc.s4b`	`ss500b.tab`	2010/05/23 08:01:00	2010/05/26 01:03:46

Table 7: Files from the S4 current meter. Times are UTC.

and will investigate. For the subsequent two deployments, the S4 was programmed to start collecting data immediately, so the files contain some useless data before the unit actually reached deployment depth.

5 Acoustic Tracking at SS500

A long-baseline acoustic system was set up at SS500 to track the 3-D motion of the suspended transmitter packages. The system consisted of four Benthos transponder balls deployed around the target site, and an acoustic interrogator suspended below the transmitter package. The signals from the acoustic interrogator were routed into the telemetry bottle and processed there by a Benthos ATM-885 PCB card; arrival times and auxiliary informa-

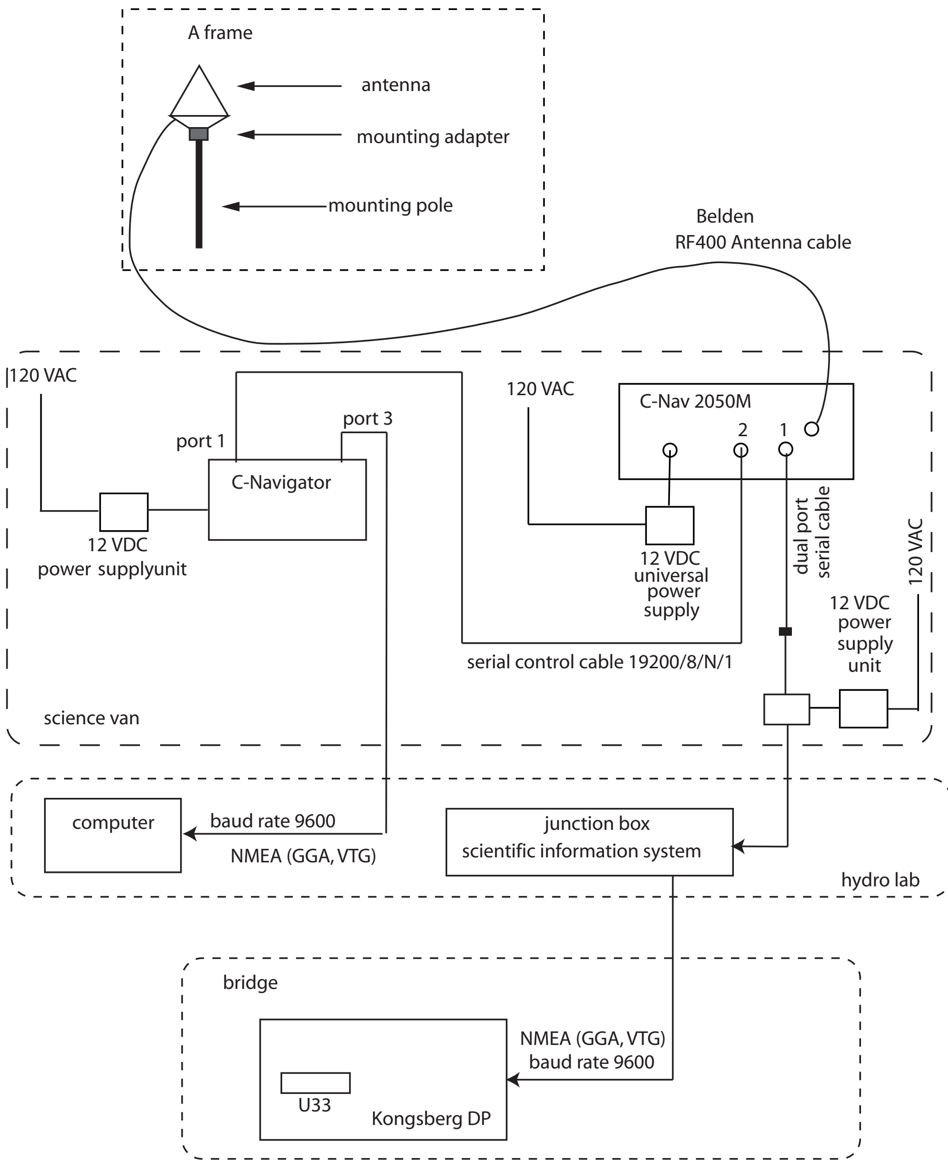

Figure 17: Cable wiring diagram, C-Nav system, R/V *Roger Revelle* 2010.

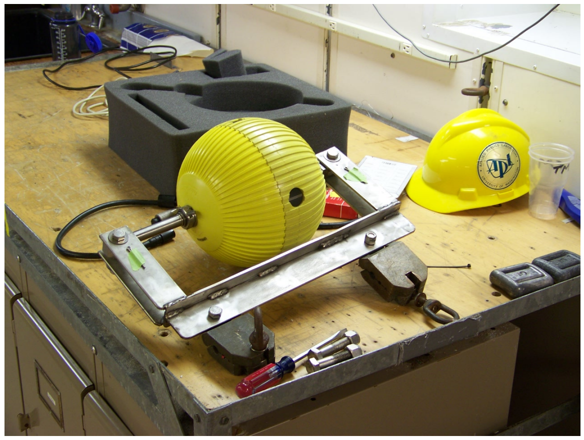

Figure 18: Mounting bracket for the S4 current meter. This bracket was returned to the R/V *Roger Revelle* after the cruise.

Site	Frequency	Time	Latitude	Longitude
X1	11.25	13:18:36	18° 57.713′	130° 10.514′
X2	11.75	12:48:29	18° 58.573′	130° 14.410′
X3	12.25	12:15:55	19° 02.285′	130° 13.494′
X4	12.75	11:43:15	19° 01.425′	130° 09.558′

Table 8: Bottom transponder drop times and drop locations. The depth at the site was approximately 5900 m. The designation X1, X2, etc. corresponds to notation used in section 7 and Fig. 20.

tion were then multiplexed up the optical fiber and reconstructed as an RS232 stream to be used by a top-side controller computer. In addition, a Benthos 7000 deck unit was used to survey the transponder balls. This unit was also controlled by computer, and its interrogator transducer was suspended temporarily over the transom of the R/V *Roger Revelle* during the surveys.

5.1 Acoustic Survey of the Transponder Net

5.1.1 Survey Design

On 8 May 2010 four transponders were launched from the R/V *Roger Revelle* at the approximate UTC time and WGS84 locations. Fig. 8 displays the frequency, time of day, latitude, and longitude of the drop point for each of the transponders (the approximate water depth was 5855 m). Herein, the positive latitude direction is north and the positive longitude direction is east. The instrumentation geometry for the survey is shown in Fig. 19.

Due to other considerations, the survey of the seafloor transponder locations was delayed

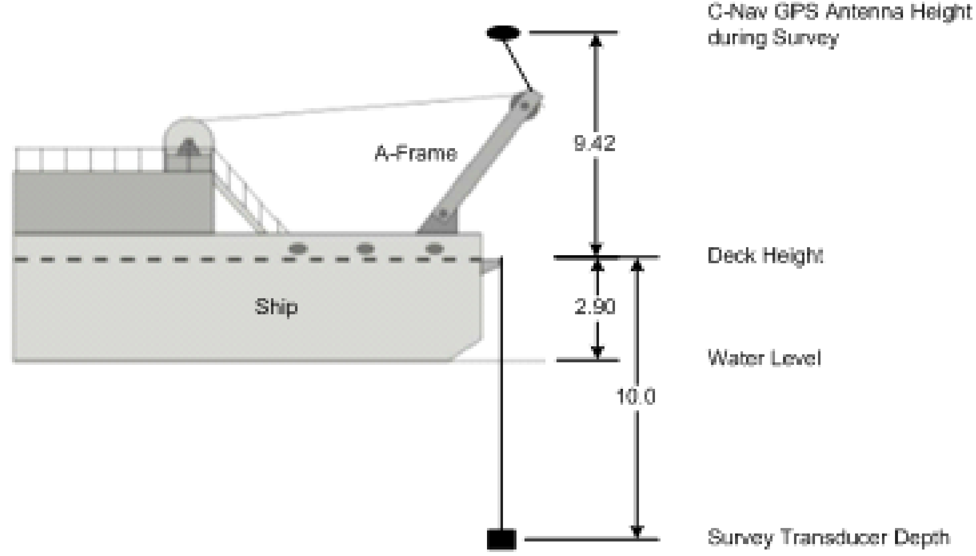

Figure 19: Survey configuration. Distances are in meters, and values are accurate to the number of digits specified.

until 11 May 2010, beginning around 2 am and ending around 12 pm UTC. During this time the ship was driven to eleven surface locations where it drifted while ranging data to the seafloor transponders were acquired. This is displayed in Fig. 20 where east and north are relative to SS500; i.e., the WGS 84 location latitude 19° 00.00′, longitude 130° 12.00′. Each seafloor transponder is labeled by its frequency. The ship's track is displayed by a solid line. The locations where ranging data were taken are denoted by '+'. The locations where the transponders were dropped are denoted by the 'o'. The locations where the survey located the transponders are denoted by 'x'. The UNIX hour of the day is plotted.

5.1.2 Estimation Method

If an approximation is based on a flat Earth, the vertical distortion in 10 km is about 8 m (see Appendix D). Because this is greater than our desired precision, careful conversions from WGS 84 coordinates to east, north, and down (ENZ) coordinates must be made; see Appendix E and Appendix F.

While there are some benefits to simultaneously fitting the location of all the seafloor transponders, we begin by presenting the method for fitting $b \in \mathbf{R}^3$, the location of one seafloor transponder. We continually measure the WGS 84 location of the ship's GPS antenna as a function of time. $g(t) \in \mathbf{R}^3$ denotes the corresponding location of the antenna in ENZ coordinates. A sequence of times t_i for $i = 1, \ldots, N$ are given when an interrogation pulse is sent from the tracking transducer and a reply pulse is received from the seafloor transponder. τ_i denotes the corresponding measured travel time. $u^i \in \mathbf{R}^3$ denotes the

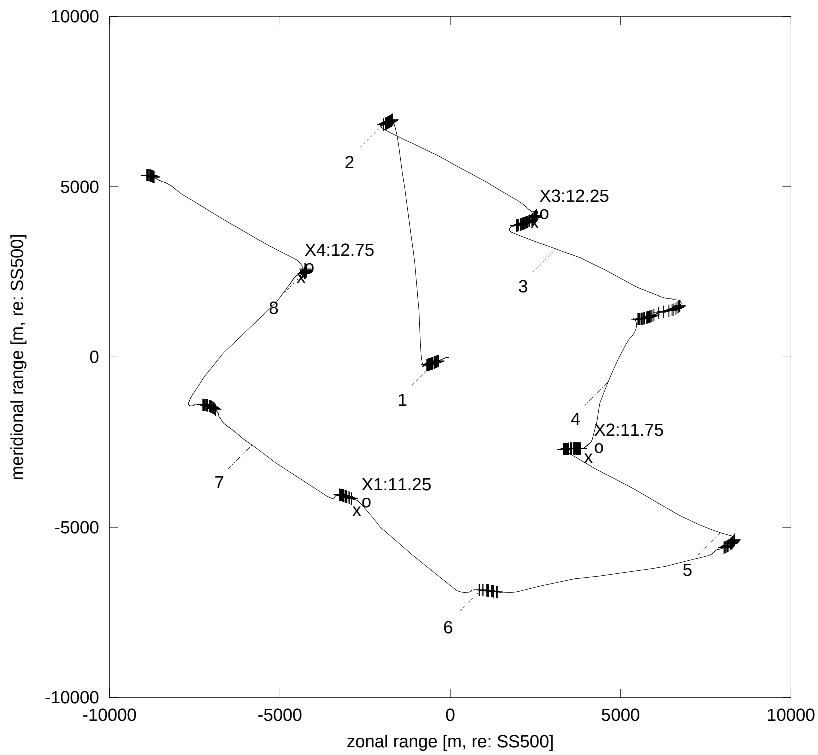

Figure 20: East–North position for ship, ranging data, seafloor transponders. Hourly (referenced to the "start" of the survey) location of ship indicated by numbers 1 through 8.

center location for the transducer midway between the transmission and reception of the corresponding reply; i.e.,

$$u^i = g(t_i + \tau_i/2) + (0, 0, 19.42)^{\mathrm{T}}$$

Note that 19.42 is the distance in the gravity direction from the GPS antenna to the tracking transducer during the survey (Fig. 19). The angle corresponding to the down direction in ENZ coordinates may differ from the gravity direction by 10 km divided by the radius of the Earth. Over a distance of 19.42 m this difference in angle is not significant. Using the transducer location midway between its transmission and reception position approximates the sum of two travel times by twice the travel time corresponding to the midpoint.

Our estimator for the location of the seafloor transponder is the value of $b \in \mathbf{R}^3$ that minimizes the objective function

$$F(b, \Delta\tau, \Delta c) = \sum_{i=1}^{N} \{\tau_i - 2\ T[\Delta c, u^i, b, \Theta_i(b)] - \Delta\tau\}^2.$$

Under the assumption that the measured travel residuals are independent and Gaussian distributed, this is the negative log likelihood (up to a constant that does not depend on b, $\Delta\tau$, or Δc). The value $\Delta\tau \in \mathbf{R}$, ($\Delta\tau \geq 0$), is the sum of the delay in the seafloor transponder plus the signal detection delay in the shipboard receiver. The travel time $T(\Delta c, u, b, \theta)$ is given by Eq. 11 and $\Theta_i(b)$ is defined by

$$R[\Delta c, u^i, b, \Theta_i(b)] = \sqrt{(b_1 - u_1^i)^2 + (b_2 - u_2^i)^2}.$$

The range function $R(\Delta c, u, b, \theta)$ is defined by Eq. 10. The transponder delay $\Delta\tau$ and the sound speed shift Δc can either be provided as *a priori* information or included in the optimization process. Including the transponder delay $\Delta\tau$ or the sound speed shift Δc in the optimization process couples the estimation of the seafloor transponders (under the assumption that it is the same for all the transponders). To be specific, if b^j is the location of the j-th transponder and τ_i^j is the corresponding travel time measurement, the objective is

$$F(b, \Delta\tau, \Delta c) = \sum_{j=1}^{J} \sum_{i=1}^{N(j)} \{\tau_i^j - 2\ T[\Delta c, u^i, b^j, \Theta_i(b^j)] - \Delta\tau\}^2, \tag{4}$$

where J is the number of seafloor transponders.

5.1.3 Survey Results

The results (Table 9) correspond to using ray tracing for travel times (see Appendix G) where $\tilde{c}(z)$ corresponds to a Seabird CTD profile measured on 20 May 2010 17:19:43 (UTC) at latitude 19° 00.01′ longitude 130° 11.96′. (This corresponds to file `dRR1006_054.cnv`, see Appendix B.) The transponder delay $\Delta\tau$ was set to 0.0097 s (as indicated by the Benthos documentation). The sound velocity shift $\Delta c = -0.94$ was the value estimated by optimizing the objective in Eq. 4.

In Table 9, frequency is in kHz, latitude is in degrees north, longitude is in degrees east, down is the negative of meters of altitude in WGS 84 coordinates, speed is distance divided by travel time for a vertical ray from the tracking transducer to the corresponding seafloor transponder, σ_r is the estimated standard deviation for the round trip travel times expressed in meters, and σ_d is the standard deviation of the position estimate (in the direction with maximum standard deviation). The values σ_r and σ_d assume the asymptotic distribution for the estimated values (and that the estimates correspond to maximizing the likelihood). Note that 10^{-6} degrees of latitude is approximately 10^{-1} m.

In Fig. 21 the solid lines display the round trip range to each transponder as a function of UNIX hour. The round trip range measurements included in the fit are plotted using the '+' symbol. The round trip range measurements removed as outliers are displayed as 'o'. Outliers that would plot outside the range are plotted on the corresponding axis limits.

In Fig. 22 the residuals corresponding to range measurements included in the fit are plotted using the '+' symbol. The residuals corresponding to round trip range measurements

Frequency	Latitude	Longitude	Down	Speed	σ_r	σ_d
11.25	18.959545	130.172674	5942.41	1512.53	1.38	0.17
11.75	18.973622	130.237384	5638.38	1510.28	1.28	0.13
12.25	19.035516	130.222356	5726.98	1510.92	1.62	0.19
12.75	19.021167	130.157130	5845.88	1511.81	1.13	0.13

Table 9: Ray tracing model results.

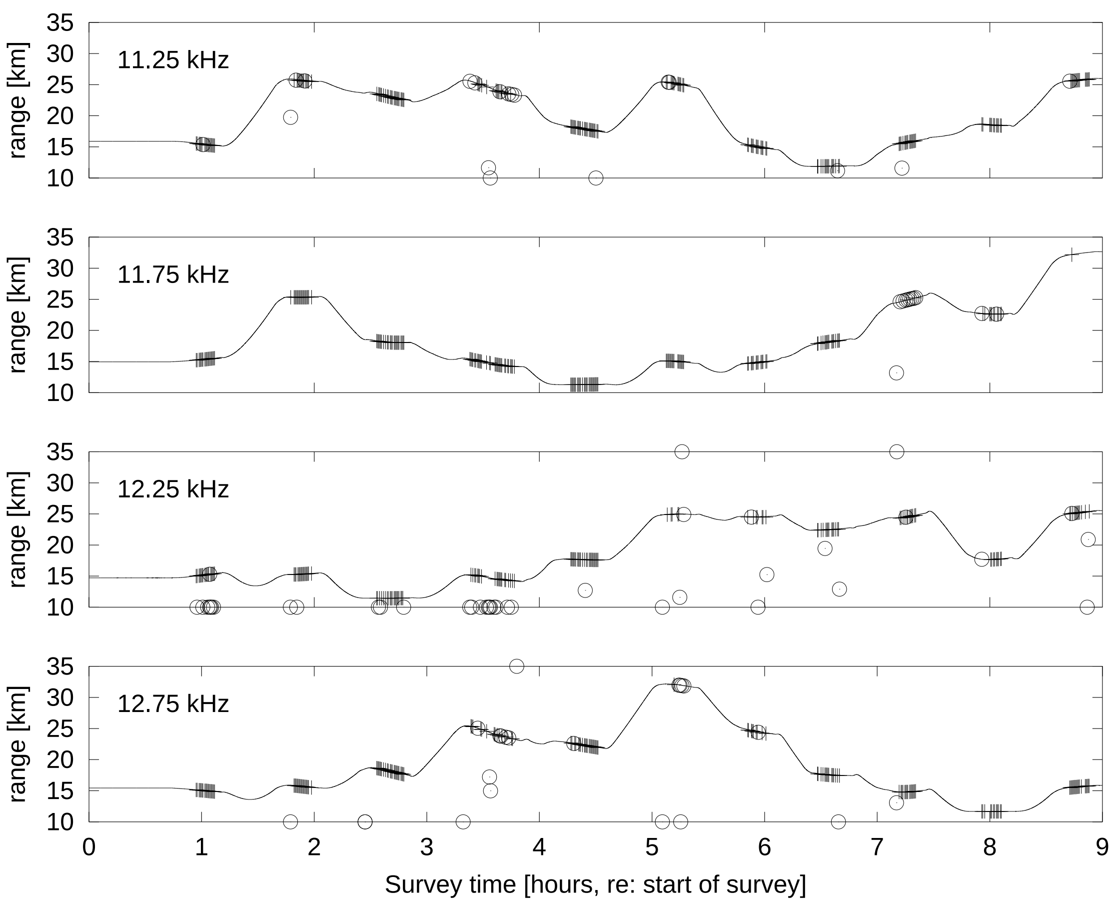

Figure 21: Round trip range distances using a ray trace model. Individual measurements deemed valid are marked +; rejected measurements are marked ∘.

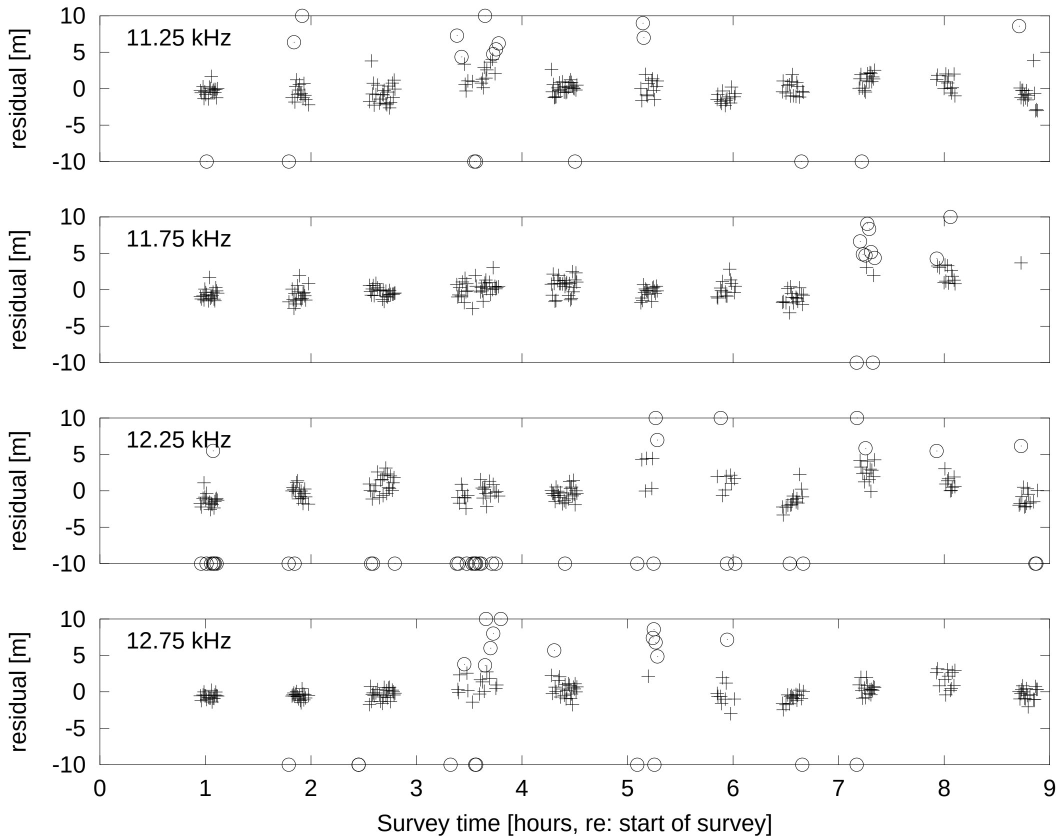

Figure 22: Round trip range residuals using a ray trace model. Individual measurements deemed valid are marked +; rejected measurements are marked ∘.

removed as outliers are displayed as 'o'. Outliers that would plot outside the range are plotted on the corresponding axis limits.

A straight line approximation for the travel times is used to test that the sound velocity profile is uniform in the horizontal, and that it did not change between 11 May (when the survey was done) and 20 May (when the profile was measured). This straight line analysis estimates an average sound velocity for each seafloor transponder during its fitting process. The objective function for each transponder is

$$G(b, s, \Delta\tau) = \sum_{i=1}^{N} \left[\tau_i - 2s \sqrt{(b_1 - u_1^i)^2 + (b_2 - u_2^i)^2 + (b_3 - u_3^i)^2} - \Delta\tau \right]^2,$$

where s is the average of the slowness for the transponder; i.e., the average $c(z)^{-1}$ between the tracking transducer and the transponder. In Table 10, speed is the corresponding sound speed estimate 1 / s and σ_c is the standard deviation of this estimate (under the assumptions that the estimate corresponds to maximum likelihood).

Note that the speed estimates are increasing with respect to the down component of the

Frequency	Latitude	Longitude	Down	Speed	σ_r	σ_d	σ_c
11.25	18.959539	130.172668	5946.97	1513.38	2.00	0.36	0.04
11.75	18.973625	130.237382	5641.74	1510.87	1.64	0.26	0.03
12.25	19.035515	130.222352	5730.28	1511.54	1.72	0.32	0.04
12.75	19.021165	130.157132	5849.78	1512.47	1.04	0.19	0.02

Table 10: Straight line model results.

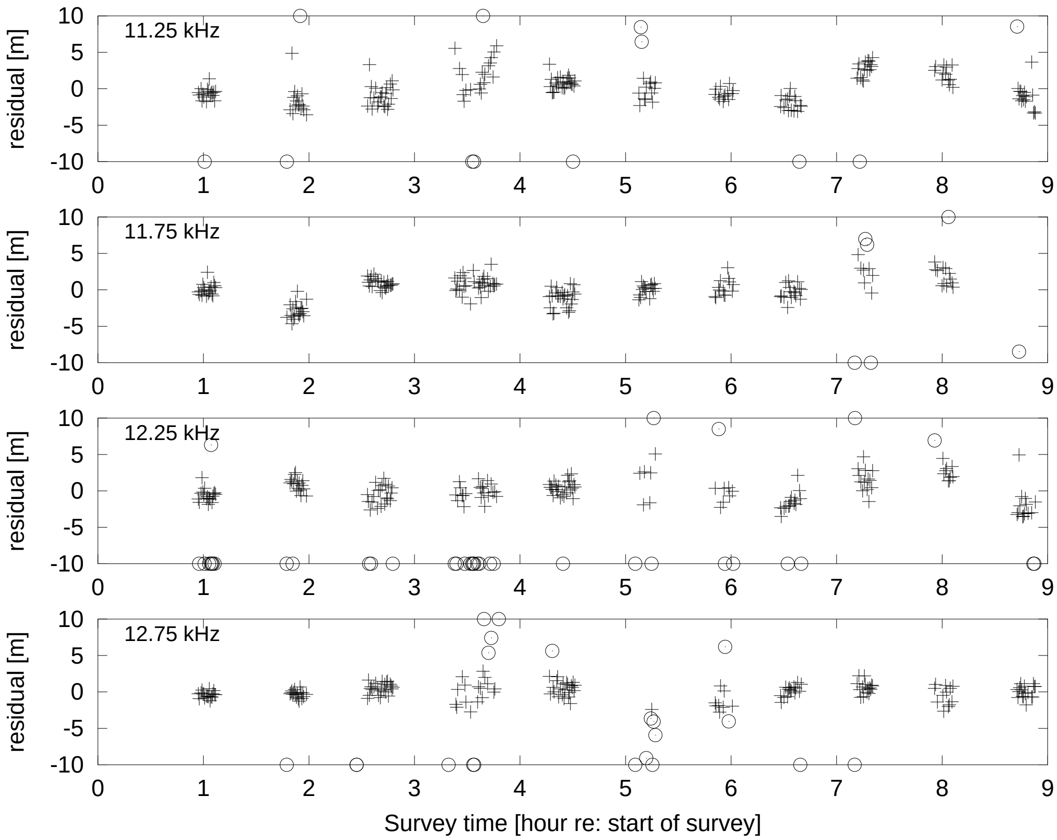

Figure 23: Range residuals using a "straight line" propagation model. Individual measurements deemed valid are marked +; rejected measurements are marked ∘.

corresponding transponder in an approximately affine fashion. This follows because sound velocity profiles are nearly linear with depth in deep water. In addition, the speed estimates are comparable with those for the ray trace fit in Table 9. The residuals corresponding to this fit are plotted in Fig. 23.

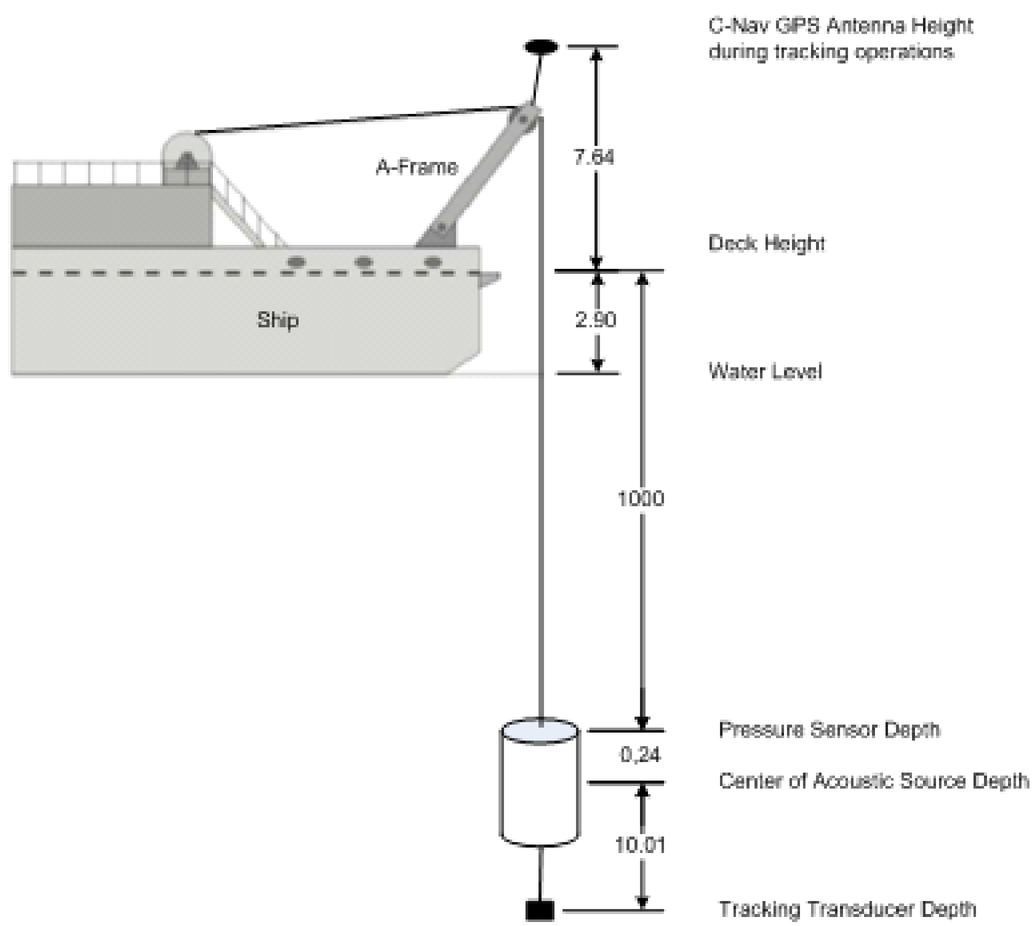

Figure 24: Diagram of the tracking configuration, distances are in meters.

5.2 Acoustic Tracking

The instrumentation geometry for the tracking effort is shown in Fig. 24. Our goal is to locate the center of the source. For the purposes of tracking, we locate the tracking transducer and then consider the source center as 10.01 m above that location. In addition, we consider the seafloor transponders to be fixed at the locations in Table 9.

The cable length is much longer during tracking of the source than during the survey (section 5.1.1). Hence, during the tracking, we do not assume that the tracking transducer is below the GPS antenna (in ENZ coordinates). We use a Kalman smoother model for the measurements and dynamics of our tracking problem. The state vector for our tracking problem is a function $x : \mathbf{R} \mapsto \mathbf{R}^7$, where the components have the meaning given in Table 11.

$x_1(t)$	:	east component of ENZ position
$x_2(t)$	:	north component of ENZ position
$x_3(t)$	:	down component of ENZ position
$x_4(t)$	:	east component of ENZ velocity
$x_5(t)$	:	north component of ENZ velocity
$x_6(t)$	:	down component of ENZ velocity
$x_7(t)$	:	shift of the measured sound speed profile

Table 11: Kalman smoothing state vector.

5.2.1 Dynamical Model

The dynamical model for a Kalman smoother expresses the mean and noise in the state vector at the current time point x^k given the state at the previous time point x^{k-1} and the state transition noise w^k;

$$x^k = g^k(x^{k-1}) + w^k.$$

It is standard for Kalman filters and smoothers to use w^k for the vector of dynamical noise at time index k. Here, $w \in \mathbf{R}^3$ denotes a WGS 84 location while $w^k \in \mathbf{R}^7$ denotes a dynamical noise vector in the Kalman smoother model.

In our case, $g^k : \mathbf{R}^7 \mapsto \mathbf{R}^7$. There is a special definition for $g^1(x^0)$ (see section 5.2.3). For $k \neq 1$ and for $i = 1, 2, 3$,

$$\begin{aligned} g_i^k(x^{k-1}) &= x_i^{k-1} + x_{i+3}^{k-1}(t_k - t_{k-1}) \\ g_{i+3}^k(x^{k-1}) &= x_{i+3}^{k-1} \\ g_7^k(x^{k-1}) &= x_7^{k-1}. \end{aligned}$$

That is, the mean of x^k given x^{k-1} is linear motion for the position, and persistence for the other components of x^k.

The dynamical model also specifies the variance $Q^k \in \mathbf{R}^{7\times 7}$ of the dynamical noise w^k. In our model, this variance is diagonal and has the following values along the diagonal:

$$\operatorname{diag}(Q^k) = (t_k - t_{k-1})(\sigma_e^2, \sigma_n^2, \sigma_z^2, \dot\sigma_e^2, \dot\sigma_n^2, \dot\sigma_z^2, \sigma_s^2),$$

where $\sigma_e = \sigma_n = .001$ are the standard deviation per second for east and north positions in meters per second, $\sigma_z = 0.01$ is the standard deviation per second for the depth position in meters per second, $\dot\sigma_e = \dot\sigma_n = 0.01$ are the standard deviation per second for east and north velocities in meters per second per second, $\sigma_z = 0.1$ is the standard deviation per second for the depth velocity in meters per second per second, $\sqrt{3600}\ \sigma_s = 0.01$ is the standard deviation per hour for the sound speed profile shift in meters per second per hour.

5.2.2 Measurement Model

We use travel time measurements from the tracking transducer to the four seafloor transponders as well as pressure measures at the pressure sensor (Fig. 24). $t_k \in \mathbf{R}$ for $k = 1, \ldots, N$ denotes the times at which there are some transponder travel time measurements $\{\tau_i^k \in \mathbf{R} \mid i = 1, \ldots, 4\}$ and / or a pressure measurement $p_k \in \mathbf{R}$. Throughout the value zero is used for components of the measurements that are not present at a particular time index k. It is standard for Kalman filters and smoothers to use z^k for the vector of measurements at time index k. Here, $z \in \mathbf{R}$ denotes a depth while $z^k \in \mathbf{R}^5$ denotes the measurement vector in the Kalman smoother model. For $i = 1, \ldots, 4$

$$
\begin{aligned}
z_i^k &= \begin{cases} 1500\,(\tau_i^k - \Delta\tau)/2 & \text{if } \tau_i^k \neq 0 \\ 0 & \text{otherwise} \end{cases} \\
z_5^k &= \begin{cases} D(\lambda, p_k) + 20.79 - a_k & \text{if } p_k \neq 0 \\ 0 & \text{otherwise,} \end{cases}
\end{aligned}
$$

where $\lambda = 19$ is the latitude in degrees for SS500, p_k is the pressure in bars of mercury (one bar corresponds to the surface of the ocean), a_k is the altitude of the GPS antenna at time t_k, and $D(\lambda, p_k)$ is the depth function defined in Appendix H. Note that (Fig. 24)

$$20.79 = 7.64 + 2.90 + 0.24 + 10.01.$$

We use $x^k \in \mathbf{R}^7$ to denote the vector $x(t_k)$; i.e., the state vector at time t_k (Table 11). A Kalman smoother models the measurement vector z^k as

$$z^k = h^k(x^k) + v^k,$$

where $h^k(x^k)$ is the model for the mean of z^k given x^k, and v^k is the noise in the measurement.

Here $h^k : \mathbf{R}^7 \mapsto \mathbf{R}^5$. The model for the mean of the pressure data z_5^k given the state vector x^k is simply

$$h_5^k(x^k) = x_3^k.$$

For $i = 1, \ldots, 4$, $h_i^k(x^k)$ is the nominal sound speed times the travel time from the seafloor transponder located at b^i to the tracking transducer located at (x_1^k, x_2^k, x_3^k) (the nominal sound speed is 1500 $\mathrm{m\,s^{-1}}$). We use the ray trace travel time from a nominal position for the transducer $\bar{u}$ to each of the seafloor transponders to get an average sound speed for that transponder $\bar{c}_i$. The nominal position for the transducer $\bar{u}$ is a depth of 1010 m at SS500; i.e., latitude 19° 00.00′, longitude 130° 12.00′, and altitude −1010 m. To be specific, $\bar{c}_i$ is defined by

$$
\begin{aligned}
R[\Delta c_k, u^k, b^i, \bar{\theta}_i] &= \sqrt{(b_1^i - \bar{u}_1^k)^2 + (b_2^i - \bar{u}_2^k)^2} \\
\bar{c}_i &= \frac{|b^i - \bar{u}|}{T(0, u^k, b^i, \bar{\theta}_i)}.
\end{aligned}
\tag{5}
$$

The function $R(\Delta c, u, b, \theta)$ is defined by Eq. 10. The function $T(\Delta c, u, b, \theta)$ is defined by Eq. 11. Note $\bar{c}_i$ depends on the function $\tilde{c}(z)$, which is an interpolated version of the sound speed profile measured as a function of depth from the surface of the ocean.

For the simple, straight line model, the functions $h_i^k(x^k)$ for $i = 1, \ldots, 4$ are given by

$$\begin{aligned} u^k &= (x_1^k, x_2^k, x_3^k)^{\mathrm{T}} \\ \Delta c_k &= x_7^k \\ h_i^k(x^k) &= 1500 \left| u^k - b_i^k \right| (\bar{c}_i + \Delta c_k)^{-1}. \end{aligned} \tag{6}$$

The first and second expressions in Eq. 6 define u^k and Δc_k in terms of the components of x^k. The third expression incorporates the sound speed shift Δc_k in the model for the travel time by the nominal sound speed.

For the ray trace model, the functions $h_i^k(x^k)$ for $i = 1, \ldots, 4$ are given by

$$\begin{aligned} R[\Delta c_k, u^k, b^i, \Theta_i(u^k)] &= \sqrt{(b_1^i - u_1^k)^2 + (b_2^i - u_2^k)^2} \\ h_i^k(x^k) &= 1500\, T(\Delta c_k, u^k, b^i, \Theta_i(u^k)). \end{aligned} \tag{7}$$

The first expression in Eq. 7 is an implicit definition for the initial angle of the ray between the tracking transducer and seafloor transponder $\Theta_i(u^k)$. The second expression models the travel time from the transducer to the seafloor transponder (times the nominal sound speed).

The measurement model also specifies the variance $R^k \in \mathbf{R}^{5\times 5}$ of the measurement noise v^k. In our model, this variance is diagonal and has the following values along the diagonal:

$$\mathrm{diag}(R^k) = (\sigma_\tau^2, \sigma_\tau^2, \sigma_\tau^2, \sigma_\tau^2, \sigma_p^2),$$

where the standard deviation for the one-way travel time measurement in meters is $\sigma_\tau = 1.5$ and the standard deviation for the pressure measurements in meters is $\sigma_p = 0.2$. Note that missing data values correspond to infinite standard deviations and zeros on the diagonal of the inverse of the covariance $(R^k)^{-1}$.

5.2.3 Tracking Results

We use the notation $\{x^k\}$ to denote the sequence of state vector values $\{x^1, \ldots, x^N\}$. The Kalman smoother estimate $\{\hat{x}^k\}$ minimizes the objective function

$$\begin{aligned} H(\{x^k\}) &= \sum_{k=1}^{N} [x^k - g_k(x^{k-1})]^{\mathrm{T}} (Q^k)^{-1} [x^k - g_k(x^{k-1})] \\ &+ \sum_{k=1}^{N} [z^k - h_k(x^k]^{\mathrm{T}} (R^k)^{-1} [z^k - h_k(x^k]. \end{aligned} \tag{8}$$

In this notation, Q^1 is the variance of the initial state estimate $g_1(x^0)$ and the function $g_1(x^0)$ is constant; i.e., it does not depend on the value of x^0. Under the assumptions that the random variables $\{w^k\}$, $\{v^k\}$ independent Gaussian distributed with mean zero and variance $\{Q^k\}$, $\{R^k\}$ respectively, maximizing the objective above is equivalent to maximizing the likelihood of the state sequence $\{x^k\}$ given the measurement sequence $\{z^k\}$. For our purposes, the initial state variance Q^1 was set large enough so that the initial estimate did not significantly affect the solution. The non-linear Kalman smoother package [7] was used to optimize the objective in Eq. 8.

Position results for the straight line measurement model (Eq. 6) are plotted in Fig. 25. These positions are relative to SS500; i.e., the WGS 84 location latitude 19° 00.00′, longitude 130° 12.00′. Components of $\{\hat{x}^k\}$ are plotted with a solid line. The corresponding locations of the ship's GPS antenna are plotted as dots for comparison. Note that 1010 meters has been added to the down component of the ships GPS antenna so that it would be easy to compare with the down component of the tracking transducer; i.e., $\{\hat{x}_3^k\}$ (Fig. 24). Also note that the time scale for the down component is shorter than for the east and north components.

Relative to SS500 the east, north, and down coordinates of the nominal tracking transducer location $\bar{u}$ are $(0, 0, 1010)$. The position results for the ray tracing model (Eq. 7) are identical to the the straight line model. This is to be expected because $\bar{u}$ was used to define the average velocities in the straight line approximation (Eq. 5), and the actual transducer location was always close to $\bar{u}$.

The velocity components of the estimate $\{\hat{x}^k\}$ are plotted in Fig. 26. The corresponding residuals $\{z^k - h^k(\hat{x}^k)\}$ are plotted in Fig. 27.

5.3 Acoustic Tracking Validation Dataset

On 20 May 2010 a validation data set was collected using the same configuration and data acquisition as during the survey (Fig. 19). That is, we ranged to the four seafloor transponders and recorded GPS position under conditions where we knew the position of the tracking transducer relative to the GPS antenna. A pseudo pressure measurement was created from the fact that the transducer was 7.10 m below the ocean surface. The measurement and dynamical model for this validation were the same as described in Section 5.2 with the following exceptions:

1. The nominal position of the tracking transducer, $\bar{u}$, is a depth of 7.10 m at SS500; i.e., latitude 19° 00.00′, longitude 130° 12.00′, and altitude −7.10 m.
2. The value used for the depth measurements, z_5^k, was $19.42 - a_k$. Note that $19.42 = 9.42 + 10.0$ and $7.10 = 10.0 - 2.90$ (Fig. 19).

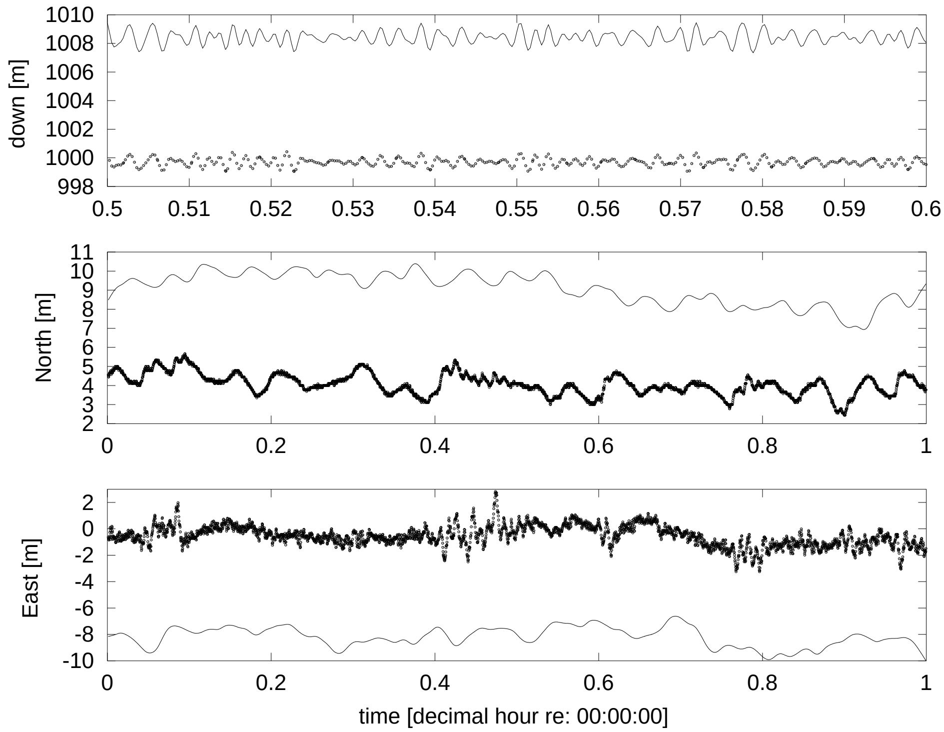

Figure 25: East, North, and Down positions. Measurements from the C-Nav GPS shown as dots, and the smoother results for the transmitter package shown as solid lines.

The position results, relative to SS500, for this validation are plotted in Fig. 28. In these plots the solid line is the Kalman smoother estimate for the tracking transducer location and the dotted line is the corresponding GPS data. The down location of the GPS antenna has been shifted by 19.42 m so that it corresponds to the location of the transducer.

The difference between GPS location and the smoother location for the tracking transducer is plotted in Fig. 29. Note that this is only a validation of the east and north directions. The down direction is not a real validation because it is determined by the pseudo depth data, which is different from the actual pressure sensor that is used when the transducer is at about 1000 m depth.

5.4 Further Suggestions on Acoustic Tracking

1. Correct the depths in the sound speed profile by integrating the pressure and using a more accurate equation of state to determine the compressibility of water.

2. Do the ray tracing in circular coordinates where range is along the circle and depth

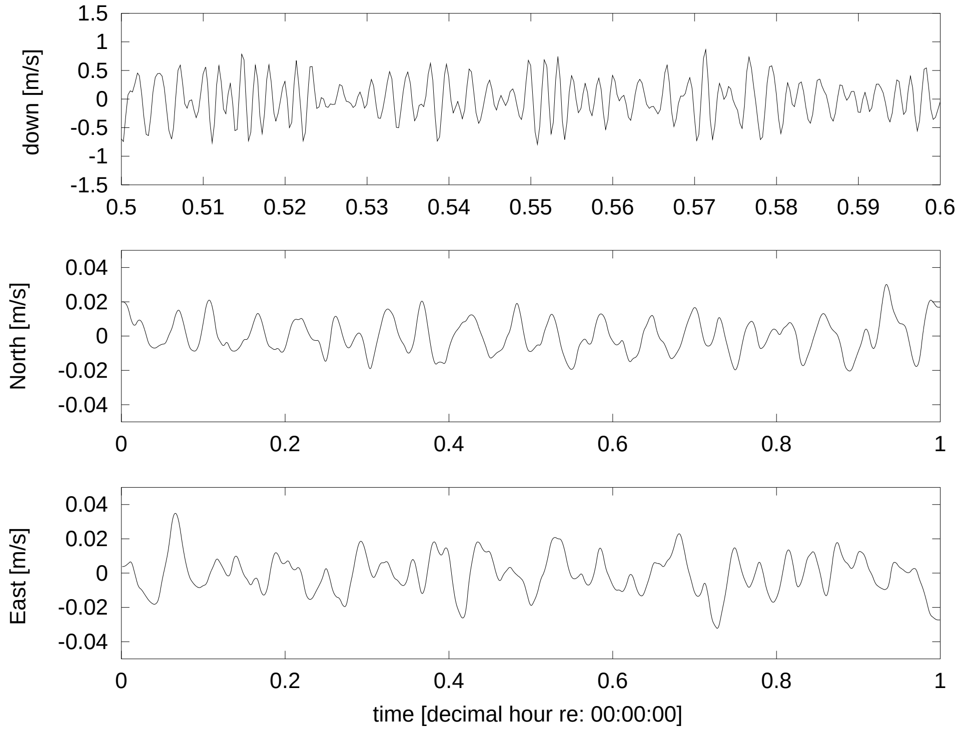

Figure 26: East, north, and down velocities. Tracking estimates.

is toward the center of curvature for the current point on the Earth.

3. Determine the time delay between the GPS time in the C-Nav data stream and when the corresponding `GPGGA` message is completed (at 9600 baud).

4. Measure the time delay between when the Benthos DS7000 (and ATM-885) is commanded to transmit and when it does transmit.

5. Measure the turn-around time in the seafloor transponders, plus the time it takes for the Benthos DS7000 to recognize that a pulse is received; i.e., the correction to the travel time that accounts for processing delay.

6. Use the ship's heading, pitch, and roll to get a more accurate estimate of the tracking transducer during the survey.

7. Provide a more detailed description of the outlier rejection method.

8. Use other robust estimators for the survey and or the tracking; e.g., the ℓ_1 Laplace estimator.

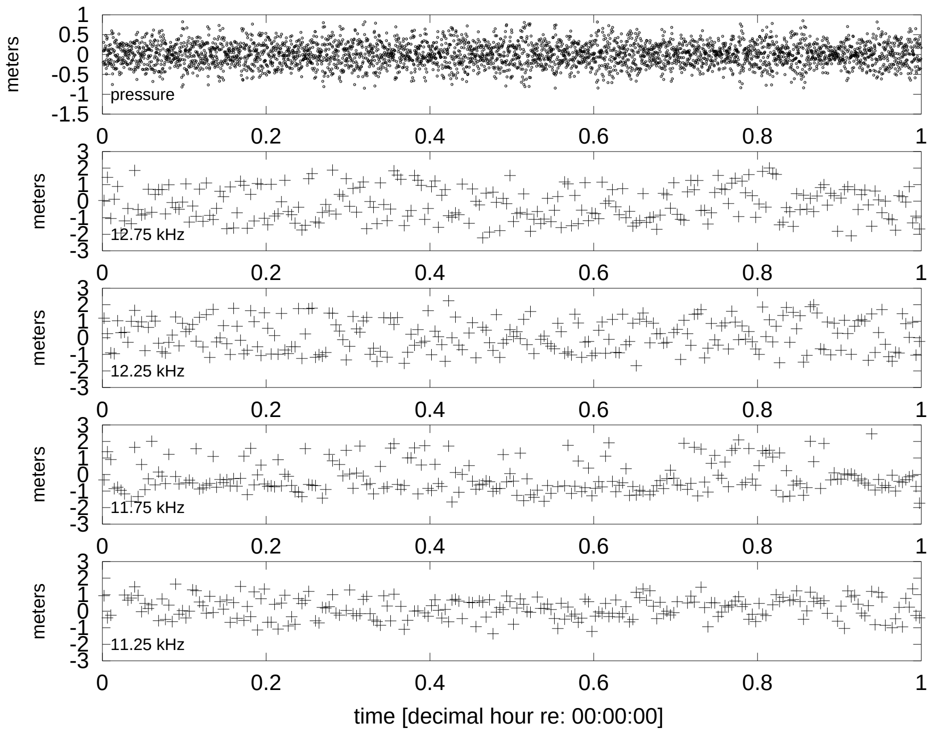

Figure 27: Pressure and one-way travel time residuals for the transducer estimates.

9. Add a correction factor for the barometric pressure at the surface of the ocean (Appendix H).

10. Replace the sound speed profile shift Δc by a more physical description of profile variation in space and time (section 5.2.2).

11. The Kalman smoother routine allows for an arbitrary dynamical model in the form of the definition of $g^k(x^k)$ and Q^k. Improve upon the dynamical model presented in Section 5.2.1.

12. The Kalman smoother routine allows for an arbitrary measurement model in the form of the definition of $h^k(x^k)$ and R^k. Improve upon the measurement model presented in Section 5.2.2.

13. The script files `report/2010/*/survey.sh` and `report/2010/*/track.sh` create and compile Matlab programs with no documentation or unit tests. These Matlab programs should be converted to documented and tested subroutines. This would make them much easier to understand and use.

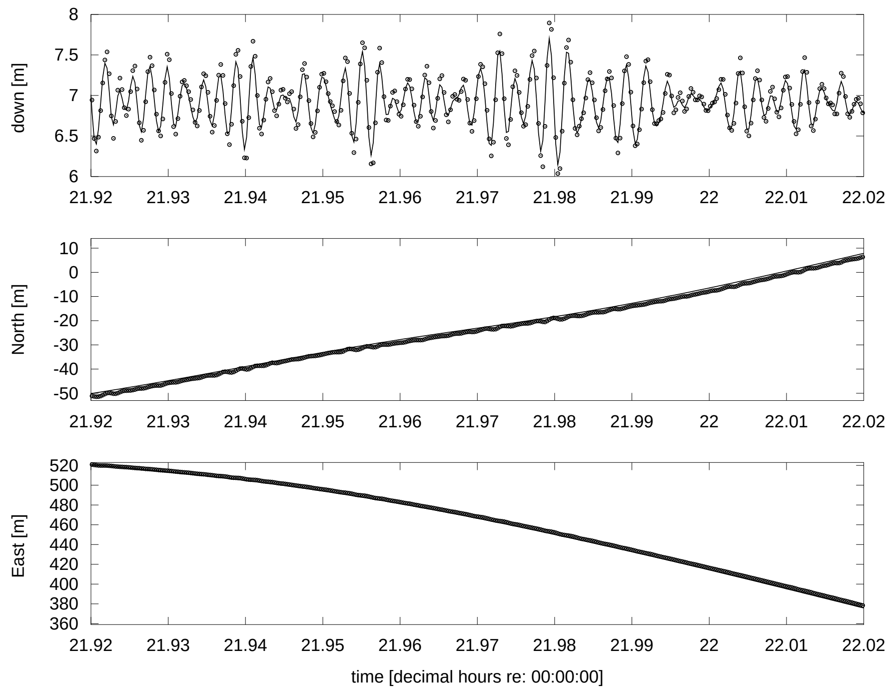

Figure 28: Validation plot of relative transducer position.

6 Environmental Measurements

6.1 Towed CTD Chain (TCTD)

The Towed CTD Chain (TCTD) is an 800-m long cable instrumented with 88 sensor fins (originally to be 100 fins but 12 from a previous field experiment were broken and unavailable at the time of our cable assembly); see Fig. 30 for a notional diagram. Each fin has onboard sensors to measure temperature, conductivity, and pressure like a traditional CTD instrument. A traditional CTD is generally cast at one geographic point location while the ship is stopped, yielding very high depth resolution CTD measurements at that single point location. In contrast, the TCTD is meant to yield a relatively high resolution (on the order of 5 m both vertically and horizontally), 2-D vertical slice of the ocean, with CTD measurements down to 500–600 m depth for as far as the cable is towed. Unlike other towed instruments such as the SeaSoar [8], the TCTD simultaneously takes measurements over the entire depth range every few seconds, resulting in much higher spatial and temporal resolution. However, while this system's concept is very attractive, and a few much smaller versions of it have been used successfully in the past, including Shallow Water 2006 (SW06) [9–11], the present large-scale version of it has numerous technical problems that greatly constrained the measurements and their usefulness. In spite of these problems, some

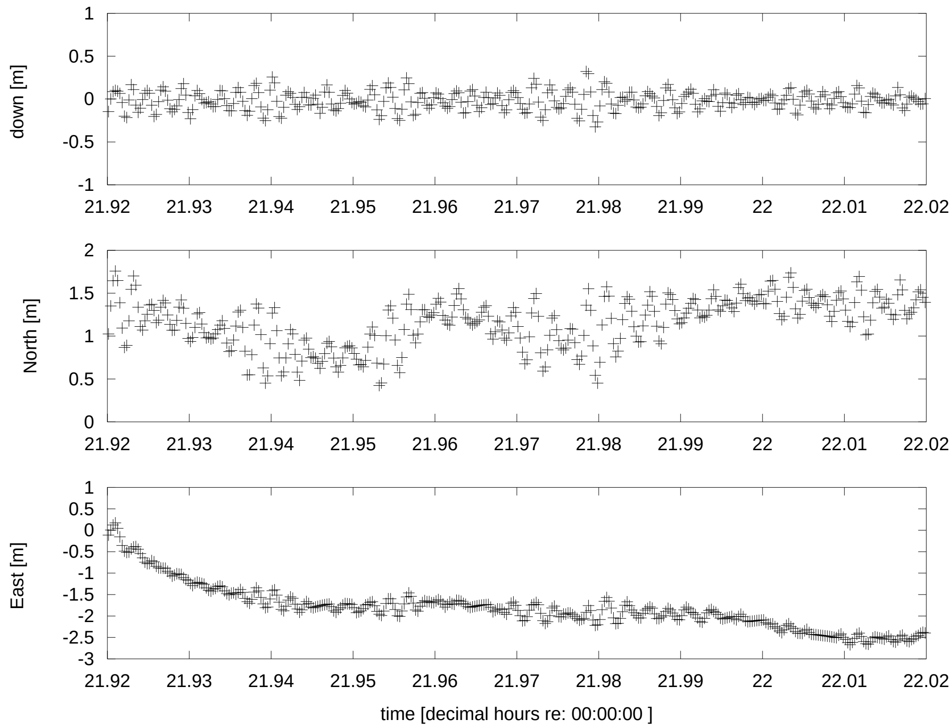

Figure 29: Validation plot of transducer position differenced with the GPS position.

TCTD data were obtained in the PhilSea10 Experiment; analysis continues to determine whether the data are scientifically useful.

6.1.1 Mechanical Operation

The TCTD chain is stored on a large powered reel, and is deployed, recovered, and towed from the fantail at the stern of the ship. During deployment and recovery the ship is slightly underway (≈1 kt) to keep the long cable from twisting under the ship, and to keep a convenient cable angle so that the sensor fins are not at risk of getting caught on the transom. A deck crew of about eight people is required for deployment or recovery, but after those operations are finished, the only operator required is one inside at the deck unit computer to monitor the system. Deployment proceeds as shown in Fig. 31, and recovery is essentially the same process in reverse; compare the following lettered items with the panels in the figure.

a) Overall layout regarding the large deployment/recovery block: during deployment and/or recovery of the depressor and cable end-termination, the large block is in raised position

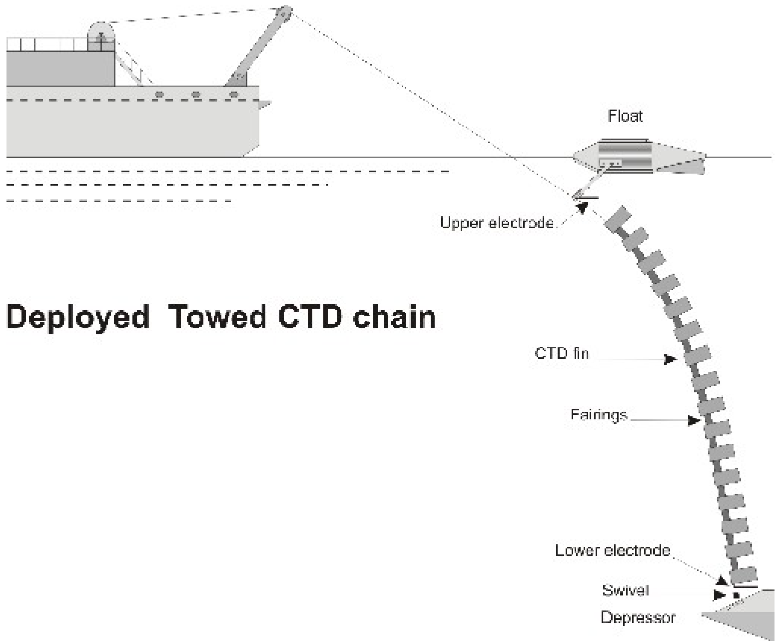

Figure 30: Notional diagram of TCTD (reproduced from website of ASD Sensortechnik [12])

(as here), then lowered close to the deck while the sensor cable itself is being deployed or recovered such that an operator can flip fins up before they enter the block. Block height is controlled via capstan at the forward end of the fantail (note an additional smaller block attached to the top of A-frame is also required). Two tag lines from the top of the block are held fast by air tuggers on each side, two tag lines from the bottom of the block are held by deck hands and fastened to cleats at the bottom of the A-frame.

b) Deploying the cable end-termination before lowering the large block: at chest level in this picture is the cable-end SBE37 CTD (#399), and at knee height is the lower termination, which is connected directly to the swivel on the depressor.

c) The large block is then lowered to a position that can be reached from deck during operation.

d) The cable runs from the large block to the level wind of the big blue powered reel. The powered reel has a dedicated operator on its control box standing nearby so that if needed the operator can stop the reel as soon as possible before a fin is damaged.

e) The big blue powered reel is about 2 m in diameter and 4 m wide — its large size is to accommodate the sensor fins remaining on the seacable on the reel (along with the armored coax tow cable at one end). On either side of each fin is a clamp-knob mounted on the cable, allowing the fin to swivel. The large reel diameter, which provides a gentle circumferential curvature, allows these clamps to hold the straight ring-core back of the fins $\approx$ 0.5-1 cm away from the curved reel surface, preventing strain on the ring cores

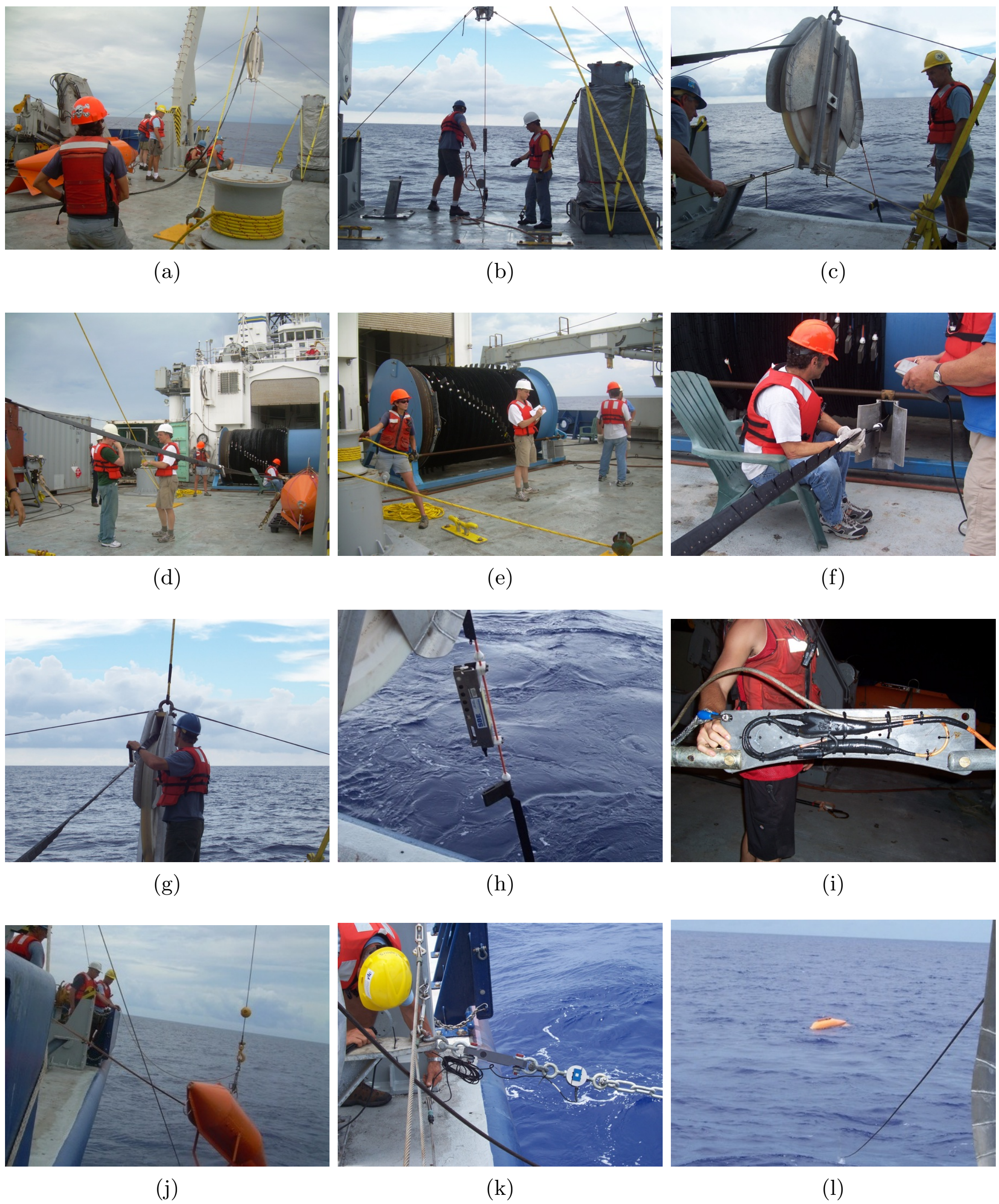

Figure 31: Deployment steps for the TCTD. (Recovery is nearly the same but in reverse). Refer to alphabetical list in text for descriptions of the step shown in each photo.

in the fins. This gentle circumferential curvature rationale also motivated the choice of diameter for the large block used at the stern.

f) A dedicated operator ensures that each fin is either lifted or flipped before transiting the level wind. It is crucial that this person is not distracted by other duties as it is easy to miss a fin, in which case the fin is destroyed, and also because **CAUTION** this level wind entry/exit is a dangerous place where a hand or arm could be injured severely.

g) Similarly, a dedicated operator flips each fin upward and guides it into the large block, whether doing so on the forward side during deployment, or on the aft side during recovery. As for the level wind, this operator must not be distracted by other duties so that a fin is not missed, and also because **CAUTION** the block entry point is a dangerous place where a hand or arm could be injured severely. Lastly, in recovery, depending on angle of cable due to current/shipspeed, it was sometimes useful to have a second person here with a pole to flip each fin on its way up so it does not catch on the transom before the operator at the block can reach it.

h) Halfway down the cable a SBE37 CTD (#397) was mounted (using standard SBE mounting pieces for 1 cm cable). Like the one at the cable end, it was attached aft of the large block, albeit with some reaching over the stern. With the problematic pressure sensors in the fins, these SBE37s were crucial to obtain a reliable cable shape/position and thus correct pressures at each fin.

i) A "fish-plate" serves as the heavy-duty connector between the float arm that attaches at top left in the photo, the sensor seacable leading down into the deep ocean and attaching at bottom right, and the towline leading to the ship and attaching bottom left. The towline is armored coax, from which one conductor goes to the electrode mounted on the fish-plate, and the other remains insulated and attaches to the top of the seacable. Within the towline connector is a "weak link" such that if tension on the seacable passes a threshold (say if snagged undersea) the weak link will break from the towline and the float will support the submerged seacable until it can be rescued.

j) With the seacable fully deployed such that the fish plate is at the stern (and all still held by the powered reel), the float is then deployed via crane, during which the fish plate is attached to the float's arm.

k) Tensiometers (two in series here, one digital unit with a cable leading to a lab computer, and the second a regular backup with local display) attach to a tow point mounted on the stern deck, and the towline is transferred to here.

l) Float is towed on order of 50 m astern. The float has a strobe and radio beacon attached in case the towline disconnects at the weak link.

6.1.2 Electronic and Software Operation

After deployment is complete, the big blue reel is dogged in place and the end of the armored coax on the reel is attached to another coax cable that leads from the fantail to the deck unit in the ship's lab. A second cable leading from the fantail into the lab is for the digital tensiometer, which attaches to an A/D unit on a lab computer. The TCTD deck unit connects to a computer for control and data acquisition, as well as to a DC power supply and to an oscilloscope for cable signal monitoring. (If the system were more stable the scope would not be required, but due to the numerous problems that remain to be solved, this monitoring oscilloscope is crucial at virtually all stages of system operation.) Finally, we used two computers — one entirely dedicated to the acquisition and control, and a second for visualization and analysis of the (networked) data acquired to avoid accidents on the acquisition computer that might jeopardize the recording of the data.

The bench-top components described above and their spares (Fig. 32a) were mounted in the TCTD station in the ship's lab. Note that the backup TCTD deck unit looks different from the main one — in fact, of the three deck units from ADM, none looked or operated quite the same, or produced precisely the same signal waveform, but the overall usage was similar. In all units there is a six-position main transformer-tap switch that changes the tradeoff between the voltage and current for a given power being sent down the seacable. By experiment, we determined the system worked best with "more current" selected (switch set to 4 or 5 out of 6). At the chosen switch setting — only changed when the DC power supply was at minimum or zero — the DC voltage was slowly turned up as the operator watched fins come online in the acquisition computer's readout display. The DC power supply's current limit was set at maximum because the cable impedance pins it to a given supply voltage. Many of the fins would not come online, and often the number of fins that did come up would begin to gradually decrease through the hours of towing. Further details on the deck unit and system operation may be found in the *TCTD How-To Procedures* document [13], instrument manuals [14, 15], and developer's website [16].

Fig. 32b shows an example of the oscilloscope display — an important system monitor during operation. The green trace is the seacable voltage at the monitor point, the yellow is the monitored seacable current, and the blue is a filtered version of the seacable voltage focused on the (higher-frequency) return signal from the fins. The numerical details of the traces can be found in the TCTD manual, how-to document, and developer website. The main concept is that between the 10 ms-long power pulses (green), the fins are called on individually to report back. Sometimes they do and sometimes they do not (blue). Monitoring whether fins report back at this electronic level helps to narrow the cause of "no data" errors that arise in the acquisition.

Towline tension via the digital tensiometer, and also the DC power supply's voltage and current monitor points, were attached to a Labjack A/D unit (Fig. 32c). The blue wires come from the DC power supply monitor points, and the four-conductor cable on left leads out to the tensiometer's interface unit on deck. The black box (Fig. 32c) is the step-down

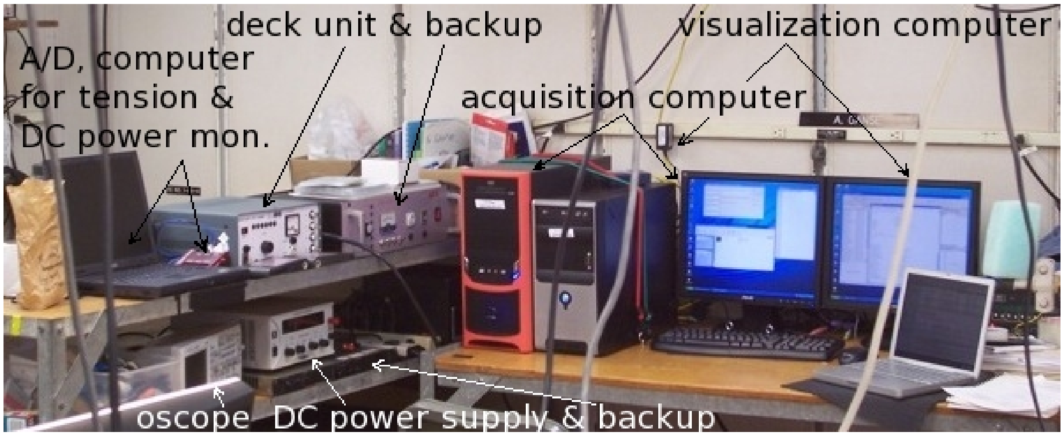

(a)

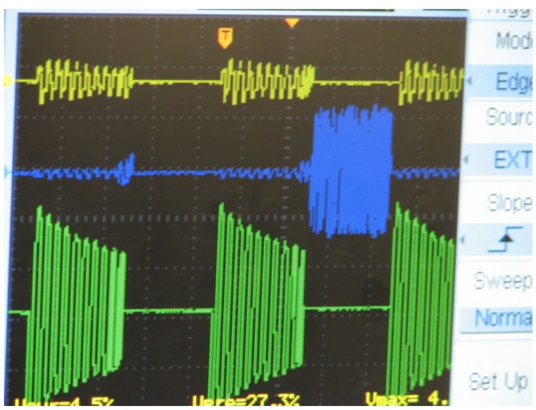

(b)

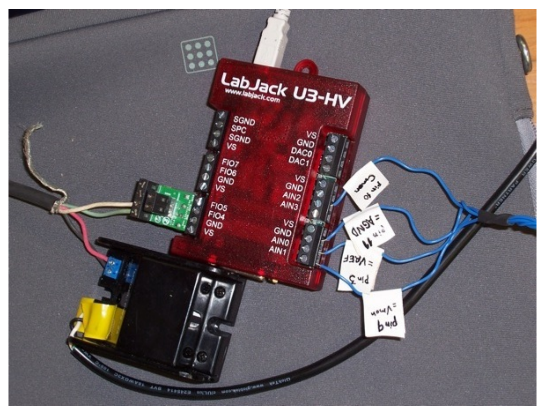

(c)

(d)

Figure 32: Elements of the TCTD electronic and computer setup. a) Components on the instrument bench, b) oscilloscope monitor trace, c) A/D connections, and d) dual-computer software display.

transformer to convert standard 120 V supply voltage to the 24 V supply voltage required by the tensiometer's little electronic interface; so two of the four conductors power the interface, and the other two carry the data. A LabView application written by Tim Wen (APL-UW) (Fig. 12) recorded and displayed the outputs of these A/D monitors, but unfortunately there was strong and unsolved radio interference from the TCTD deck unit into the A/D, even across the lab room, rendering the tension and power supply monitoring data essentially useless. Ultimately tension monitoring was a combination of the backup tensiometer and the fact that our tow speed remained quite low due to the other problems with the system, and power supply monitoring was recorded by hand in operation notes.

Lastly, Fig. 32d shows the use of the dual-computer arrangement during acquisition. One computer (TCTDrec, on left) ran the acquisition software, which had limited ability to show the recorded data graphically and list numerical values. There were, in fact, two versions of this software, one for DOS via RS232 and one for WindowsXP via USB, but the deck unit USB circuitry was extremely unstable, forcing the use of the DOS/RS232 version. The acquisition software writes the data simultaneously to the acquisition computer locally and over the network to the second computer, allowing further visualization and analysis during the potentially days-long acquisition. The second computer (TCTDvis, on right) had Matlab installed and a GUI-based Matlab application written by Linda Buck (APL-UW) to allow the user to produce various types of pre-planned plots from the streaming data, in additional to other analyses via Matlab.

6.1.3 History and Technical Problems

In spite of an appealing and conceptually clever design, there have been many problems with the TCTD system since it was shipped to APL-UW before the 2009 cruise, and the system has officially failed its acceptance test. Still in progress is analysis to determine if the limited data obtained are useful scientifically, because besides the limited spatial and temporal coverage, there are also some nontrivial calibration problems. Though this report is on the 2010 cruise, the system has failed its acceptance test and we have been learning the nature of the problems over the past two years (which may be useful in analyzing the limited dataset), so occasional references to things previous to the 2010 cruise are mentioned here for clarification. A brief history of APL-UW researchers' experience with the instrument follows. More may be found on Andrew Ganse's TCTD website [17].

- **2006.** Eighteen fins (addr #1-#18) from Penn State University were combined with 32 newer fins (addr #19-#50) for use on a 50-fin, 75-m-long seacable for the SW06 experiment. This small version of the instrument worked, in the sense of having data returned from all fins, although the data were somewhat noisy. These 50 fins are referred to collectively as the "old" fins.

- **October 2008.** Arrival of new large NPAL towed CTD chain at APL-UW. Fifty additional fins (the "new" fins, addr #101-#150) were ordered so that altogether 100 fins could be placed along the new 800-m cable. The manual was lacking in detail and instructions for use, and information from our communications with ASD/ADM was limited, making it difficult to know what was needed to run and test the system.

- **November–December 2008.** Bench testing and wet testing in UW oceanography saltwater test pool of fins on 150-m cable. Whether wet in pool or spread out dry on the floor, very few sensor fins could be pulled up online, even with assistance (via email) from ASD/ADM/Sellschopp.

- **January 2009.** Puget Sound test on R/V *Robertson* with all sensor fins on 150-m cable. An almost immediate system failure ended the test. It was later found to be due to ADM's lack of heatsinking the termination resistor in the lower electrode, causing a poorly made solder connection to melt and disconnect. (This did not happen in pool tests presumably because the cable had to be looped to fit the pool, adding a very large inductive load that greatly reduced the power going into resistor given the same input from the DC supply.)

- **January–February 2009.** Bench testing and wet testing in UW oceanography saltwater test pool yielded little improvement even with input from ASD/ADM/Sellschopp.

- **February–March 2009.** Assembly of the 800-m tow cable with 88 sensor fins and fairings (32000 screws!) down the whole cable length took six staff one week of full time. The confusing results of the bench and pool tests (i.e., no clear patterns of which fins worked) were used to determine the mixed order of the fins on the 800-m cable, trying to spread the seemingly more reliable fins over the cable length, and spread old and new fins somewhat equally over the cable length. Twelve of the 50 old fins had been determined "dead" by Penn State researchers who used them previously, and these were sent by PSU to ADM for analysis and were not available by the time of assembly to add to the cable. Thus instead of the originally planned 100 fins, only 88 were placed on the cable, leaving out every other fin at the top end of the cable.

- **April 2009.** Sellschopp accompanied us in the PhilSea09 cruise, but even he was not able to get the system working, neither with the deck unit nor with the backup he brought. The TCTD system failed its acceptance test. Its best performance was at the beginning of the cruise with 60–65% of sensor fins online; it degraded from there. Sellschopp signed a document authored by the science party that lists all the problems with the instrument, including the obvious lack of system testing before delivery. With him on board we learned a lot more about how the system works and how to use it. The powered reel worked well; the reel itself was fabricated and sold by ADM but APL-UW (Fred Karig) designed and added the powered drive. The chute (also fabricated at APL-UW) broke during use in rough seas, and the cable slipped off the chute and was gashed many times. The connection to the upper termination was weak and disconnected repeatedly, preventing cable operation until recovery of the upper termination and reconnection.

- **May–October 2009.** During a period of more wet testing at UW oceanography saltwater test pool, Sellschopp sent new firmware and minor circuit change instructions to allow several different power-pulse frequencies to be produced by the deck unit. ASD/ADM sent a new deck unit with a transformer with different winding to send more current down the seacable. Different termination resistors were tried. Greater power supplies were tried. Clamp-on current meter measurements were made to explore the possibility of electrical standing waves. None of the hardware changes helped, and evidence contradicted the standing wave hypothesis.

- **November–December 2009.** During dry testing at Sand Point and NOAA, 60–70% of fins worked in the best case. The hardware changes tried in May–October 2009 were tried dry here, with no improvement.

- **January 2010.** A Puget Sound test deployment included an end-to-end electrical test with the new armored coax cable and fish-plate/electrode connections. A meticulous meter-by-meter check of cable-jacket integrity was done via an electrical insulation tester as the cable was gradually deployed into the salt water, and previously unseen cable faults from the 2009 cruise were repaired. At best, data were obtained from 40% of sensors. The various hardware variations were tried again, including a large power supply as strongly recommended by Sellschopp, but with no improvement.

- **May 2010.** For the PhilSea10 cruise a new, much stronger mechanical arrangement at upper termination was used. The tow cable is now armored coax, serving as both tow and electrical cable. All upper termination electrical connections are on a strong steel "fish-plate," with a specially designed weak link to release the tow cable from the float/seacable in the case of an over-tension event. Instead of a chute, a specially designed, very large block was used, similar to but larger than previously used in SW06, to better protect fins via radius of curvature. Deployment and recovery went quickly and flawlessly, aided by the perfect weather. Sixty percent of sensor fins were brought online at the beginning of the cruise (presumably the meticulous checks and repairs on Puget Sound returned the cable to its state at the beginning of the 2009 cruise). However, in the ensuing hours and days, that percentage of sensors online dropped to as low as 20%. During recoveries and deployments seawater was seen squirting out of the seacable, and it seemed likely that the gradual reduction in fin percentage was due to water gradually seeping into the cable and improving the electrical connection with the surrounding seawater ground. The various hardware variations discussed above were tried again with no improvement. At the end of the cruise, the cable was cut to two shorter lengths, but even a 320-m cable could not bring all its sensors online. Correlating all these tests showed that there is a set of fins that do not respond in any test, but there are others that do not fit any clear performance/failure pattern from test to test.

- **June 2010.** For Ren-Chieh Lien's short, follow-on test cruise, a completely new seacable was reassembled on the pier in just a few days. Alas, a 60% response was obtained at the beginning of cruise, but it dropped to around 20%, presumably due to seawater seeping into small cable faults again.

For future communications with the manufacturer, it is helpful to know the hierarchy of people and businesses who design, manufacture, and sell the TCTD. There are several companies involved, but the people all know each other and communicate regularly. The TCTD system was sold to APL-UW by ASD Sensortechnik GmbH (Germany), originally run by René Heise and now by his daughter Stephanie Heise; ASD is only a technical sales/marketing company with the Heises as the sole employees. The system was manufactured by ADM Elektronik (Analoge und Digitale Meßsysteme-Elektronik), which appears to have a very close connection with ASD. When we had technical requests, René Heise would instruct the ADM technician, Mr. Haushahn, to fix or manufacture something. We currently know of no other employees of ADM. Lastly there is Dr. Jürgen Sellschopp, who is the original designer of the TCTD . He is now retired from FWG Kiel (similar to our NRL) but spent some time at SACLANTCEN where he made numerous connections with U.S. and European Union underwater acoustics research communities, and he still continues incremental development of this system. FWG policy prevented direct production/sales of the instrument to outside entities, so separate sales and manufacturing companies (ASD and ADM) had to be created. But Sellschopp is the scientific and engineering source of the system; all technical designs and decisions come to him, and he accompanied us on our PhilSea09 cruise.

The exact technical problems are still not understood, even after one and one-half years of engineering analysis, testing, and implemention of equipment revisions suggested by ADM and Sellschopp. There are two primary problems, both of which have no satisfactory explanation. First, response is missing from at least 40% of the sensor fins even when the cable is run dry, stretched out straight on a runway. Second, concerns remain about the calibration and addressing of the sensor fins. They are not only out of calibration, which might be remedied by factory re-calibration, but we observed unexplained time changes in the calibrations of the pressure and temperature sensors of one fin that was compared against a collocated Seabird SBE37 MicroCAT CTD mounted on the seacable. There are also a number of instances of sensor fins responding on addresses of other fins, in ways that cannot be currently predicted, which means that it is not possible to know which pressures go with which temperature and conductivity measurements. (Perhaps some kind of cross-correlation based analysis might be useful to solve this problem if interest in gaining those parts of the data were enough to justify the effort.)

One of the main troubling symptoms of the TCTD is that many fins do not respond. However, they are not always the same fins; some that appear dead for some time suddenly work in another arrangement. Fig. 33 shows that the pressure sensors responded consistently less reliably than the temperature and conductivity sensors, regardless of whether or not the data were accurate. Plotted at top are raw temperature data (missing data are the dark blue background) for each sensor over sample number. Results from five different tests are concatenated on the sample number axis; Table 12 defines each segment of data based on sample number. Plotted on the bottom are percentages of non-missing data for the temperature, conductivity, and pressure sensors for the same data segments referenced in the upper plot. Thus the green temperature curve in the bottom plot is computed from the columns of the matrix in the top plot.

The maximum performance ever achieved (approximately 60% of sensor fins responding) was at the beginning of the 2009 cruise before the cable was first gashed in a deployment snafu, and about the same when laid out dry on a NOAA runway (Table 12). This percentage was not obtained again in PhilSea10, though 55% was obtained for a short time at the beginning of the first tow, perhaps because the cable interior was driest. In this plot of raw on/off fin response (ignoring whether fin data is accurate) that the pressure sensors consistently responded less reliably than the temperature and conductivity sensors.

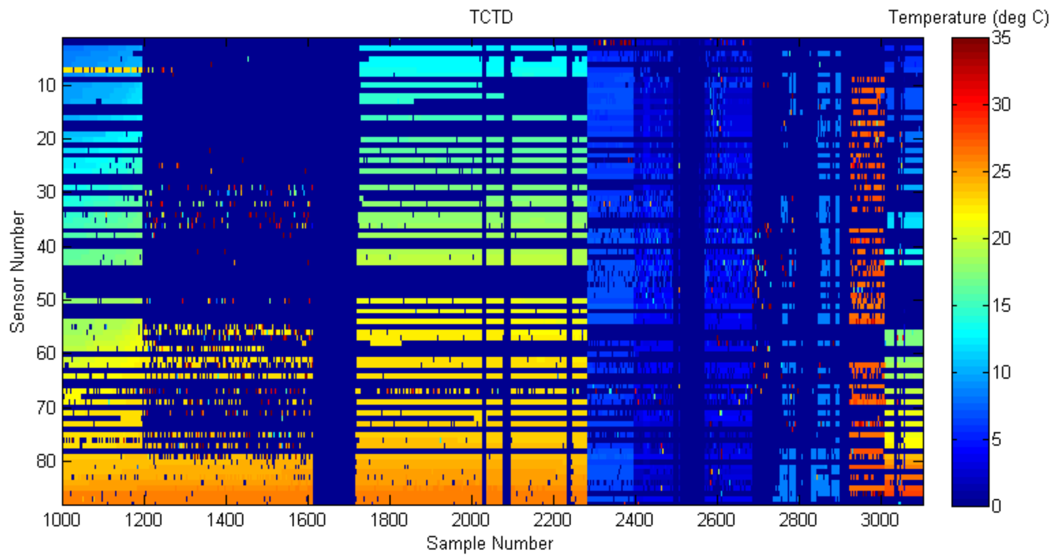

(a)

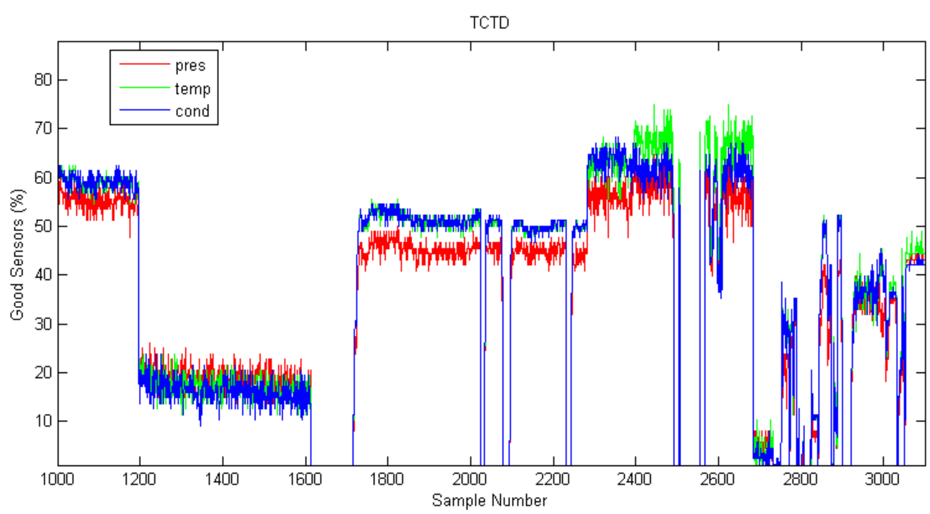

(b)

Figure 33: Comparison of TCTD sensor response over various tests and tows in 2009 and 2010. Plotted on top are raw temperature data (missing data are the dark blue background) for each sensor over sample number. Results from five different tests are concatenated on the sample number axis; Table 12 defines each segment of data based on sample number. Plotted on the bottom are percentages of non-missing data for the temperature, conductivity, and pressure sensors for the same data segments referenced in the upper plot. So the green temperature curve in the bottom plot is computed from the columns of the temperature matrix in the top plot.

Samp # range in Fig. 33 plots	Data filename	Note
1000-1200	RUN4-25A.DAT	PhilSea09 beginning of tow1, new deck unit
1200-1600	(same file/tow)	new deck unit blew out at sample 1200 so limited power after that
1700-2300	(same file/tow)	now using old APL-UW deck unit
2300-2700	DEC22H.DAT	testing DRY laid out on runway at NOAA in December (cold day!)
2700-2900	JAN27J.DAT	January test in Puget Sound
2900-3000	10051017.D26	PhilSea10 test DRY on reel before first deployment (hot day!)
3000-3010	10051120.D20	PhilSea10 beginning of tow1

Table 12: Breakdown of data comparison segments in the plots in Fig. 33.

At each time sample, a quadratic curve with respect to down-cable position was fitted to all measured pressure data, including TCTD and SBE37s, but strongly weighted toward the SBE37s (middle and end of cable) as well as zero pressure at the top of cable. Fig. 34 shows an example of such a fit at one time sample when a relatively high number of pressure sensors responded. While the quadratic fit appears appropriate for all times in the tow, notice in Fig. 34 that many TCTD fin pressure sensors are out of calibration — they are very consistent in their offset from the quadratic cable shape over all times. In this profile, fin pressures by functioning but out-of-calibration sensors are off by as much as 15 dBar (the sensors themselves are specified with an accuracy of 0.5 dBar). In contrast, the two sensors reading 0 dBar and the one reading more than 600 dBar near the top of the cable were that far off the whole tow and were considered malfunctioning (temperature and/or conductivity sensors may have been functional for those fins). These offsets for the functioning, but out of calibration, sensors are correctable by re-estimating the pressure calibration coefficients for the fins using the SBE37-based fit. These new calibration coefficients are then more reliable when less SBE37 coverage is available, such as in tow #1 or in the 2009 data.

Sensor accuracy was explored in a limited sense by comparing readings from one TCTD fin (#30, mid-cable, 41st from bottom), to those of a SBE37 CTD mounted adjacent to it (within 50 cm) on the seacable. The pressure and temperature values were compared directly between these collocated sensors by analyzing patterns in their difference. The conductivity sensor on that fin did not respond, so comparisons to conductivity measurements on nearby fins were made. In this limited comparison, we saw that the noise levels for the sensors matched their specified values in the manual, as evaluated in Table 13. A constant offset in these instrument difference values could be explained by instruments being slightly out of calibration. However, the pattern in both the pressure and temperature differences is a time-varying offset, which has no immediate explanation and thus could be problematic in analysis. The main change in the pressure differences is the shift in pressure difference between the collocated sensors when the ship sped up from 1 to 2.5 kt at about 15:00. Note there also appears some drift in the difference. A second concern is the spontaneously changing bias in the fin's temperature reading. Fig. 35 plots the differences between sensors of fin #30 and those of the collocated SBE37 CTD. Because the conductivity sensor of fin #30 did not respond at all, the conductivity plot shows the variations from mean difference between the CTD and the closest three fins with available conductivity data (fins are 8 m apart on cable), in hopes of at least some kind of comparison with the CTD. Conductivity differences are shown for fin #123 (36th from bottom), fin #121 (38th from bottom), and fin #26 (47th from bottom), not all of which reported data the whole time. (Note the fins were not in numerical address order on the cable.) The shifts in bias of the pressure and temperature sensors do not appear to correspond to any changes in instrument settings or values of the sensor readings, the latter of which can be seen in Fig. 36 along with the conductivity readings of the same nearby fins. The calibration errors for the sensors can also be seen in Fig. 36. Although the CTD was mounted just 50 cm away from fin #30, the pressure difference is consistently about 4 dBar and the temperature difference is about 0.2°C.

The sensor accuracies stated in the manual were compared to standard deviations of these differences at a few locations in the time series (Table 13). Four time ranges were chosen over the span of the tow to consider segments of distinct characters in tow #2 (Fig. 35). In contrast to the subtracted means used to plot the conductivity difference curves in Fig. 35, the means subtracted in computing the standard deviations in this table are over the 100 samples in the sample population. The standard deviations for the pressure and temperature differences are remarkably close to the specifications listed in the manual. Given that conductivity data were not available on fin #30, conductivity standard deviations are with respect to more distant fins, the standard deviations for conductivity should not be expected to be as small as the specifications. Yet, not only are they close, but as the sample size N is reduced (effectively reducing trend difference between the sensors because the means are subtracted), the standard deviations for conductivity converge to the manual's specification.

While there were numerous problems with the system that caused many sensors to drop out, based on these comparisons for just a few sensors we have some idea of the limitations of the sensors in the TCTD: DC calibration offsets, spontaneous changes in those offsets, and yet sensor noise that otherwise matches the specified values.

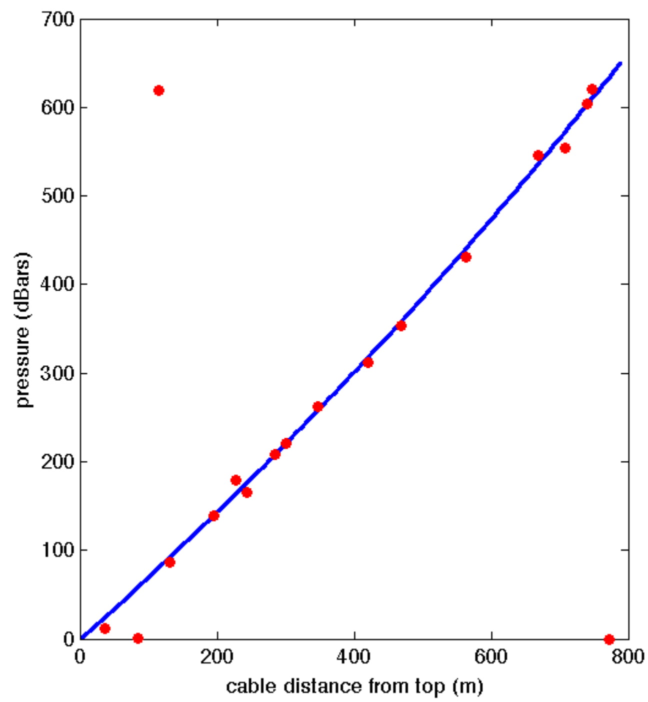

Figure 34: An example of TCTD pressure measurements compared to quadratic cable shape, at a time of a relatively high percentage of fins responding.

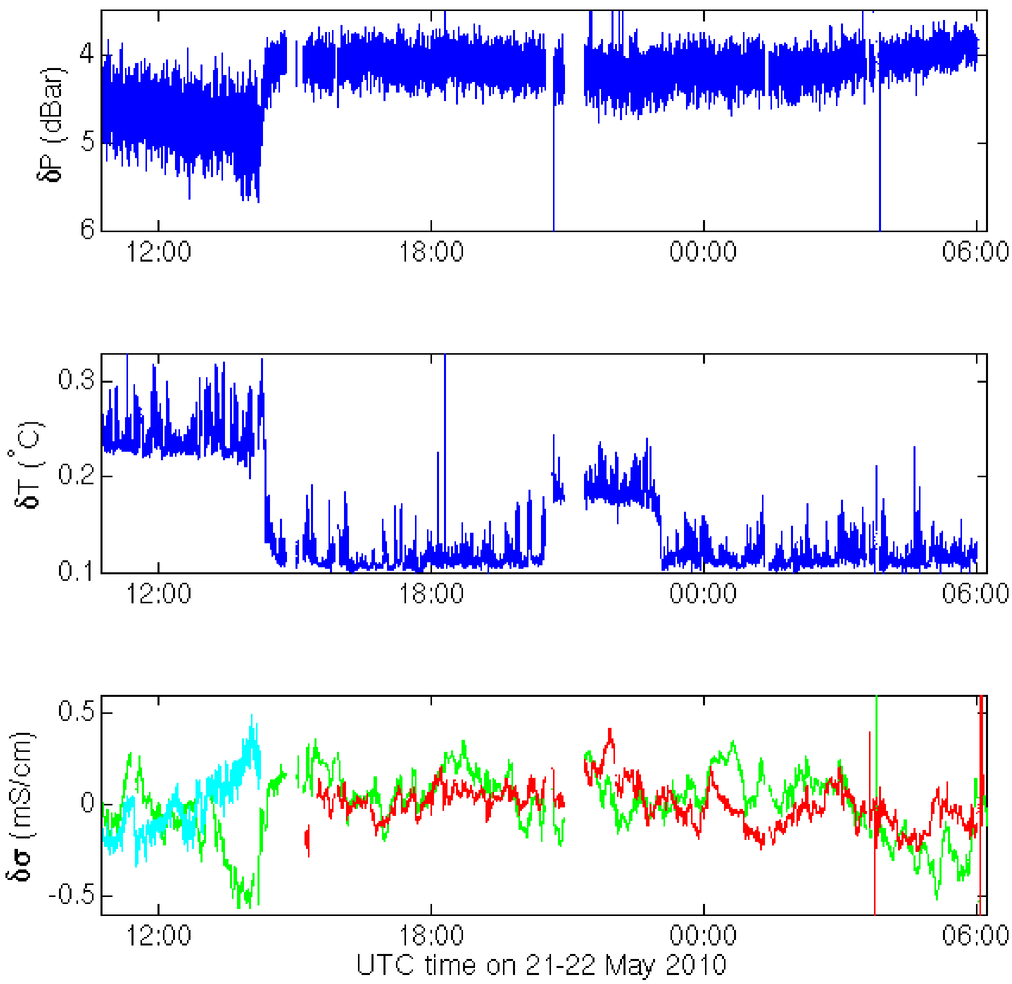

Figure 35: Differences between sensors of fin #30 (mid-cable, 41st from bottom) and those of the SBE37 CTD mounted 50 cm above it, shown in blue (pressure in top plot and temperature in middle plot). Conductivity data were missing from fin #30, so bottom plot shows differences between nearest fins with available conductivity data and the SBE37. Fin #123 (36th from bottom) in cyan, fin #121 (38th from bottom) in red, and fin #26 (47th from bottom) in green. Note that fins #36 and #38 each only had data for part of the time, with endpoints roughly around 15:00.

Time at 1st sample	Which sensors	Stdev(diff-mean) , N=100	Spec
21 May, 12:00	$\text{pres}_{SBE37} - \text{pres}_{41stfin}$	0.19 dBar	0.5 dBar
(initial deep/slow	$\text{temp}_{SBE37} - \text{temp}_{41stfin}$	0.01 $°C$	0.01 $°C$
segment)	$\text{cond}_{SBE37} - \text{cond}_{36thfin}$	0.03 mS/cm	0.01 mS/cm
	$\text{cond}_{SBE37} - \text{cond}_{47thfin}$	0.03 mS/cm	0.01 mS/cm
21 May, 17:00	$\text{pres}_{SBE37} - \text{pres}_{41stfin}$	0.13 dBar	0.5 dBar
(seemingly quiescent	$\text{temp}_{SBE37} - \text{temp}_{41stfin}$	0.01 $°C$	0.01 $°C$
period during least	$\text{cond}_{SBE37} - \text{cond}_{38thfin}$	0.01 mS/cm	0.01 mS/cm
temperature sensor bias)	$\text{cond}_{SBE37} - \text{cond}_{47thfin}$	0.04 mS/cm	0.01 mS/cm
21 May, 22:00	$\text{pres}_{SBE37} - \text{pres}_{41stfin}$	0.17 dBar	0.5 dBar
(during period of	$\text{temp}_{SBE37} - \text{temp}_{41stfin}$	0.01 $°C$	0.01 $°C$
increased temperature	$\text{cond}_{SBE37} - \text{cond}_{38thfin}$	0.05 mS/cm	0.01 mS/cm
bias)	$\text{cond}_{SBE37} - \text{cond}_{47thfin}$	0.05 mS/cm	0.01 mS/cm
22 May, 05:00	$\text{pres}_{SBE37} - \text{pres}_{41stfin}$	0.09 dBar	0.5 dBar
(very end, during period	$\text{temp}_{SBE37} - \text{temp}_{41stfin}$	0.01 $°C$	0.01 $°C$
of apparent decreased	$\text{cond}_{SBE37} - \text{cond}_{38thfin}$	0.03 mS/cm	0.01 mS/cm
pressure variation)	$\text{cond}_{SBE37} - \text{cond}_{47thfin}$	0.03 mS/cm	0.01 mS/cm

Table 13: Field evaluation of sensor uncertainties based on comparisons to collocated SBE37 CTD, with reference to the sensor specifications listed in the TCTD manual. These are the same sensor fins referred to in Figs. 35 and 36. The four time ranges are in segments of different character in tow #2 (Fig. 35).

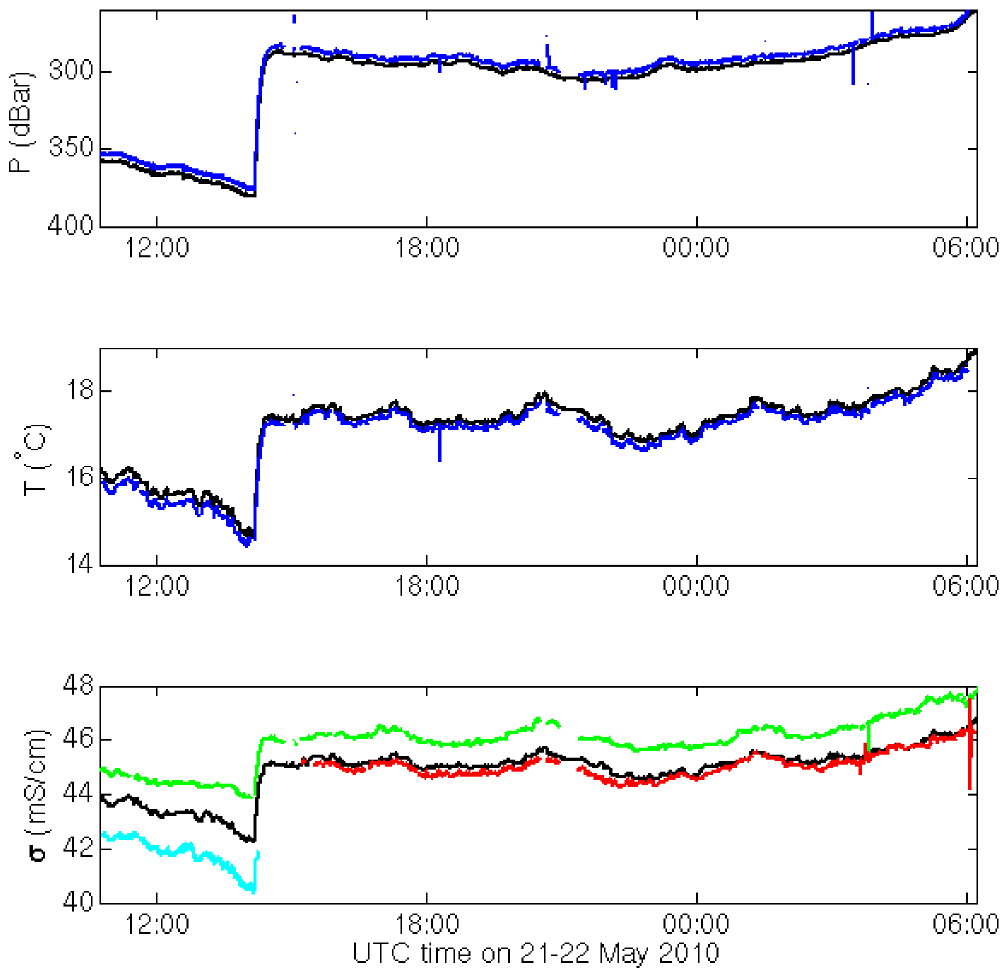

Figure 36: Co-plotted comparisons of sensors of fin #30 (mid-cable) and those of the SBE37 CTD mounted 50 cm above it. In all three plots: black = SBE37 CTD (ser#397), blue = fin #30 (41st from bottom), cyan = fin #123 (36th from bottom), red = fin #121 (38th from bottom), green = fin #26 (47th from bottom). Fins #123, 121, and 26 are shown because the conductivity sensor of fin #30 did not respond, and these three are the nearest three with available conductivity data (fins are 8 m apart on cable).

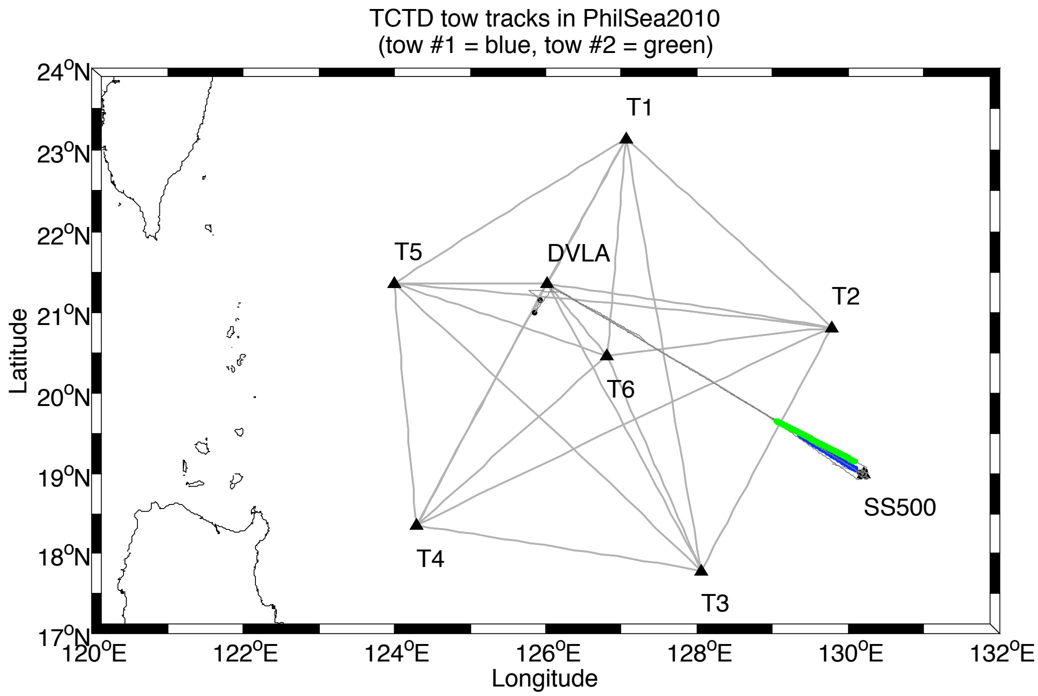

Figure 37: The locations of TCTD tows 1 and 2 in the PhilSea10 Experiment. The two tows are roughly collocated, but they are separated in time by eight days. The first tow (blue) was 93 km for about 39 hr and the second tow (green) was 124 km for about 30 hr.

Tow Endpoint	Lat	Lon	Date/Time UTC
tow #1 begin	19° 03.079651′ N	130° 06.483234′ E	2010-05-11 Z 15:00:00
tow #1 end	19° 29.335061′ N	129° 21.339935′ E	2010-05-13 Z 06:00:00
tow #2 begin	19° 09.272539′ N	130° 05.492690′ E	2010-05-21 Z 07:30:00
tow #2 end	19° 39.945547′ N	129° 02.846721′ E	2010-05-22 Z 13:00:00

Table 14: Endpoints of the straight-line (geodesic) TCTD tows in PhilSea10.

6.1.4 Data Products and Results

In spite of the aforementioned technical difficulties, measurements at sampling periods of 3–5 s were obtained in two main tows in this cruise, with one to three dozen sensors distributed over 700 m depth. The first tow was 93 km for about 39 hours and the second tow was 124 km for about 30 hours. These tows were along approximately the same segment of the track between the DVLA and SS500 (Fig. 37 and Table 14), separated in time by about eight days. Note that during those eight days, a sequence of CTD casts were made along that same track.

A SBE37 CTD (ser#399) was mounted at the bottom of the cable (and additionally –

ser#397 – in the middle of the cable in the second tow) to improve cable modeling, as the temperature and conductivity measurements were more reliable than pressure measurements. These CTDs proved vital in the estimation of the pressures at the sensor locations, as the pressures measured by the TCTD fins themselves were fraught with problems.

The data of tow #1 require more effort to clean than those of tow #2, for in tow #1 we used the fin-power monitoring capability of the system. In this mode, diagnostic fin-power data replace the environmental data. Unfortunately, the diagnostic data are transmitted in the same bytes reserved for the environmental data, and are not flagged to automatically distinguish when one or the other are being transmitted. The diagnostic data had been recorded frequently in this tow and are the source of much (but not all) of the extraneous scatter in the tow #1 plots of temperature and conductivity (Fig. 38), as well as the cause of the red band between 300 and 400 dBar (Fig. 38b). Further processing should be able to remove this extraneous noise with some “elbow grease” or cleverness. One option used in tow #1 was to record the diagnostic data such that it filled the environmental data bytes every Nth sample. This feature was turned off and on a number of times, reseting the position of the Nth sample pattern, and also the N value was not always the same. Meanwhile, in spite of the extra scatter, the plots in Fig. 38 show an overview of what data coverage is available in tow #1 — the data in these plots were cleaned manually, just enough to show the structure of the tow; more rigorous cleaning methods should be used for actual analysis.

The focus of this report’s analysis is on tow #2. The plots in Fig. 39 show the result of extensive cleaning of problematic data segments, and then identifying scattered values that are greater than two sigma away from the mean curve for a sensor. Note that the conductivity sensors failed much more often than the temperature sensors, a limiting factor for calculating sound speed. The pressure data measured by the TCTD sensors were of poor quality, so for each individual time sample the pressure profile (importantly including data from SBE37 CTDs) was fitted with a quadratic curve and missing pressure readings were interpolated along that curve, then combined with the originally measured temperatures and conductivities. The large “jump” feature at about 14:30 on 21 May is when the ship speed was increased from approximately 1 kt speed-over-ground to approximately 2.5 kt speed-over-ground, which caused the seacable to rise in the water column. The more subtle “waviness” of the pressure curves is similarly due to variability in ship speed over time.

Percentages of TCTD sensors responding over the course of the tows are shown in Fig. 40. Fig. 40a shows the raw on/off response of fins in tow #1, ignoring whether sensor data were good quality. Notice that the highest percentage of fins obtained in either tow was at the very beginning of tow #1. Presumably the cable was dry to begin, and gradually water entered the cable through small faults and thus improved the electrical connection with the seawater. Fig. 40b shows the raw on/off response of fins in tow #2, ignoring whether sensor data were good quality; Fig. 40c was computed after the processing described for Fig. 39 resulting in usable data from each sensor. In terms of raw on/off response, the temperature and conductivity sensors responded approximately equally and the pressure

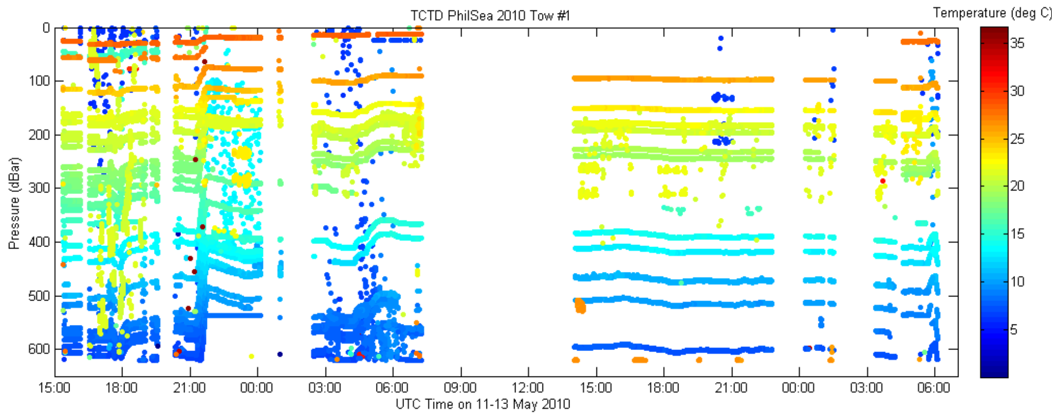

(a)

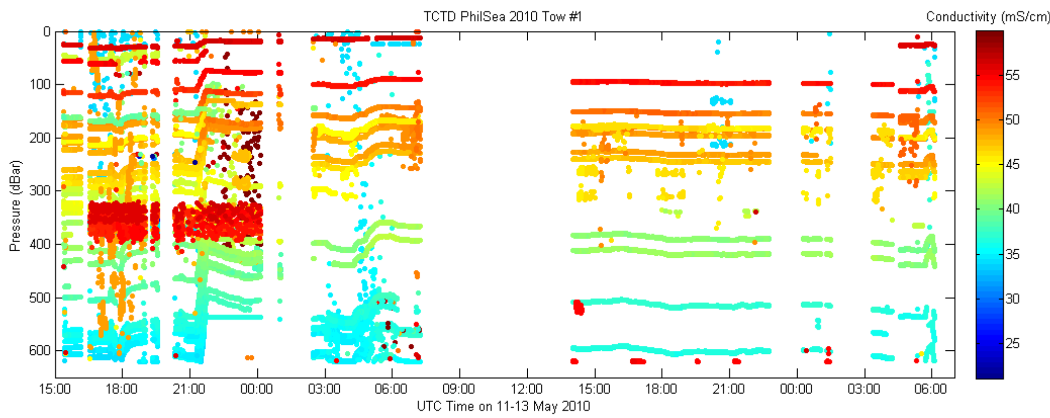

(b)

Figure 38: Measured temperatures and conductivities of PhilSea10 tow #1 (partially cleaned).

sensors performed much worse. After processing to determine usable data, temperature sensor response decreased slightly (i.e., most temperature data on responding fins were good) and the conductivity sensors had very poor performance — about half that of the temperature sensors. The pressure response result shown is the same in (b) and (c) to aid comparison. Because the pressure data were processed heavily and superceded by the SBE37 CTD data, the actual response for pressure sensors in (c) would be effectively 100%.

Fig. 41 shows preliminary results for 2-D slices of temperature, conductivity, and sound speed perturbations from background mean profiles, based on the collocated temperature and conductivity measurements. The fins with successful conductivity measurements are a subset (about half the size) of those with successful temperature measurements. So the interpolation between sensors is heavy, which suggests some caution in the interpretation of feature scale sizes and shapes in these plots. Still, it appears clear there is a broad region of higher sound speed and possibly bimodal depth structure that was transited from 06:00

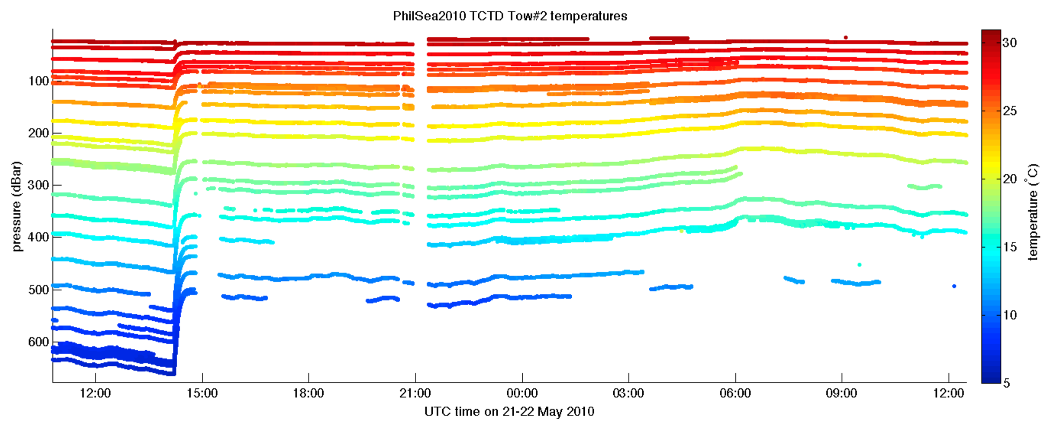

(a)

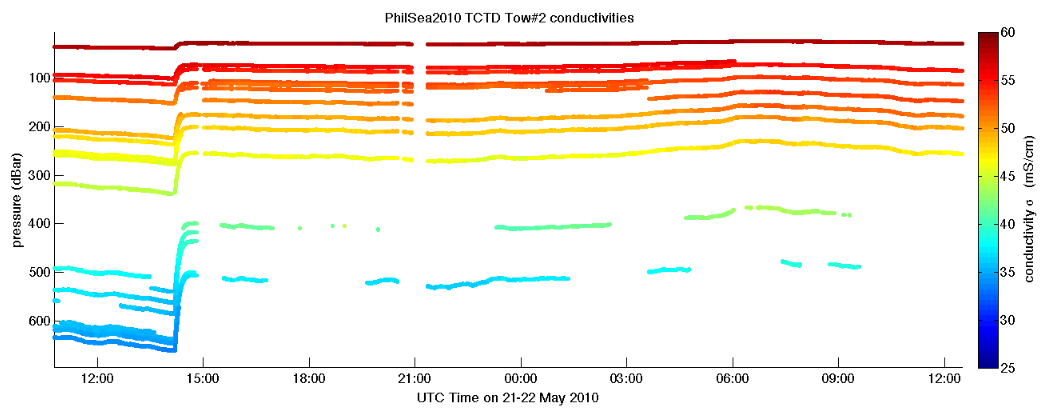

(b)

Figure 39: Measured temperatures and conductivities of PhilSea10 tow #2 (fully cleaned).

to past 12:00, and a warm blob around 21:00. Some similar broad-scale features appear to exist in the respective locations in the CTD dataset measured between the two TCTD tows.

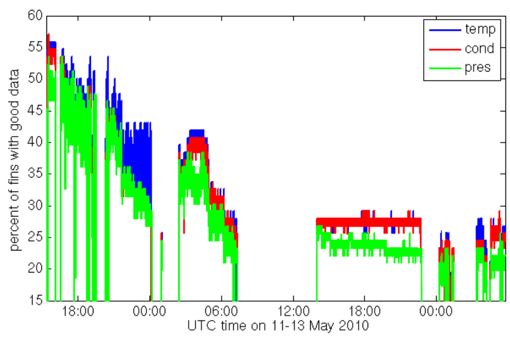

(a)

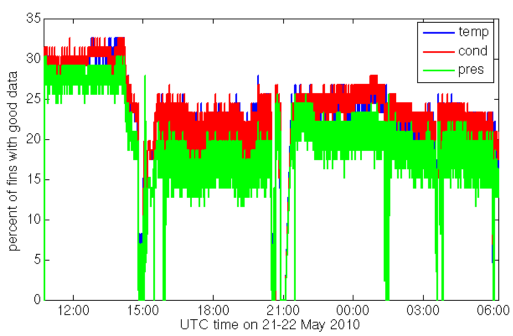

(b)

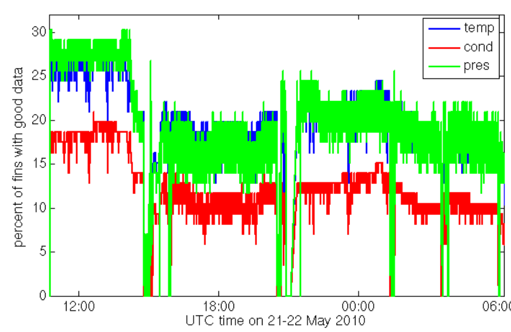

(c)

Figure 40: Percentages of responding TCTD fins over time in (a) tow #1 and (b-c) #2. a) Raw on/off response of fins in tow #1, ignoring whether sensor data were good/usable. b) Raw on/off response of fins in tow #2, ignoring whether sensor data were good/usable. c) Computed after the processing described for Fig. 39 resulting in usable data from each sensor.

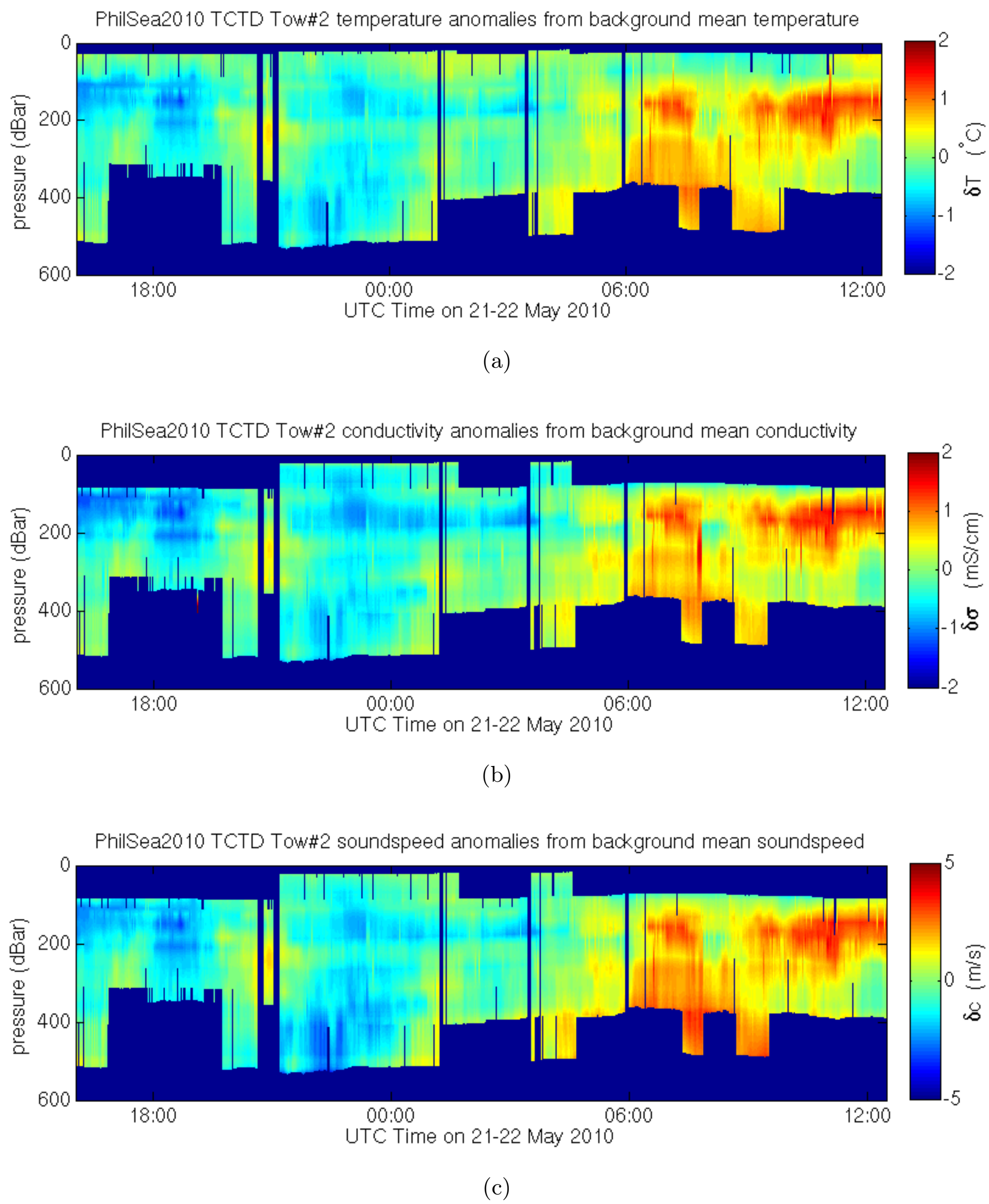

Figure 41: Preliminary results for anomalies from background mean temperature, conductivity, and sound speed in tow #2.

6.2 Ship Instrumentation

The R/V *Roger Revelle* has a Seabird SBE-911plus CTD, two acoustic current profilers, a Bell BGM-3 gravimeter, a Kongsberg EM122 multibeam echosounder, a Knudsen 320 B/R subbottom profiler, a suite of meteorological sensors, a gyrocompass, a Doppler knotmeter and three GPS receivers. All data logged from these instruments were obtained by APL-UW. The following sections provide some examples of these datasets.

6.2.1 CTD Casts

Over the entire cruise, 54 casts were made with the ship's Seabird SBE 911plus. A list of downcast files (processed according to the prescription described below in this section) is provided in Appendix B.

We detected a problem with the instrument on cast RR1006_001, and subsequently the primary sensor was found to be faulty and was replaced. Cast RR1006_001a is the next cast, same place, and both sensors were deemed to be functioning properly. Note that the primary sensor (the one that was replaced) was also the primary sensor on the previous cruise, RR1005 (P. Worcester, Chief Scientist) and therefore all those casts should be inspected. (And probably the casts on the cruise before that, RR1004, with Chief Scientist R.-C. Lien.)

From 15 to 21 May, the R/V *Roger Revelle* took a CTD section along the nominal acoustic propagation path between SS500 and the DVLA. Casts were made about every 10 km to 1500 m. Every fifth cast was to within several hundred meters of the bottom, roughly 5000–6000 m, depending on location. This section involved 51 casts. The temperature, salinity, and sound speed sections (as computed or derived under the processing prescription described below in this section) are shown in Fig. 42. Difference plots of these quantities versus May climatologies from WOA2005 [18] and GDEM-V [19] are shown in Figs. 43 and 44, respectively.

It was requested by the sponsor that the ship's CTD casts be forwarded to NAVOCEANO. (The data will be sent to NAVOCEANO at a future date.) This requirement has consequences that originate at the processing of the raw Seabird cast data. Processing CTD data and sending it to NAVOCEANO is a detailed and complex operation.

NAVOCEANO takes in CTD data two ways: near-real-time and later. In the near-real-time operation, the sound speed profile is compressed into an email message and sent to NAVOCEANO, where it is assimilated once daily in their forecasting program. When the CTD data becomes older than (approximately) this near-real-time window (i.e., at the end of the cruise), they are used in the NAVOCEANO historical database.

In both cases, the CTD data must be reformatted. NAVOCEANO provides a program `SVPG.exe` to do this. A zip file called `svpg_setup.zip` containing the program and some

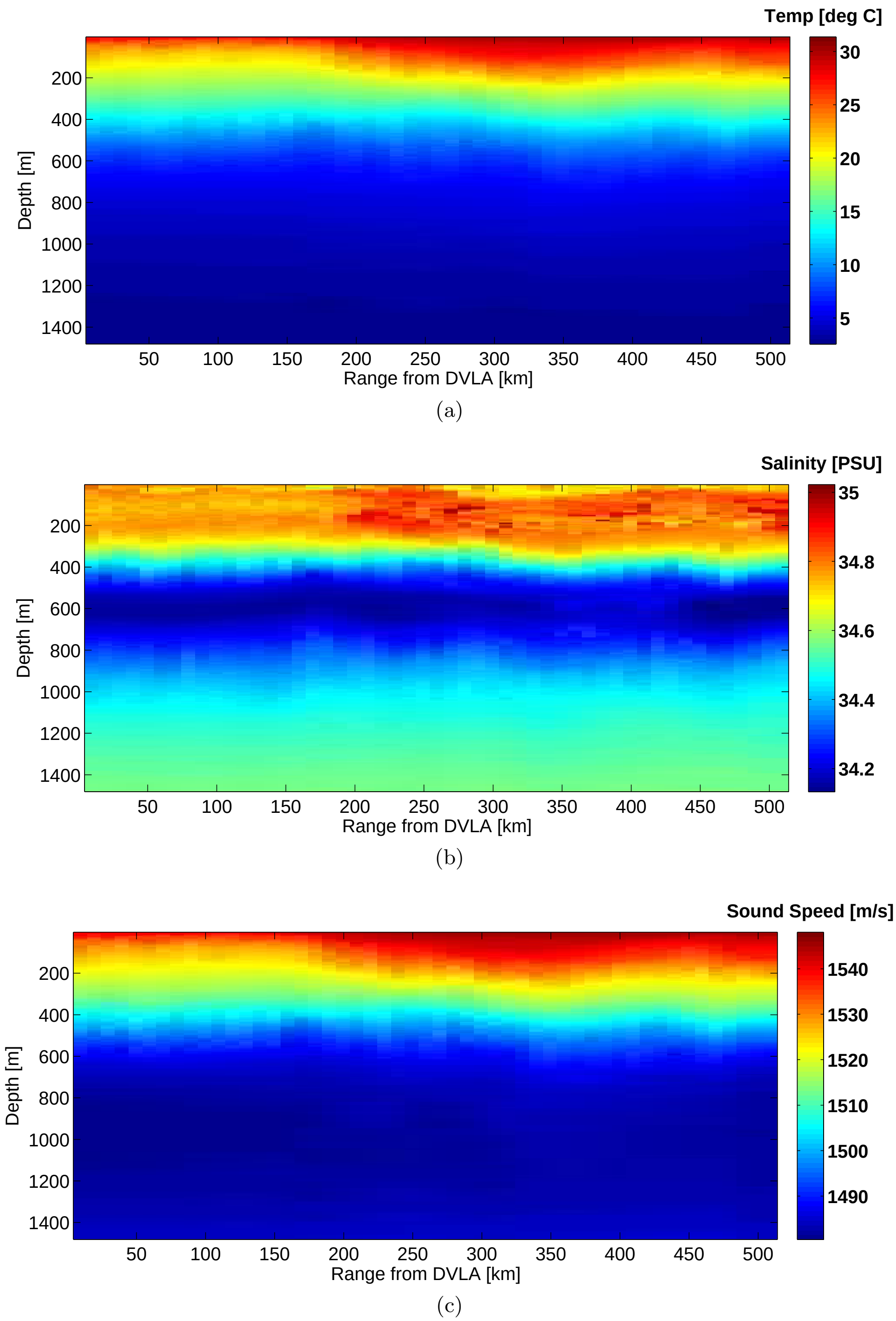

Figure 42: Oceanographic section along the DVLA – SS500 path. Top: temperature. Middle: salinity. Bottom: sound speed.

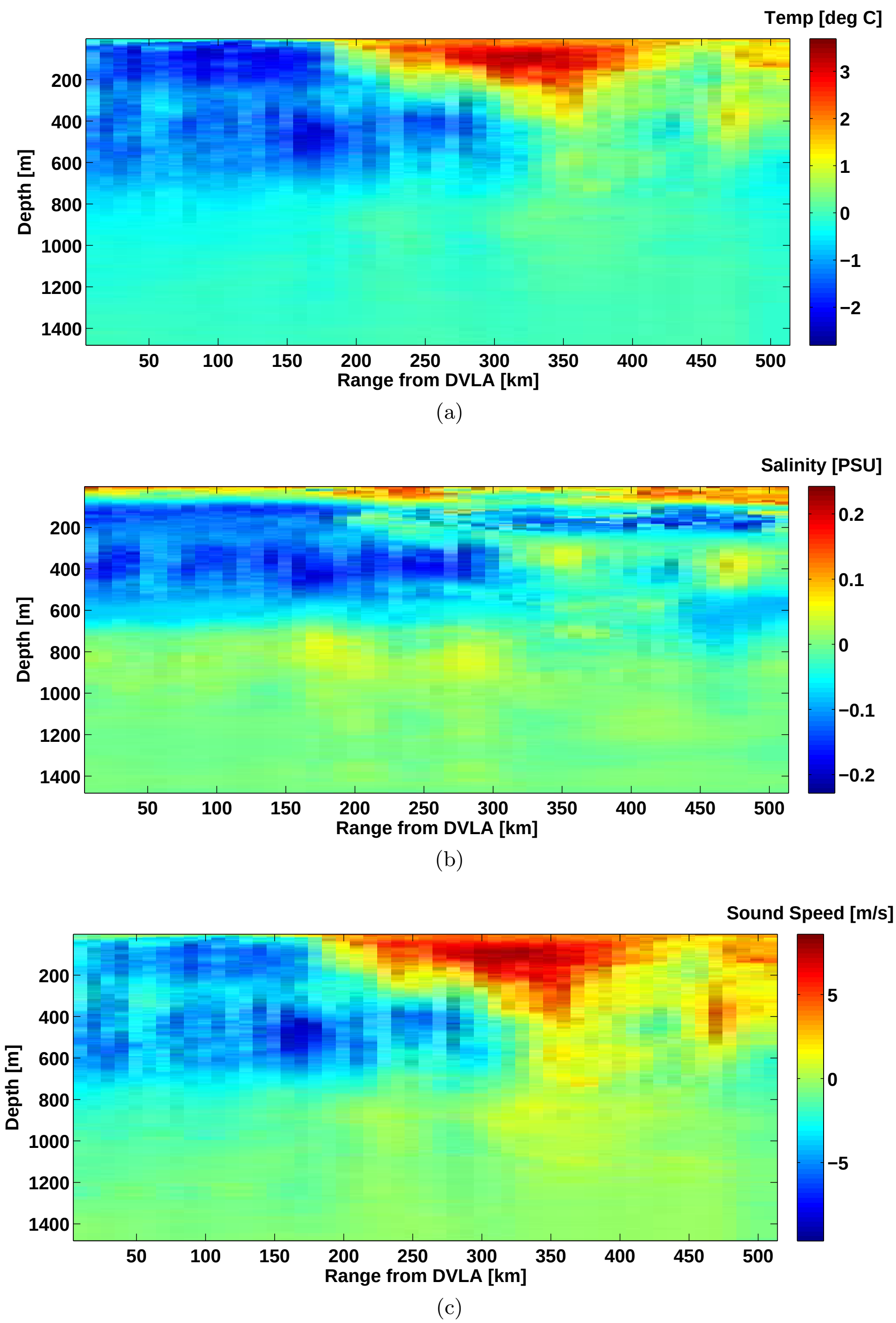

Figure 43: Section difference, Seabird value minus May WOA2005 value. Top: temperature. Middle: salinity. Bottom: sound speed. Pressure and sound speed computed using the CSIRO Seawater Toolkit [20].

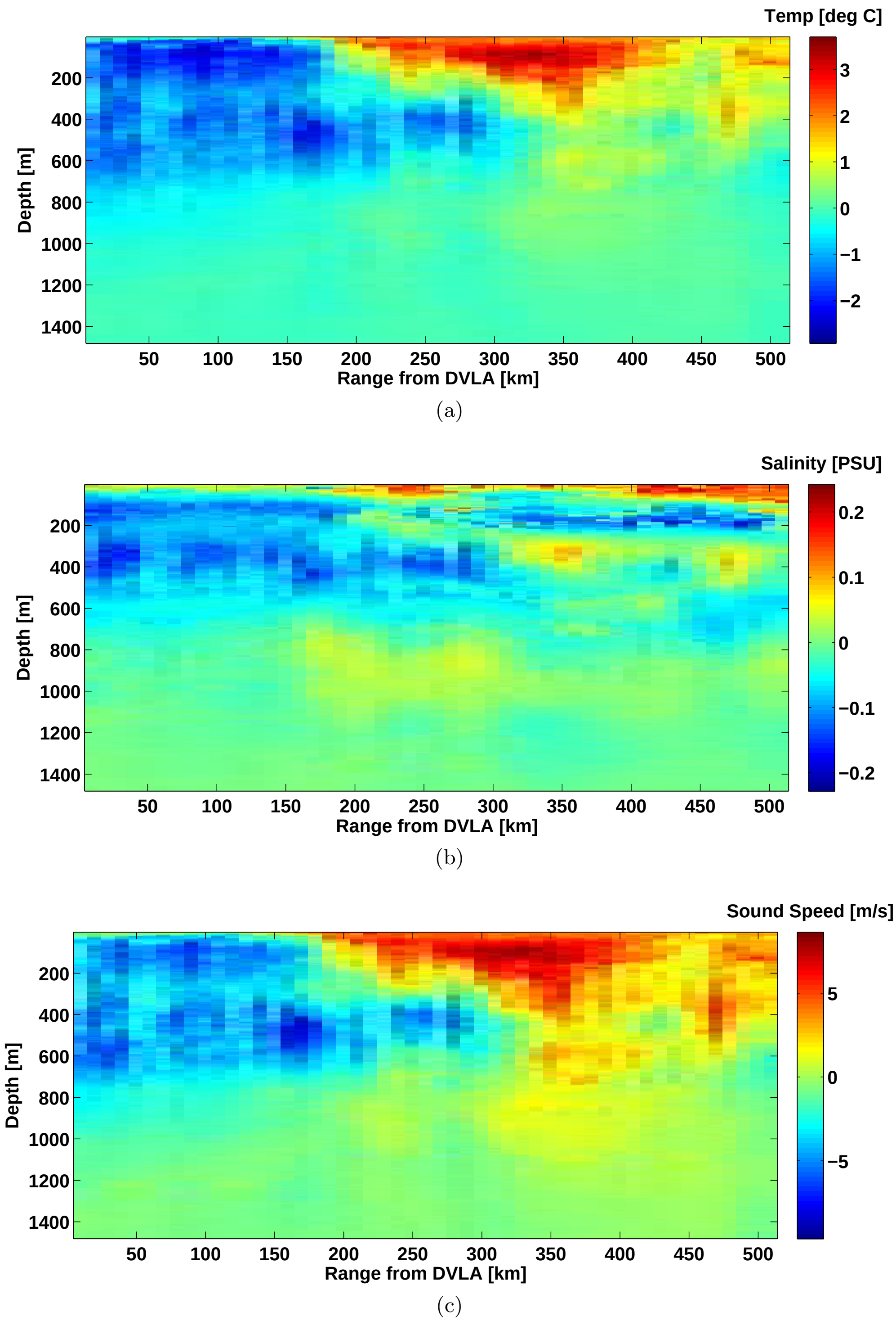

Figure 44: Section difference, Seabird value minus May GDEM-V value. Top: temperature. Middle: salinity. Bottom: sound speed.

(partially obsolete) documentation can be downloaded from the NAVOCEANO FTP site `ftp://ftp7320.nrlssc.navy.mil`. Look in the directory `/pub/ko/NGLI_Data/`. (Last accessed Spring 2010.)

This is a Windows executable that accepts processed CTD files from several standard CTD instruments in use throughout the oceanographic community, subsamples the profile using a published algorithm (this is a form of data compression) and emits output data files in both the real-time email format (called an R-T message) and in post-real-time format.

The program `SVPG.exe` can be difficult to run, but it worked under Windows XP. The program also requires the input data file (i.e., the final processed data from the CTD cast) to have a certain format. For the specific case of Seabird data, the program uses the converted ".cnv" output file, and then only the first 12 columns. Depth must be in columns 1 or 2. Terry Rago of the Naval Postgraduate School (`tarago@nps.edu`) suggested the following column sequence:

1. Pressure (db)
2. Depth [saltwater, m]
3. Julian day
4. Temperature (ITS-90, degrees C)
5. Temperature for secondary sensor (ITS-90, degrees C)
6. Conductivity [S/m]
7. Conductivity for the second sensor [S/m]
8. Salinity (PSU)
9. Salinity for secondary sensor (PSU)
10. Sound Velocity (m/s, Del Grosso)
11. Sound Velocity for secondary sensor (m/s, Del Grosso)

The requirement to forward the CTD data to NAVOCEANO defined in part the post-cast processing applied to the data from every cast. Additional post-processing program parameters were determined by Lora Van Uffelen (SIO) and circulated in a memo. (These were based on suggestions from experts who routinely process Seabird CTD data.) Merging all this wisdom, the following prescription was developed and applied to all the raw Seabird data with the Seabird Seasoft package.

1. **[Data Conversion]** Converts from .hex to ASCII. A successful identification of output variables that produces the final output columns given above is:

1. Pressure (db)
2. Depth [saltwater, m] (make this the SECOND variable)
3. Julian day
4. Temperature (ITS-90, degrees C)
5. Temperature for secondary sensor (ITS-90, degrees C)
6. Conductivity (S/m)
7. Conductivity for secondary sensor (S/m)
8. Elapsed time [s]

The elapsed time is a convenient diagnostic for problems. It is stripped out later so as not to confuse `SPVG.exe`.

2. [**Wild Edit**] Run on pressure, temperature, and conductivity data. The data were kept within two standard deviations for pass 1 and ten standard deviations for pass 2. This was done for twenty scans per block.

3. [**Cell Thermal Mass**] Run on both primary and secondary temperature sensors with a thermal anomaly amplitude (alpha) of 0.03 and a thermal anomaly time constant (1/beta) of 7.

4. [**Filter**] Run on the pressure with a low-pass filter with a time constant of 0.15. Do not change the filters from their defaults.

5. [**LoopEdit**] Run with a minimum velocity of 0.1 m/s. In the lower parameter box, check Remove Surface Soak, and use a surface soak depth of 10 m, a minimum soak depth of 5 m and a maximum soak depth of 20 m. Enable "Use deck pressure as pressure offset."

6. [**Bin Average**] Run to average the data by depth into bins of 1 m (recommended). Include the surface bin, with minimum bin value -0.5 m, maximum bin value 0.5 m and surface bin value 0.

7. [**Derive**] Run to calculate salinity, salinity 2, sound velocity, and sound velocity 2.

8. [**Strip**] Run to exclude elapsed time.

9. [**Split**] Run to divide the data into an upcast and downcast.

We experienced a problem getting the step **LoopEdit** to properly handle the data before and after a nearsurface soak. "Proper handling" is defined here as retaining data from the surface (around 1 or 2 m depth) downward, particularly after an initial soak at 10 m or deeper. Some detective work ensued: the steps above were found to successfully retain all the downcast data from the surface down through the near-surface layer, while flagging and ignoring any soak exercise. These steps were deduced by examining the processing parameters embedded in the header of "successfully" post-processed PhilSea09 files.

Note that retaining the upper 20 m of the ocean in the downcast is not explicitly required (that we know of) by NAVOCEANO, but meets the needs of the NPAL researchers.

Once the converted ".cnv" file for the downcast has been produced, the program `SVPG.exe` must be used to process the .cnv file for transmission to NAVOCEANO. `SVPG.exe` makes several directories for itself. It is best to delete these before starting a new set of cruise CTD profiles. Thus: delete `C:\_TEMP` and `C:\DATASETS.`

1. Open Explorer to `C:\SVPG`.
2. Click on `SVPG.EXE`. (This is the only way to get the graphics to load.)
3. Click OK .
4. Set the target filetype to ".cnv", OK.
5. Open the raw data file. You may get several warning dialog boxes. Ignore them, click OK as necessary.
6. You get a header dialog box. Enter a few things:
   1. Cast: enter the cast number.
   2. Cruise number. for example, RR0510 represents R/V *Roger Revelle* cruise in May 2010.
   3. Shipname: set to other.
   4. Depth: enter the Kongsberg EM122 multibeam depth.

   After OK, you will get a blank screen.
7. <enter>, this brings up "next Step" dialog widget.
8. Click on SV profile.
9. Another dialog box pops up. Do not use a previous SVP. OK.
10. Dialog will report GDEM not found. Click OK
11. Enter the usable cast depth for the maximum depth. Leave the extrapolation method per default. OK.

12. Blank graph, with “Final Data” dialog. Click “ADD” then Ctrl-S.

13. Should get a graph now. Click OK.

14. Should you increase the number of points to 100? Why not? Yes.

15. OK.

Done. Kill the program. The output files are stored in a “temp” directory. The documentation provided in the .zip file describes this in greater detail, but now mail (i.e., on a CD, through ground mail) all contents of the directory `C:\_TEMP` to NAVOCEANO (address below.)

The contact (as of this writing) at NAVOCEANO is

Carl Szczechowski
Oceanographer
Ocean Prediction Department
Ocean Observations Technical Lead (Code NP1O) 8232 Naval Oceanographic Office
1002 Balch Blvd., Stennis Space Center, MS 39522-5001
phone: 228-688-4622
e-mail: carl.szczechowski@navy.mil

6.2.2 Echosounder

The R/V *Roger Revelle* had a Kongsberg EM122 echosounder used to map bottom bathymetry. This instrument was generally disabled during stationary acoustic operations at SS500 and also during the drifting exercise SS25.

Preliminary bathymetric results are shown in Appendix I.

6.2.3 Current Profilers

The R/V *Roger Revelle* has two acoustic systems for interrogating the velocity profiles remotely (i.e., from the surface). The standard instrument is an RDI OceanSurveyor that operates in both narrowband mode (150 kHz) and broadband mode (75 kHz). Examples of processed data products from this instrument are shown in Figs. 45 and 46.

The other instrument, unique to the R/V *Roger Revelle* , is the Hydrographic Doppler Sonar System (HDSS), developed by the Ocean Physics Group at SIO. There are two modes —

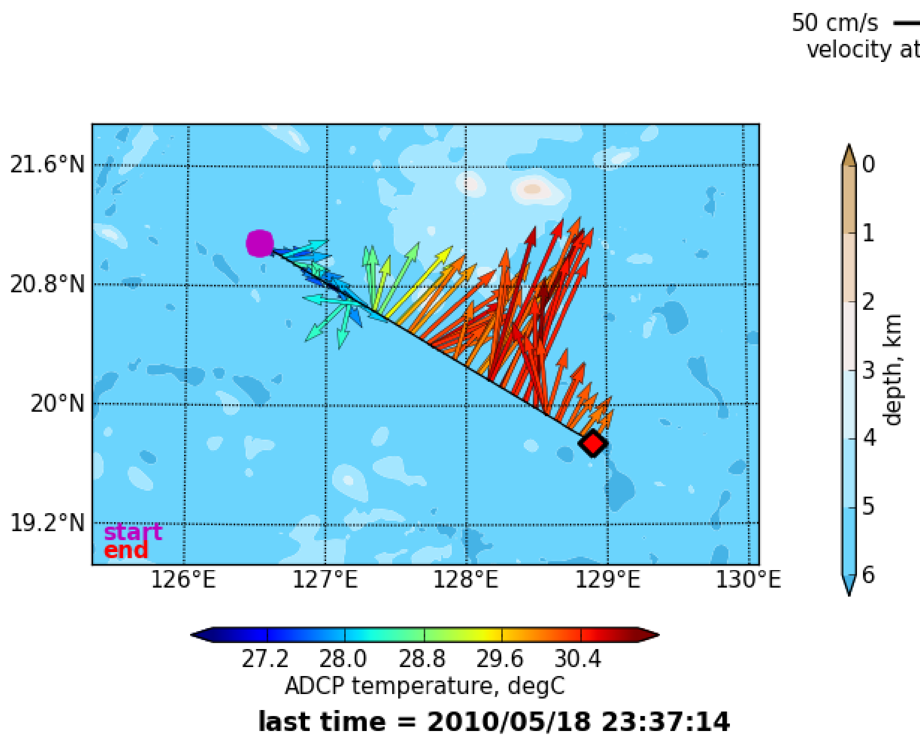

Figure 45: ADCP example. Shallow currents up to 18 May 2010. Sample depth 51 m.

continuous operation at 50 kHz and 140 kHz. Data from the acquisition is streamed to disk: every 44 minutes, the disk files are closed and archived, and new files started. We obtained archive data files every 44 min from about 8 May 2010 01:31 to 28 May 2010 11:48 (times UTC) for both modes.

Processing software was not supplied: contact the Ocean Physics Group at SIO.

6.2.4 Sub-Bottom Profiler

The Knudsen sub-bottom profiler operates at 3.5 kHz and can interfere with the APL-UW equipment. Therefore, it was not always enabled. Raw SEG-Y format files were obtained from 11 to 20 May 2010 with some gaps. Fig. 47 displays an example output from the Windows PlotSurvey program from file `2010_131_1600_000.keb`, showing the layered structure in the bottom at this location.

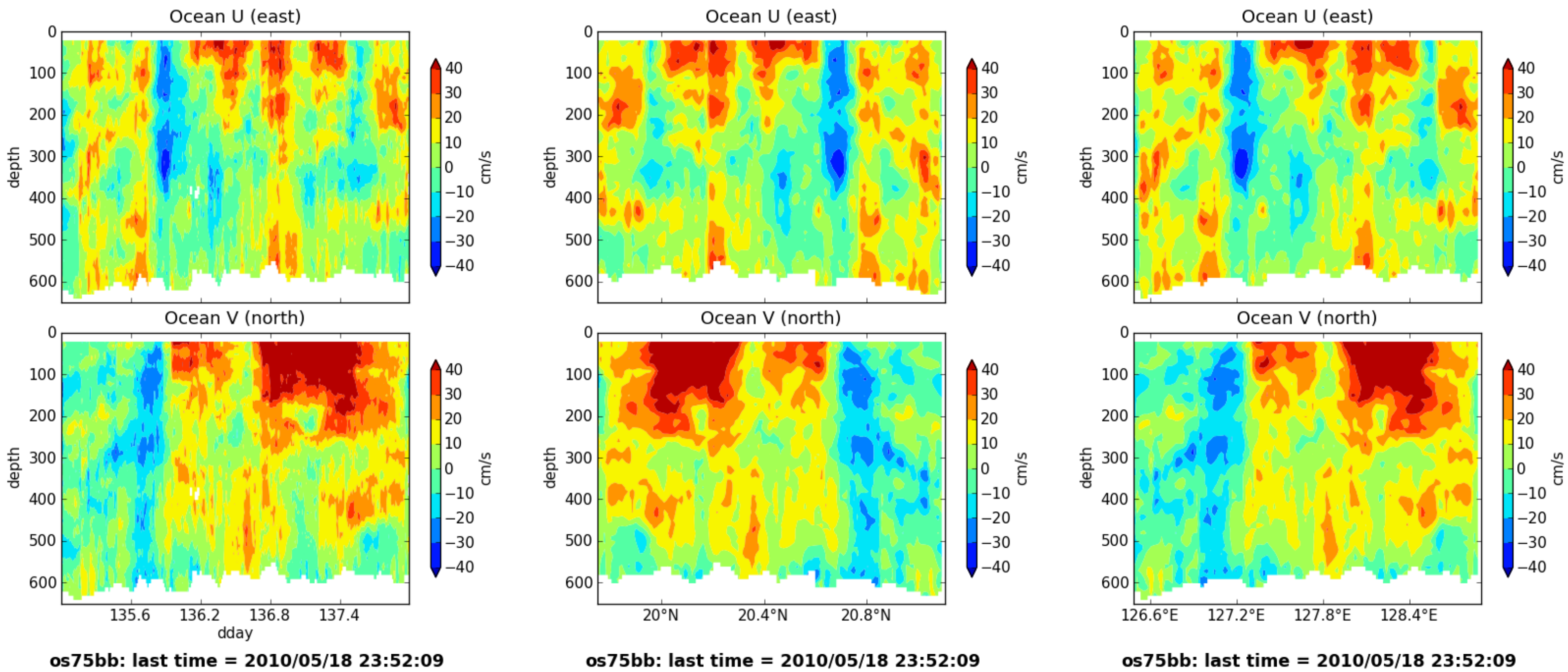

Figure 46: ADCP example. Sections from 18 May 2010. Left: sections for current components along the ship track, parameterized by time along the track. Middle: projected meridional current components, parameterized by latitude. Right: projected zonal current components, parameterized by longitude.

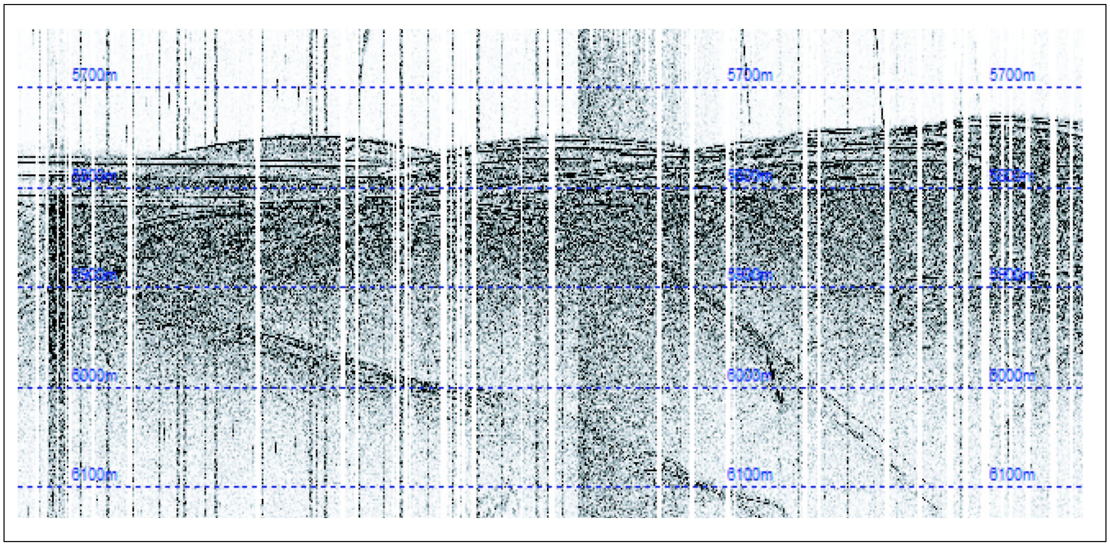

Figure 47: Knudsen sub-bottom profiler example from 11 May 2010.

6.2.5 Navigation

The ship has three GPS systems, an Ashtech ADU2, a Furuno GP-90, and an MX Marine MX421. NMEA strings from all three instruments were logged the entire cruise. In addition, the ship has a Sperry MK-37 gyrocompass, and data from this instrument were logged as well.

6.2.6 MET Data

All auxiliary instrument measurements were logged every ~ 30 s throughout the cruise. In addition to standard meteorological measurements (wind speed, wind direction) there are a suite of other environmental and shipboard machinery (e.g., winch) and instruments (e.g., Doppler log) readings.

As an example, Fig. 48 shows the wind speed through the cruise. This was measured on an RM Young 2-axis ultrasound anemometer mounted 17 m above the mean water level. This figure shows very mild conditions throughout the cruise.

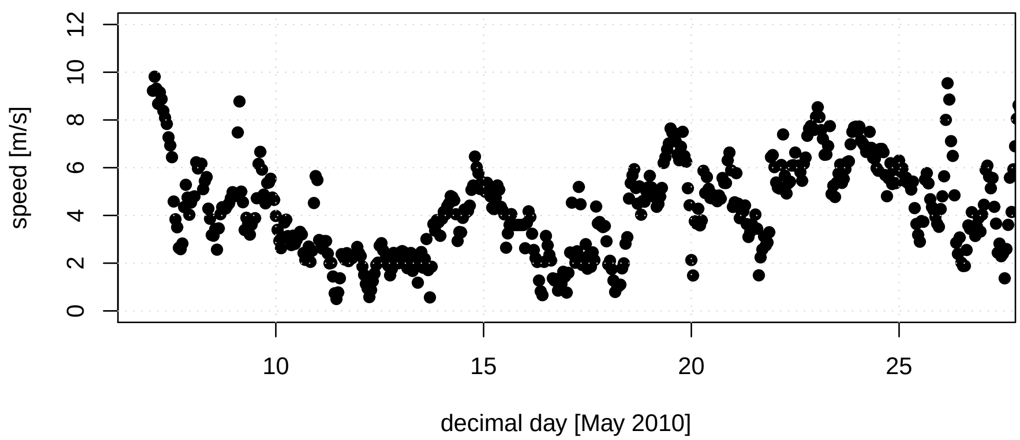

Figure 48: Wind speed record, entire cruise, 17 m above the sea surface. Plot points are true wind speed averaged over each hour.

7 Chronology of Events

The following is a condensed account of events from several sources. Dates are local time unless otherwise noted.

1 May — Arrived in Kaohsiung late last night after flying Seattle to Tokyo, Tokyo to Kaohsiung. The crew is staying at the Grand Hi-Lai Hotel again this year. Because there is uncertainty about the location of the ship on 2 May, it may be anchored out in the harbor, we have decided to unload all four containers today. Surprisingly, all four containers and their contents were aboard the R/V *Roger Revelle* by noon.

2–3 May — Mobilization.

4 May — Mobilization has gone well and is nearly complete. Both sources, the HX and the MP, have been deployed dockside to test handling issues and the various sensors associated with the fiber optic data stream. This included actuating the gas valve via the fiber optic channel. Rex has created a new transmission for the MP source. It includes an m-sequence for each of the two MP resonances. The Q for the lower resonance is 4 and the Q for the upper resonance is 6. The exact frequencies and laws were chosen to make the transmissions the same length.

All electronic equipment appears to be working. There was some concern about the rack computer in the science van because it was obvious that the van had been dropped prior to its arrival at the dock. The screws for the rear mounting brackets on the computer were completely sheared. Nevertheless, the computer and all of the other electronics in the van appear to be working.

Considerable effort was taken to mount the C-Nav GPS antenna. The antenna location is critical for both the transponder survey operation and during the source transmissions. During the transmissions the antenna needs to be over the aft edge of the block supporting the source cable. During the survey the antenna needs to be over the edge of the fantail where the survey interrogation transducer is suspended. When the A-Frame is moved from one position to the other, the antenna's vertical angle changes and the number of satellites it detects may be affected. Rex decided to bias the angle in favor of the position while source transmissions are taking place. The position of the A-frame is fixed (against its stops) during source transmission, so that is a known geometry. No such position exists for the A-frame in the survey configuration. We therefore jockied the A-frame back and forth and sighted from the shore along the stern of the R/V *Roger Revelle* to identify the A-frame angle that put the GPS antenna most nearly over the transom. (See Fig. 15.) Rex, Andrew, and Brad agreed on the final angle. Then Jim changed it. The angle was marked with tape on the A-frame.

Because the R/V *Roger Revelle* A-Frame is about 20 ft wide there was enough space to mount the source deployment block on the port-side of center and the block for the Towed CTD Chain (TCTD) on the starboard side of center. This will alleviate the problem of changing blocks during the cruise.

It was also possible during the mobilization to test the launching of the TCTD surface float and array using the new TCTD block. Although it is impossible to duplicate the conditions at sea, it appears that the geometries for the spooler and block are workable.

Although it is likely that we would be ready to depart earlier than scheduled on 5 May, a Coast Guard inspection is likely to prevent an early departure and may even delay our scheduled departure.

5 May Final securing of equipment is taking place. The clamps that hold the TCTD fins in place are also being adjusted so that each CTD fin is not stressed while passing over the block.

We have now learned that the cruise will be delayed 24 hr. All personnel are to be on board by 1200 on 6 May. All APL-UW personnel will stay on board tonight rather than returning to the hotel.

6 May Finally departed Kaohsiung at 6:55 PM local time.

7 May Transiting all day. Jim designed survey geometry. Jim raised temperature in science van to 75°F to reduce condensation. Jim, Lyle, and Chuck plugged air holes into the science van to reduce condensation. Discussions on how to adjust our schedule seem to be converging. At the moment, we expect to arrive on site tomorrow around 8 PM. We will proceed to deploy the seafloor transponders and then get into DP at SS500. It will be very close but we may get the MP source deployed and calibrated before the reception window opens at midnight. Following the reception window we will most likely conduct the acoustic survey. This will cut into the time available for the TCTD leg. In addition, we must get to the DVLA with enough time to calibrate the HX source. If the TCTD appears to be working exceptionally well, we may re-deploy it for some distance on our way back to SS500. On the other hand, if the acoustic tracking during the first reception window does not work, we can skip the acoustic survey and get closer to the original schedule.

It was noticed that water inside the TCTD array cable was passing out of the upper termination. An air hose and venture connection were used to suck air out of the cable and the termination was re-potted.

8 May This morning the estimated arrival time at transponder site X1 is still about 8 PM tonight. Discussed the location of the S4 current meter with Rex, Tim, and Eric. The concern is the drag from the S4 pulling the Benthos interrogator off the source vertical axis. We are considering placing the S4 above the source. There is some concern that proximity to the source cable may be a problem for the S4 but we will not know until we try it.

Eric and Tim will consider making a bracket for the S4 similar to the one that holds the monitor hydrophone.

Rex computed a propagation time from SS500 to the DVLA of 344 s based upon a May Levitus profile.

Because the dew point is 25.7°C (78.2°F), Jim suggested that we raise the temperature setting in the Science Van to 80°F, at least until we start transmitting.

Andy reports that more elements of the USB circuitry have apparently failed, and therefore the "new" TCTD deck unit is no longer operational. This means that the chain will have to be controlled by the DOS computer, as was done last year. The corollary is that all the Windows-based acquisition software he developed over the past year will not be available. It will still be possible to transfer data files over to the Windows machine and use the GUI-based analysis tools written by Linda.

Jim asked Tim McGinnis to test increasing the separation from the MP source to the Benthos interrogator by putting two cables in series and looking at the receptions on deck. It might be advantageous to increase the separation in order to reduce interference from the source. Two cables increases the distance to the acoustic center of the MP from 5 to 10 m. Interrogations on the deck indicated that the quanta level of receptions with two cables was about half that with one cable.

All transponders will be interrogated at 10 kHz. The first one to go in replies at 12.75 kHz and was dropped at X4 at 11:43:15 UTC. The second transponder (X3) replies at 12.25 kHz and was dropped at 12:15:55 UTC. The third transponder (X2) replies at 11.75 kHz and was dropped at 12:48:29 UTC. The fourth transponder (X1) replies at 11.25 kHz and was dropped at 13:18:36 UTC. All four transponders enable with code "A."

After 298 wraps off the winch the MP source reached 992 meters by 10:55 PM. Two more wraps for a total of 300 brought the MP source to 998 meters. A tape indictor in the cable gave the 992 depth but it was from the R/V *Melville* where the winch was closer to the A-frame.

We calibrated the dual frequency transmission at 191.1 dB. Selecting a different tap (848/7.7) for the amplifier allowed greater current for operating near the resonances. The voltage is running about 550 V rms and the current around 5.5 A rms. The actual transmission began at about 12:47 AM on 9 May.

Figure 49: The chiller.

9 May Transmissions continued through the night. The Liebert chiller (see Fig. 49) is keeping pace with the L50 heat output. The chiller does not create as much noise in the electronics compartment as expected, but while it is running, it definitely gets chilly. Temperature measurements with the Craftsman IR meter show air at about 40°F coming out of the chiller. Once the chiller goes off, the temperature rises. Again using the Craftsman meter, the temperature looking at the fan grilles (and further inside) on the back of the L50 shows about 110 to 120°F (highest temps on the upper fans) right before the chiller kicks in again. The temperature on a small digital thermometer on the work desk does not register significant deviations from a "shirtsleeve" environment, but the draft from the chiller when it is operating usually requires watchstanders to wear sweaters and hats and a couple wool blankets.

Concern has arisen over the rate at which the telemetry battery voltage is falling. At 9:30 AM the 12 V battery was at 11.13 V and the 24 V battery was at 22.92 V. The acoustic tracking ping rate was changed to once every 40 s from once every 20 s. The rate was changed again at 9:30 AM to once every 60 s. A power spectrum of the C-Nav GPS indicated that most of the large-scale motion would be captured at this tracking rate. We will continue to monitor the battery voltages closely. We checked last year's log at the end of roughly 60 hr of deployment and the 12 V battery was still at 11.4 V. At 4:30 PM the battery voltage was 11.0 but we are still tracking.

10 May Around 4 AM the monitor hydrophone went dead and around 5 AM the tracking gave out, both due to battery failure.

Transmissions continuing all day without incident.

There is some question about the DP offsets for the C-Nav GPS. We seem to be holding the A-frame at 18° 59.98′, 130° 11.98′ instead of 19° 00′ and 130° 12.00′.

The transmission will end shortly before 7 AM tomorrow morning. We plan to start raising the MP source immediately thereafter and continue the recovery until breakfast at 7:30 AM. After breakfast the source will be recovered and placed out of the way on the deck. The HX source will then be moved into position. Interspersed with this activity we will try to get the acoustic survey started at the SS500 location.

11 May The source recovery was completed after breakfast this AM. The MP source was moved near the storage van and the HX was placed in the throat of the A-Frame for the next deployment.

Rex determined that the S4 contained no data. The unit apparently woke up on time, then immediately aborted operations due to a "watchdog timeout" and went back to sleep. InterOcean has been notified.

The acoustic survey of the transponders began around 9:50 AM and was completed around 5:55 PM.

A deep CTD cast was initiated near 6:00 PM.

The CTD cast was aborted at 6:40 PM because the CTD was giving false readings. The unit will be retrieved after reaching a depth of over 1000 m. Replacement components will be mounted and the cast repeated. This time the maximum depth will be limited to about 1500 m for the sake of time.

CTD temp 2 was replaced and pump 1 replaced. The new CON file is RR1006_002.CON. The next cast was RR100_001a. This lowered to 100 m, then raised back to the surface, then lowered to 1500 m — a good example of a yo-yo. The entire cast went well. The CTD was fixed.

The TCTD was deployed without the float but attached to the hard point on the stern. A little more than 50% of the sensors were responding at first but there was some indication that there might be a downward trend in the percentage. It was decided to continue a slow tow without the float and if things went well through the night to put the float out in the morning.

Tim McGinnis put the charger on the SeaBattery deployed with the multiport, and reported that one side is not holding a charge. This battery is deemed unhealthy. He will run a discharge test on the HX554 SeaBattery for comparison.

12 May Unfortunately the downward trend in the percentage of sensors that were providing good data continued through the early hours of this morning. We have decided to bring the upper termination of the TCTD on board and inspect it for moisture. We are considering the option of towing the chain from the hard point with the upper termination on the deck and grounding the TCTD to the ship.

Grounding the upper termination to the deck did not improve performance. The day was spent trying to diagnose the problems.

The bridge determined that the 9600 baud data rate from the C-Nav was not integrating well with their navigation systems, so Tim Wen reconfigured the C-Nav to output at 4800 baud.

Rex heard from InterOcean that the watchdog timeout is a very unusual error message, and they think there is an intermittent connection inside the unit. The wake-up mode of operation is not to be trusted. Tests are showing that the S4 operates reliably if logging is commanded to begin immediately (i.e. during bench set-up). That will be the mode used for the remainder of the cruise.

The survey analysis was completed in a preliminary form. The residuals are sub-meter in all three coordinates.

13 May Efforts to diagnose the poor performance (20–22 CTD fins working properly) of the TCTD continued until about 2 PM when the ship scheduled a safety drill. The TCTD was recovered between 3 and 4 PM without incident. The performance of the new block and other new hardware appeared to be very good; however, the seas were very calm so it is not possible to grade the new hardware during severe conditions.

The ship began the transit to a position about 25 km from the DVLA at 4 PM and we expect to arrive around 11 AM tomorrow.

14 May Arrived at a position (21° 14.9364′N, 126° 13.2852′E) 25 km short of the DVLA at 9:30 AM. We conducted a drift test that indicated a 0.5-kt drift in a true bearing direction of 250° and estimated the start position for the 10-hr drift to be 21° 17.1012′N and 125° 47.2056′E. This should take us from roughly 25 to 35 km from the DVLA during the 10-hr drift. We will check the drift one more time from this new location.

Upon arriving at the anticipated location of the start of the drift, another drift test was completed. That test indicated a drift direction of 202° and a speed of about 0.6 kt. Hence the starting point for the source deployment and the beginning location for the drift will be 21° 09.096′N and 125° 55.340′E. This location is 25 km from the DVLA and was determined graphically on the bridge. Because of unpredictable changes in the current and wind between now and the source transmission it is likely that we will need to execute some form of a controlled drift.

The source deployment to 150 m began around 7:15 PM and was completed at 7:45 PM. Pressurization with the fiber control was initiated at 8:15 PM and the admittance loop appeared to remain constant by 8:30 PM.

Because of the short range for this test (25 to ? km) the source was calibrated at only 185.4 dB.

15 May By 7 AM this morning the current had changed directions slightly and increased to 1 kt, while the wind had rotated significantly and increased to 10 kt. So rather than just drifting we are going to start a controlled drift. In other words, most of the impetus for our motion will come from the 1 kt current, but the ship's propulsion will keep us on the track line heading of 202 degrees. Because of the higher current, we will actually cover roughly 20 km, from 25 to 45 km from the DVLA. There was insufficient time to reposition the ship to 20 km from the DVLA at the start.

There is considerable knocking heard in the monitor hydrophone channel. There is a periodic knocking with a period of about 5 s, and occasionally a double-knock. Sometimes it sounds like the hydrophone cable hitting the hydrophone frame. Note, however, that the current past the suspension cable does not appear excessive, but there is a lot of strumming on it. Subsurface currents? The hydrophone mount (i.e., frame) should be revisited to determine how resistant it is to vibration induced knocking.

The HX source transmission began at 7:55 AM so that the schedule for the first hour would be the same for every hour of this 10-hr period (we stop transmitting every hour for a few minutes while the DVLA is collecting navigation data).

During the night and this morning while the ship was in DP, there was significant strumming on the source cable. When the ship began the assisted drift at 8 AM the strumming disappeared. However at 8:07 AM the telemetry from the source stopped. This is not important for this section of the cruise because we have C-Nav GPS to tell where the source is approximately, we know the depth, and the amplifier voltage and current tell us that the signal is still as desired. We just hope that the repairs to the telemetry will be successful for the next series of transmissions. We have spare parts for all telemetry components. It would be unfortunate if this sea battery were to have shorted out because it is superior to our other sea battery.

At 10:15 AM the ship is tracking down the line at 202 degrees very smoothly even though the directions of the wind and the current have shifted slightly.

The ship continued down the track line very smoothly all day. At the end of the 10-hr recording period the ship had reached 21° 0.1′N, 125° 51.3′E (43.2 km from the DVLA). The recovery took less than a half hour and the source was on the deck by 6:30 PM. The ATOC source, at about 61 Hz center frequency, worked with no variation for the 10-hr period.

The S4 was recovered and found to contain data for the duration of the deployment.

Upon opening the telemetry bottle we found a circuit card that had worked its way out of its socket in spite of the fact that set screws (supposedly) secured the card. This is an easy fix, so all should be well for the next transmissions from SS500.

The start point for the CTD transit will be 10 km from the DVLA along a geodesic back to SS500. This start point is 21° 19.0224′N, 126° 05.7906′E. This CTD cast will go to within 10 m of the bottom and should start around 9 PM. Subsequent casts will be 10 km apart.

16 May Based on progress with the CTD transit (four casts to 1500 m and one deep cast, all in 13 hr), it appears that we will be able to make every fifth CTD cast a deep cast. The intervening casts will be to 1500 m.

The CTD transit has proceeded smoothly today with a cast spacing of 10 km and every fifth a cast a deep one. The intervening casts are to 1500 m. If this schedule takes us back to SS500 sufficiently early, we may collect some CTD data between SS500 and the tomography mooring T3.

Watchstanding shifts are 0000 – 1200 and 1200 – 2400.

17 May The CTD transit proceeded without incident.

18 May About four hours were lost today while the TCTD was repaired. It still appears that we will make it back to SS500 three days ahead of schedule. Three options have presented themselves 1) conduct a CTD survey from SS500 to T3, 2) spend more time on the acoustic survey, and 3) re-deploy the TCTD in a vertical suspension.

19 May The CTD transit continued without incident throughout the day.

20 May The CTD transit continued without incident throughout the day.

21 May The CTD transit ended back at SS500 early this morning. Additional acoustic transponder survey data were taken at SS500 and at survey location SG. Additional survey data will be taken at location SH later in the cruise.

The CTD casts went faster than expected so we will have some extra time before the next transmission. After consulting with others, Rex chose to redeploy the TCTD because if more than a couple of fins are OK, then a long tow without repeatedly changing system parameters (such as tow speed and voltage levels) might still be of high quality and useful. A tow was selected over a vertical dangle because a tow could reveal horizontal scales. Horizontal scales here might be different than usual because of the strong shear due to neighboring eddies (although eddy size is generally greater than an IW correlation length.) There are arguments for deploying the orange float. This is partially to give Eric some experience deploying it (an investment in the future) and also to actually deploy "the entire system." The float will decouple the ship motion from the chain to some degree, so peak loads might be less with it than without it. (This is, however, not an issue with the mild seas we are experiencing.) In the end, Eric's most compelling reasoning seemed to focus not on any of the aforementioned issues but on the survivability of the chain. If the upper end of the chain were secured to the tow-point and the chain snagged an undersea obstacle, the entire chain would likely rip off and be lost. If the chain were secured per design to the float, the weak link from the float to the ship would break, but the chain would remain attached to the float and hence could still be recovered. This was probably the deciding factor for Eric.

Deployment of the TCTD began shortly before 9 AM. Up to 10 people supported the tow from the deck: two air tugger operators and two additional tag lines for the block; one slip line between the depressor and a deck cleat; the A-Frame operator, the capstan operator controlling a line through the small block to raise and lower the large block; one operator of the TCTD spooler; one person to raise the chain and fins as they passed out of the spooler; and one person to control the operation. The array was completely in the water by about 10 AM and will be towed from the spooler. Later we may deploy the surface float to suspend the array.

When the array was powered up, only the upper half of the array showed fins giving good returns. After the power to the fins was increased, 43 (50%) of the fins gave returns and these 43 were fairly evenly distributed along the array.

Between 11 and 11:30 AM the surface float was deployed. The knuckle crane was used to get the float over the side and behind the stern. Additional tag lines would have been required in rougher weather. Winds were light and the sea state was 1 or 2. Initial tow speed was 1.5 kt. Problems with the deck box and the USB card have delayed the acquisition of data.

After much investigation it was decided that the array circuit was also open so it was decided to bring the surface float back on deck so the upper termination can be inspected. Once on deck an open circuit was found in the upper termination. A temporary fix will be established and the array will be energized with the top termination still on the deck.

When the array was re-powered with the upper termination on the deck, but all of the fins except the top one in the water, we found about 35% of the fins working; and they were fairly evenly distributed along the array.

Since the temporary fix seemed to identify the problem, the array was turned off around 6:30 PM and a more permanent repair was initiated. The repair ingredients will have to cure after application, but the array can be energized while the termination remains on deck.

22 May The collection of TCTD data continued through the night with the upper termination of the deck. The number of fins reporting dropped to about 25% when the speed was increased to 2.5 kt late last night and the same number continued until 8:30 AM. A short interruption in the data occurred when the primary deck box failed. It took about 30 min to replace it with a spare deck box. This happened around 5 AM. Unless a failure occurs we will continue towing the TCTD until roughly 10:30 PM.

After collecting data for approximately 140 km we put the upper termination in the water around 8:30 PM to check its integrity — it seemed to work fine and about the same 23% of the fins returned. The speed was kept at 1.5 kt until 10:45 PM when the system was turned off and recovery of the TCTD began.

A 1500 m CTD cast began at roughly 11:30 PM and when that is complete we will begin a transit to transponder survey site SH.

23 May Transponder survey data were taken this morning at location SH and near SS500. Location residuals from a preliminary analysis appear to be well below one meter.

Because of concerns about the sea battery lasting long enough to provide telemetry data for the 55-hr transmission window and the pre-window testing, it was decided to wait until 4 PM to start deploying the HX source at SS500. By 5 PM the source had reached a depth of 444 meters and we dogged the winch at that point to break for dinner. On this deployment we were also applying a corrosion inhibitor to the cable as it went out.

After dinner the process continued until the HX reached a depth of 998 meters. Initial admittance plots revealed a loop with an apparent resonance near 50 Hz. When the air valve was opened, the loop increased in size and the 50 Hz resonance shifted to a slightly lower conductance over the first 10 minutes but showed insignificant changes after that. There is a slight kink in the loop around 70 Hz. These results were inconsistent with our expectations for a source depth of 1000 meters. The expected resonance was closer to 75 Hz. A 100-V test signal with an 81-Hz carrier was sent and produced a source level of nearly 182 dB. A 61-Hz signal was then sent with a similar voltage level and only produced a source level of 179 dB. It was decided that there must be something wrong with the admittance software, and that the primary resonance was indeed at approximately 70 Hz. We settled on the 81-Hz signal and an amplifier voltage of 500 V. This voltage level produced a source level of 186 dB.

The HX554 signal consisted of an m-sequence with 2047 bits and a processing gain of 33 dB. Assuming an ambient noise level of 80 dB, spherical propagation loss over the entire 500-km path, no absorption loss, and the 33-dB gain in coherent processing, we expected an SNR of 24 dB at the DVLA. This was considered adequate and a safe level for the damaged HX source.

(In retrospect, Rex could not find any indication that the calculations were wrong. Thus, it still seems like the HX was strongly resonant at a non-pressurized frequency. This makes no physical sense.)

A schedule was prepared to control the HX transmissions with appropriate gaps during the DVLA receptions of navigation data. The 55-hr window actually began at midnight.

Acoustic tracking of the HX source appeared to be working fine with the 11.25-kHz transponder receptions being somewhat less consistent than the others. The interrogation interval was reduced to once every 60 s to save battery power until the transmission window begins when the interval will be reduced to 10 s.

Just before the main transmission schedule started, some faint but interesting moanings and whirrings could be heard on the monitor hydrophone. It seemed to be strongly correlated to the ship heave. The pressure time series should identify this. Rex thinks it sounds like water flowing up and down through the source structure as it drops and lifts. Jim thinks it may be the binding of the ship's propeller shaft as the ship bends while heaving in the waves (which was actually right.) Rex took a couple long ambient noise recordings.

24 May HX transmissions at site SS500 and a depth of 1000 m began at 0000 AM along with acoustic tracking of the source. This continued throughout the day with the exception of a short hiatus every hour so that the DVLA can perform acoustic navigation.

25 May The HX source, telemetry, and acoustic tracking worked flawlessly throughout the day.

26 May The HX source, telemetry, and acoustic tracking continued to work until terminated today at the end of the 55-hr transmission window. At 8 AM we began the recovery of the HX source.

The S4 contained data for the entire deployment, although CRC errors cut short downloading all the data in the device. This seemed to only cut off data captured after the last transmission.

The inductive cable on the TCTD has been cut in half. Later this AM we will deploy the top half of the cable with half of the CTD fins. About 50% of these fins were working. Between 4 and 5 PM, another 12 CTD fins were cut off. This removed two previous cable repairs. The shortened array was then deployed for a short time, but no significant improvement in performance (number or ID of responding fins) was realized. The array was recovered between 6 and 7 PM.

This ended the science activities of this cruise.

27 May In transit to Kaohsiung

28 May In transit to Kaohsiung

8 Science Party

name	affiliation	email
Dr. Jim Mercer	APL-UW	mercer@apl.washington.edu
Dr. Rex Andrew	APL-UW	randrew@apl.washington.edu
Dr. Brad Bell	APL-UW	bradbell@apl.washington.edu
Eric Boget	APL-UW	boget@apl.washington.edu
Meghan Donohue	SIO/UCSD	mkdonohue@ucsd.edu
Charles Fletcher	—	N/A
Andy Ganse	APL-UW	aganse@apl.washington.edu
Lyle Gullings	APL-UW	lyle@apl.washington.edu
Brett Hembrough	SIO/UCSD	bhembrough@ucsd.edu
Fred Karig	APL-UW	fred@apl.washington.edu
Tim McGinnis	APL-UW	tmcginnis@apl.washington.edu
Kristopher Weeks	SIO/UCSD	kris@ucsd.edu
Tim Wen	APL-UW	tim@apl.washington.edu
Andrew White	APL-UW	andrew8@apl.washington.edu

Table 15: Science party, PhilSea10 Experiment.

References

[1] "PSIEX 2009 Lake Washington Engineering Test Results," dated March 19, 2009, NPAL investigators, Applied Physics Laboratory, University of Washington, unpublished notes.

[2] "PSIEX 2010 Lake Washington Engineering Test Results," dated April 19, 2010, NPAL investigators, Applied Physics Laboratory, University of Washington, unpublished notes.

[3] T. McGinnis, "Acoustic Source Monitoring and Positioning System (MPS) Software Specification," revision 1.2, dated 9 February 2009, Applied Physics Laboratory, University of Washington, engineering notes.

[4] J. A. Mercer, R. K. Andrew, B. M. Howe, and J. A. Colosi, *Cruise Report: Longe-range Ocean Acoustic Propagation EXperiment (LOAPEX)*, Applied Physics Laboratory, University of Washington, APL-UW TR 0501, 2005.

[5] M. R. Zarnetske, *Long-range Ocean Acoustic Propagation EXperiment (LOAPEX): Preliminary Analysis of Transmitter Motion and Tidal Signals*, MS thesis, School of Oceanography, University of Washington, Seattle, WA, October 2005.

[6] J. Hummon, personal communication, on the R/V *Roger Revelle* in port in Kao-Hsiung between cruises RR1005 and RR1006, April 2010.

[7] A Constrained Kalman–Bucy Smoother, version `ckbs-0.20100325.0`, `http://www.coin-or.org/CoinBazaar/ckbs/ckbs.xml`. Last accessed July 2010.

[8] SeaSoar developers' website, `http://www.chelsea.co.uk/Vehicles%20SeaSoar.htm`

[9] The Shallow Water 2006 Experiment is described in a series of articles in the *IEEE J. Ocean. Eng.* **35**(1), January 2010. An introduction is provided in N. R. Chapman and J. F. Lynch, "Editorial: Special issue on the 2006 Shallow Water Experiment," pp 1–2.

[10] M. S. Ballard, and K.M. Becker, "Inversion for range-dependent water column sound speed profiles on the New Jersey shelf using a linearized perturbative method", *J. Acoust. Soc. Am.*, **127**(6), 2010.

[11] D. J. Tang, et al, "Shallow Water '06: A joint acoustic propagation/nonlinear internal wave physics experiment,', *Oceanography*, **20**(4), 2007.

[12] ASD Sensortechnik website, `http://www.asd-sensors.de/index.php?option=com_content&task=view&id=18`, last accessed August 2010.

[13] A. A. Ganse, "TCTD How-to Procedures," APL-UW/NPAL internal document, May 2009.

[14] *TOWED CTD CHAIN Users Manual*, ADM Elektronik, Germany, Edition October 2008.

[15] *TOWED CTD CHAIN DECK UNIT Users Manual supplement*, ADM Elektronik, Germany, Edition September 2009.

[16] Towed CTD Chain developer's website, `http://www.ctdchain.info`, last accessed August 2010.

[17] APL-UW/NPAL Towed CTD Chain Experiences/Notes Repository, `http://staff.washington.edu/aganse/ctdchain` (restricted website – request access from A. A. Ganse, `mailto:aganse@apl.washington.edu`).

[18] *World Ocean Atlas 2005 (WOA2005)* climatologies and related statistics in netCDF format. `http://www.nodc.noaa.gov/OC5/WOA05/woa05nc.html`. Last accessed August 2010.

[19] *Generalized Digital Environmental Model (GDEM-V)*, version 3.0, October 2003. Naval Oceanographic Office, Oceanographic Data Bases Division, Stennis Space Center, MS 39522-5003.

[20] *CSIRO Seawater Toolkit*, release 3.2, April 2006, `http://www.cmar.csiro.au/datacentre/ext_docs/seawater.htm`, last accessed 30 July 2010.

[21] F. B. Jensen, W. A. Kuperman, M. B. Porter, and H. Schmidt, *Computational Ocean Acoustics*, New York: Springer-Verlag, 2000.

[22] T. Schaad, *Digiquartz depth sensor ocean-depth conversion*, Paroscientific, Inc., application note Doc. G8033.

[23] See `http://www.ldeo.columbia.edu/res/pi/MB-System`. Last accessed 6 August 2010.

[24] U. Zajaczkovski, "EM 120 Multibeam Echosounder," unpublished notes described in the file `RR0901_report_multibeam.pdf`, downloaded from `http://www.marine-geo.org/tools/search/Document_Accept.php?url_uid=860&client=DataLink`, last accessed 6 August 2010.

A Transmission Schedules and Files

A.1 SS500 — Multiport System

All transmissions from the MP200/TR1446 system were captured in the files listed in Table 16. All transmissions used a 40-s ramp, all files have length 240553421 bytes, and all had durations of 3300 s. The first second in the IRIG-M channel in every file decoded to HH:47:30. The telemetry system failed around 18:00 on 8 May, and consequently no valid monitor hydrophone data and therefore source level estimates are available after that.

A.2 SS25 — HX554 System

All transmissions from the HX554 system were captured in the files listed in Table 17. All transmissions used a 40-s ramp. All files except the last one have length 111995371 bytes; all had durations of 3000 s. The first second in the IRIG-M channel in every file decoded to HH:53:57. The last file was from a short transmission scheduled at the last minute to insonify the receiver during the last few minutes of its collection window.

We noticed significant strumming around the suspension cable, and initially considerable loud "knocking" in the monitor hydrophone channel. Shortly after deployment, the telemetry system failed. This was later traced to a fiber optic multiplexer board that came out of its connector — possibly due to the vibration — in the telemetry bottle. Due to this failure, no acoustic data were collected during this exercise, and therefore no source level estimates could be made.

A.3 SS500 — HX554 System

All transmissions from the HX554 system were captured in the files listed in Table 18. All transmissions used a 300-s ramp. The first second in the IRIG-M channel in every file decoded to HH:47:10.

Table 16: MP200/TR1446 system transmission files at SS500, PhilSea10. Marktime is in Unix seconds. Date and time are the marktime rendered into UTC units. "Yday" is the yearday, with 1 being January 1. SL is the source level in dB re 1 μPa^2 @ 1 m. The power amplifier input drive level is in units of RMS volts, the cable voltage level is in units of RMS volts, and the cable current is in units of RMS amperes.

filename	marktime	date	time	Yday	SL	drive levels			comments
						input	V_{cable}	I_{cable}	
1273337290.sam	1273337290	2010/05/08	16:48:10	128	190.5	3.98	549.2	5.47	
1273340890.sam	1273340890	2010/05/08	17:48:10	128	189.9	3.98	548.3	5.44	possible glitch?
1273344490.sam	1273344490	2010/05/08	18:48:10	128	189.9	3.98	548.8	5.45	
1273348090.sam	1273348090	2010/05/08	19:48:10	128	189.8	3.98	549.7	5.46	
1273351690.sam	1273351690	2010/05/08	20:48:10	128	189.8	3.98	549.7	5.45	
1273355290.sam	1273355290	2010/05/08	21:48:10	128	189.8	3.98	549.5	5.45	
1273358890.sam	1273358890	2010/05/08	22:48:10	128	189.9	3.98	550.0	5.46	
1273362490.sam	1273362490	2010/05/08	23:48:10	128	189.8	3.98	549.7	5.45	
1273366090.sam	1273366090	2010/05/09	00:48:10	129	189.9	3.98	549.7	5.45	
1273369690.sam	1273369690	2010/05/09	01:48:10	129	189.9	3.98	550.0	5.45	
1273373290.sam	1273373290	2010/05/09	02:48:10	129	189.9	3.98	550.0	5.45	
1273376890.sam	1273376890	2010/05/09	03:48:10	129	189.8	3.98	550.0	5.45	
1273380490.sam	1273380490	2010/05/09	04:48:10	129	189.7	3.98	550.0	5.45	
1273384090.sam	1273384090	2010/05/09	05:48:10	129	189.6	3.98	550.0	5.45	
1273387690.sam	1273387690	2010/05/09	06:48:10	129	189.6	3.98	550.0	5.44	
1273391290.sam	1273391290	2010/05/09	07:48:10	129	189.6	3.98	550.2	5.44	
1273394890.sam	1273394890	2010/05/09	08:48:10	129	189.6	3.98	550.2	5.45	
1273398490.sam	1273398490	2010/05/09	09:48:10	129	189.6	3.98	550.2	5.45	
1273402090.sam	1273402090	2010/05/09	10:48:10	129	189.6	3.98	550.2	5.45	
1273405690.sam	1273405690	2010/05/09	11:48:10	129	189.6	3.98	550.2	5.45	

Table 16: ... *continued*

filename	marktime	date	time	Yday	SL	drive levels			comments
						input	V_{cable}	I_{cable}	
1273409290.sam	1273409290	2010/05/09	12:48:10	129	189.6	3.98	550.2	5.45	
1273412890.sam	1273412890	2010/05/09	13:48:10	129	189.6	3.98	550.2	5.45	
1273416490.sam	1273416490	2010/05/09	14:48:10	129	189.6	3.98	550.2	5.45	
1273420090.sam	1273420090	2010/05/09	15:48:10	129	189.5	3.98	550.2	5.45	
1273423690.sam	1273423690	2010/05/09	16:48:10	129	189.5	3.98	550.2	5.45	
1273427290.sam	1273427290	2010/05/09	17:48:10	129	189.4	3.98	550.2	5.45	
1273430890.sam	1273430890	2010/05/09	18:48:10	129	N/A	3.98	550.0	5.45	
1273434490.sam	1273434490	2010/05/09	19:48:10	129	N/A	3.98	548.3	5.43	
1273438090.sam	1273438090	2010/05/09	20:48:10	129	N/A	3.98	548.8	5.44	
1273441690.sam	1273441690	2010/05/09	21:48:10	129	N/A	3.98	550.2	5.45	
1273445290.sam	1273445290	2010/05/09	22:48:10	129	N/A	3.98	550.2	5.45	
1273448890.sam	1273448890	2010/05/09	23:48:10	129	N/A	3.98	550.2	5.45	
1273452490.sam	1273452490	2010/05/10	00:48:10	130	N/A	3.98	550.5	5.45	
1273456090.sam	1273456090	2010/05/10	01:48:10	130	N/A	3.98	550.5	5.45	
1273459690.sam	1273459690	2010/05/10	02:48:10	130	N/A	3.98	550.5	5.45	
1273463290.sam	1273463290	2010/05/10	03:48:10	130	N/A	3.98	550.2	5.45	
1273466890.sam	1273466890	2010/05/10	04:48:10	130	N/A	3.98	550.5	5.45	
1273470490.sam	1273470490	2010/05/10	05:48:10	130	N/A	3.98	549.5	5.43	
1273474090.sam	1273474090	2010/05/10	06:48:10	130	N/A	3.98	548.3	5.42	
1273477690.sam	1273477690	2010/05/10	07:48:10	130	N/A	3.98	550.5	5.44	
1273481290.sam	1273481290	2010/05/10	08:48:10	130	N/A	3.98	550.5	5.44	
1273484890.sam	1273484890	2010/05/10	09:48:10	130	N/A	3.98	550.5	5.45	
1273488490.sam	1273488490	2010/05/10	10:48:10	130	N/A	3.98	550.5	5.45	
1273492090.sam	1273492090	2010/05/10	11:48:10	130	N/A	3.98	550.5	5.45	
1273495690.sam	1273495690	2010/05/10	12:48:10	130	N/A	3.98	550.5	5.45	
1273499290.sam	1273499290	2010/05/10	13:48:10	130	N/A	3.98	550.5	5.45	
1273502890.sam	1273502890	2010/05/10	14:48:10	130	N/A	3.98	550.5	5.45	
1273506490.sam	1273506490	2010/05/10	15:48:10	130	N/A	3.98	547.3	5.42	
1273510090.sam	1273510090	2010/05/10	16:48:10	130	N/A	3.98	539.5	5.34	
1273513690.sam	1273513690	2010/05/10	17:48:10	130	N/A	3.98	550.5	5.45	
1273517290.sam	1273517290	2010/05/10	18:48:10	130	N/A	3.98	550.5	5.45	
1273520890.sam	1273520890	2010/05/10	19:48:10	130	N/A	3.98	550.5	5.45	
1273524490.sam	1273524490	2010/05/10	20:48:10	130	N/A	3.98	550.7	5.46	
1273528090.sam	1273528090	2010/05/10	21:48:10	130	N/A	3.98	550.7	5.46	

Table 17: HX554 system transmission files, SS25 (drift exercise), PhilSea10. Marktime is in Unix seconds. Date and time are the marktime rendered into UTC units. “Yday” is the yearday, with 1 being January 1. Duration is in seconds, filesize is in bytes. The power amplifier input drive level is in units of RMS volts, the cable voltage level is in units of RMS volts, and the cable current is in units of RMS amperes.

filename	marktime	date	time	Yday	duration	SL	file size	drive levels			comments
								input	V_{cable}	I_{cable}	
1273881277.sam	1273881277	2010/05/14	23:54:37	134	3000	????	111995371	1.38	331.4	2.56	telemetry failed during
1273884877.sam	1273884877	2010/05/15	00:54:37	135	3000	N/A	111995371	1.38	331.6	2.56	
1273888477.sam	1273888477	2010/05/15	01:54:37	135	3000	N/A	111995371	1.38	331.6	2.56	
1273892077.sam	1273892077	2010/05/15	02:54:37	135	3000	N/A	111995371	1.38	331.4	2.56	
1273895677.sam	1273895677	2010/05/15	03:54:37	135	3000	N/A	111995371	1.38	331.4	2.56	
1273899277.sam	1273899277	2010/05/15	04:54:37	135	3000	N/A	111995371	1.38	331.4	2.56	
1273902877.sam	1273902877	2010/05/15	05:54:37	135	3000	N/A	111995371	1.38	331.4	2.56	
1273906477.sam	1273906477	2010/05/15	06:54:37	135	3000	N/A	111995371	1.38	331.4	2.56	
1273910077.sam	1273910077	2010/05/15	07:54:37	135	3000	N/A	111995371	1.38	331.4	2.56	
1273913677.sam	1273913677	2010/05/15	08:54:37	135	3000	N/A	111995371	1.38	331.4	2.56	
1273916850.sam	1273916850	2010/05/15	09:47:30	135	1200	N/A	45704984	1.38	331.4	2.56	DVLA nav overlap

Table 18: HX554 system transmission files, SS500, PhilSea10. Marktime is in Unix seconds. Date and time are the marktime rendered into UTC units. "Yday" is the yearday, with 1 being January 1. Duration is in seconds, filesize is in bytes. SL is the source level in dB re 1 μPa^2 @ 1 m. The power amplifier input drive level is in units of RMS volts, the cable voltage level is in units of RMS volts, and the cable current is in units of RMS amperes.

filename	marktime	date	time	Yday	duration	SL	file size	drive levels			comments
								input	V_{cable}	I_{cable}	
1274626330.sam	1274626330	2010/05/23	14:52:10	143	2700	185.8	76923058	2.03	492.9	2.64	
1274629930.sam	1274629930	2010/05/23	15:52:10	143	2700	185.8	76923058	2.03	493.1	2.64	
1274633530.sam	1274633530	2010/05/23	16:52:10	143	2700	186.0	76923058	2.03	493.1	2.64	
1274637130.sam	1274637130	2010/05/23	17:52:10	143	2700	185.9	76923058	2.03	493.1	2.64	
1274640730.sam	1274640730	2010/05/23	18:52:10	143	2700	185.8	76923058	2.03	493.1	2.63	
1274644330.sam	1274644330	2010/05/23	19:52:10	143	2700	185.8	76923058	2.03	493.1	2.63	
1274647930.sam	1274647930	2010/05/23	20:52:10	143	2700	185.8	76923058	2.03	493.1	2.63	
1274651530.sam	1274651530	2010/05/23	21:52:10	143	2700	185.7	76923058	2.03	493.1	2.63	
1274655130.sam	1274655130	2010/05/23	22:52:10	143	2700	185.7	76923058	2.03	493.1	2.63	
1274658730.sam	1274658730	2010/05/23	23:52:10	143	2700	185.6	76923058	2.03	493.1	2.63	
1274662330.sam	1274662330	2010/05/24	00:52:10	144	2700	185.6	76923058	2.03	493.1	2.63	
1274665930.sam	1274665930	2010/05/24	01:52:10	144	2700	185.6	76923058	2.03	493.1	2.63	
1274669530.sam	1274669530	2010/05/24	02:52:10	144	2700	185.6	76923058	2.03	493.1	2.63	
1274673130.sam	1274673130	2010/05/24	03:52:10	144	2700	185.5	76923058	2.03	493.1	2.63	
1274676730.sam	1274676730	2010/05/24	04:52:10	144	2700	185.5	76923058	2.03	493.1	2.63	
1274680330.sam	1274680330	2010/05/24	05:52:10	144	2700	185.5	76923058	2.03	493.1	2.63	
1274683930.sam	1274683930	2010/05/24	06:52:10	144	2700	185.5	76923058	2.03	493.1	2.63	
1274687530.sam	1274687530	2010/05/24	07:52:10	144	2700	185.5	76923058	2.03	493.1	2.63	
1274691130.sam	1274691130	2010/05/24	08:52:10	144	2700	185.5	76923058	2.03	493.1	2.63	
1274694730.sam	1274694730	2010/05/24	09:52:10	144	2700	185.5	76923058	2.03	493.4	2.63	
1274698330.sam	1274698330	2010/05/24	10:52:10	144	2700	185.5	76923058	2.03	493.1	2.63	
1274701930.sam	1274701930	2010/05/24	11:52:10	144	2700	185.5	76923058	2.03	493.1	2.63	
1274705530.sam	1274705530	2010/05/24	12:52:10	144	2700	185.5	76923058	2.03	493.1	2.63	
1274709130.sam	1274709130	2010/05/24	13:52:10	144	2700	185.5	76923058	2.03	493.1	2.63	
1274712730.sam	1274712730	2010/05/24	14:52:10	144	2700	185.5	76923058	2.03	493.1	2.63	

Table 18: ... *continued*

filename	marktime	date	time	Yday	duration	SL	file size	drive levels			comments
								input	V_{cable}	I_{cable}	
1274716330.sam	1274716330	2010/05/24	15:52:10	144	2700	185.4	76923058	2.03	493.1	2.63	
1274719930.sam	1274719930	2010/05/24	16:52:10	144	2700	185.4	76923058	2.03	493.4	2.63	
1274723530.sam	1274723530	2010/05/24	17:52:10	144	2700	185.4	76923058	2.03	493.4	2.63	
1274727130.sam	1274727130	2010/05/24	18:52:10	144	2700	185.4	76923058	2.03	493.4	2.63	
1274730730.sam	1274730730	2010/05/24	19:52:10	144	2700	185.4	76923058	2.03	493.4	2.63	
1274734330.sam	1274734330	2010/05/24	20:52:10	144	2700	185.4	76923058	2.03	493.1	2.63	
1274737930.sam	1274737930	2010/05/24	21:52:10	144	2700	185.4	76923058	2.03	493.4	2.63	
1274741530.sam	1274741530	2010/05/24	22:52:10	144	2700	185.4	76923058	2.03	493.4	2.63	
1274745130.sam	1274745130	2010/05/24	23:52:10	144	2700	185.4	76923058	2.03	493.4	2.63	
1274748730.sam	1274748730	2010/05/25	00:52:10	145	2700	185.4	76923058	2.03	493.1	2.63	
1274752330.sam	1274752330	2010/05/25	01:52:10	145	2700	185.4	76923058	2.03	493.1	2.63	
1274755930.sam	1274755930	2010/05/25	02:52:10	145	2700	185.4	76923058	2.03	493.4	2.63	
1274759530.sam	1274759530	2010/05/25	03:52:10	145	2700	185.4	76923058	2.03	493.4	2.63	
1274763130.sam	1274763130	2010/05/25	04:52:10	145	2700	185.3	76923058	2.08	503.4	2.69	
1274766730.sam	1274766730	2010/05/25	05:52:10	145	2700	185.4	76923058	2.08	503.4	2.68	
1274770330.sam	1274770330	2010/05/25	06:52:10	145	2700	185.4	76923058	2.08	503.4	2.68	
1274773930.sam	1274773930	2010/05/25	07:52:10	145	2700	185.4	76923058	2.08	503.4	2.68	
1274777530.sam	1274777530	2010/05/25	08:52:10	145	2700	185.4	76923058	2.08	503.6	2.68	
1274781130.sam	1274781130	2010/05/25	09:52:10	145	2700	185.4	76923058	2.08	503.4	2.68	
1274784730.sam	1274784730	2010/05/25	10:52:10	145	2700	185.4	76923058	2.08	503.4	2.68	
1274788330.sam	1274788330	2010/05/25	11:52:10	145	2700	185.4	76923058	2.08	503.4	2.68	
1274791930.sam	1274791930	2010/05/25	12:52:10	145	2700	185.4	76923058	2.08	503.4	2.68	
1274795530.sam	1274795530	2010/05/25	13:52:10	145	2700	185.4	76923058	2.08	503.4	2.68	
1274799130.sam	1274799130	2010/05/25	14:52:10	145	2700	185.4	76923058	2.08	503.4	2.68	
1274802730.sam	1274802730	2010/05/25	15:52:10	145	2700	185.3	76923058	2.08	503.4	2.68	
1274806330.sam	1274806330	2010/05/25	16:52:10	145	2700	185.4	76923058	2.08	503.4	2.68	
1274809930.sam	1274809930	2010/05/25	17:52:10	145	2700	185.4	76923058	2.08	503.4	2.68	
1274813530.sam	1274813530	2010/05/25	18:52:10	145	2700	185.3	76923058	2.08	503.4	2.68	
1274817130.sam	1274817130	2010/05/25	19:52:10	145	2700	185.3	76923058	2.08	503.4	2.68	
1274820730.sam	1274820730	2010/05/25	20:52:10	145	2700	185.3	76923058	2.08	503.4	2.68	
1274824330.sam	1274824330	2010/05/25	21:52:10	145	2700	185.3	76923058	2.08	503.4	2.68	
1274827930.sam	1274827930	2010/05/25	22:52:10	145	180	185.3	12330429	2.08	503.9	2.69	

Filename	Lat	Lon	Range	Type	Filename	Lat	Lon	Range	Type
dRR1006_001a.cnv	19.05	130.11	498.62	SH	dRR1006_029.cnv	20.17	128.16	259.24	DP
dRR1006_003.cnv	21.25	126.21	23.51	DP	dRR1006_030.cnv	20.12	128.25	269.22	SH
dRR1006_004.cnv	21.32	126.10	9.29	DP	dRR1006_031.cnv	20.08	128.33	279.23	SH
dRR1006_005.cnv	21.27	126.18	19.28	SH	dRR1006_032.cnv	20.03	128.41	289.19	SH
dRR1006_006.cnv	21.23	126.26	29.32	SH	dRR1006_033.cnv	19.98	128.49	299.21	SH
dRR1006_007.cnv	21.18	126.35	39.31	SH	dRR1006_034.cnv	19.94	128.57	309.20	DP
dRR1006_008.cnv	21.14	126.43	49.15	SH	dRR1006_035.cnv	19.89	128.66	319.25	SH
dRR1006_009.cnv	21.09	126.51	59.27	DP	dRR1006_036.cnv	19.84	128.74	329.28	SH
dRR1006_010.cnv	21.04	126.60	69.32	SH	dRR1006_037.cnv	19.80	128.82	339.21	SH
dRR1006_011.cnv	21.00	126.68	79.37	SH	dRR1006_038.cnv	19.75	128.90	349.21	SH
dRR1006_012.cnv	20.95	126.76	89.31	SH	dRR1006_039.cnv	19.70	128.98	359.18	DP
dRR1006_013.cnv	20.91	126.84	99.25	SH	dRR1006_040.cnv	19.66	129.06	369.21	SH
dRR1006_014.cnv	20.86	126.93	109.24	DP	dRR1006_041.cnv	19.61	129.15	379.15	SH
dRR1006_015.cnv	20.82	127.01	119.15	SH	dRR1006_042.cnv	19.56	129.23	389.25	SH
dRR1006_016.cnv	20.77	127.09	129.25	SH	dRR1006_043.cnv	19.52	129.31	399.18	SH
dRR1006_017.cnv	20.72	127.18	139.20	SH	dRR1006_044.cnv	19.47	129.39	409.14	DP
dRR1006_018.cnv	20.68	127.26	149.19	SH	dRR1006_045.cnv	19.42	129.47	419.19	SH
dRR1006_019.cnv	20.63	127.34	159.22	DP	dRR1006_046.cnv	19.38	129.55	429.24	SH
dRR1006_020.cnv	20.59	127.42	169.30	SH	dRR1006_047.cnv	19.33	129.63	439.17	SH
dRR1006_021.cnv	20.54	127.51	179.31	SH	dRR1006_048.cnv	19.28	129.72	449.18	SH
dRR1006_022.cnv	20.49	127.59	189.37	SH	dRR1006_049.cnv	19.24	129.80	459.25	DP
dRR1006_023.cnv	20.45	127.67	199.26	SH	dRR1006_050.cnv	19.19	129.88	469.26	SH
dRR1006_024.cnv	20.40	127.75	209.32	DP	dRR1006_051.cnv	19.14	129.96	479.21	SH
dRR1006_025.cnv	20.36	127.84	219.26	SH	dRR1006_052.cnv	19.09	130.04	489.19	SH
dRR1006_026.cnv	20.31	127.92	229.26	SH	dRR1006_053.cnv	19.05	130.12	499.18	SH
dRR1006_027.cnv	20.26	128.00	239.24	SH	dRR1006_054.cnv	19.00	130.20	508.97	DP
dRR1006_028.cnv	20.22	128.08	249.30	SH	dRR1006_055.cnv	19.69	128.99	360.96	SH

Table 19: CTD downcast files produced for NAVOCEANO

B CTD Files

Table 19 lists the CTD downcast files produced for NAVOCEANO and available for modeling and analysis. There is also a corresponding upcast file for each downcast file. Latitude is in degrees North, longitude in degrees East, and range is in kilometres from the target DVLA site. The type is either DP for deep (actual depth varies, but is roughly 5000 to 6000 m) and SH for shallow (usually 1500 m.)

C Tracking Computer: Logging and Timing Issues

The NPAL tracking computer used a single program to acquire data from various serial ports. After an input record completed, Unix second and microsecond were read and written.. The end of record character (or characters) was (were) changed to a newline character. This UNIX time (corresponding to the beginning of the file) was used to create file names of the form *device-yymmdd.hh*, where *device* is the instrument recording the data, *yy* is the last two digits of the year; i.e., 10, *mm* is the month; i.e., 05, *dd* is the day, and *hh* is the hour.

There was a mistake in setting the UNIX time on the tracking computer, hence all of the file names are about one hour less than they should be. To be more specific, at 01:00:07 UTC, the tracking computer UNIX time to the nearest second was 1273536000, (which corresponded to 00:00:00 on 2010-05-11). This was deduced by inspecting the beginning of the file `cnav-100511.00`.

In general, the C-Nav GPS set is continually providing UTC time as part of its input. Hence the corresponding data files can be used to map UNIX time to UTC time. For most of the time, the C-Nav communication link was set at 9600 baud (it was set at 4800 baud for a short period when we were not tracking).

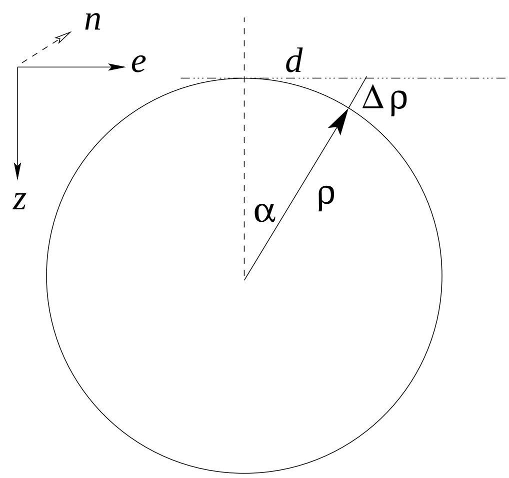

Figure 50: Tangent plane notation. ρ is the radius of Earth, $\rho \approx 6 \times 10^6$ (m); d is the maximum distance for flat Earth approximation, $d \approx 10^4$ (m); α is the angle from center of Earth corresponding to d; $\Delta\rho$ is the flat Earth error at distance d (m) .

D ENZ Coordinates

There are three measures of depth to consider in long baseline tracking. A GPS tracking system provides an elevation (negative of depth direction) where zero corresponds to the surface of the WGS 84 ellipsoid. In East, North and Down coordinates (ENZ), down is relative to the tangent plane to zero WGS 84 elevation at the origin of the ENZ coordinates. The sound speed velocity profiles are given in terms of ocean depth (as estimated from pressure). Ocean depth is different from ENZ down for two reasons. The first is that there is a displacement between the WGS 84 ellipsoid and the current height of the ocean. The second is that the earth curves away from the tangent plane at the origin of the ENZ coordinates.

The amount of distance that the Earth curves away from the tangent plan in ENZ coordinates is about 8 m in 10 km. We use the notation in Fig. 50 and derive this result as follows:

$$\begin{aligned} \rho + \Delta\rho &= \sqrt{\rho^2 + d^2} \\ \Delta\rho &= \rho\left(\sqrt{1 + (d/\rho)^2} - 1\right). \end{aligned}$$

Using a first order Taylor series approximation for square root near one we have

$$\Delta\rho \approx d^2/(2\rho) \approx .5 \times 10^2/6 \approx 8,$$

which is a distance in meters.

E Conversion Between WGS 84 and ECEF Coordinates

We use the notation in Table 20 to convert from WGS 84 coordinates to Earth centered, Earth fixed (ECEF) coordinates (which are rectangular).

We use $\rho = 6378137(m)$ for the semi-major axis and $f = 1/298.257223563$ for the flattening of WGS 84 ellipsoid. Given a latitude, longitude, and altitude $w \in \mathbf{R}^3$ in WGS 84 coordinates, the corresponding ECEF coordinates $x \in \mathbf{R}^3$ are given by

$$\begin{aligned} \varepsilon^2 &= 2f - f^2 \\ R &= \rho\left[1 - \varepsilon^2 \sin^2(w_1)\right]^{-1/2} \\ x_1 &= (R + w_3)\cos(w_1)\cos(w_2) \\ x_2 &= (R + w_3)\cos(w_1)\sin(w_2) \\ x_3 &= [R(1-\varepsilon^2) + w_3]\sin(w_1). \end{aligned} \tag{9}$$

Note that routines for transforming from WGS 84 to ECEF and from ECEF to WGS 84 are readily available.

w_1	latitude of point in WGS coordinates
w_2	longitude of point in WGS coordinates
w_3	altitude of point in WGS coordinates
x_3	axis of Earth's rotation
x_1	$x_1 \perp x_3$ from center of Earth to zero lat, lon
x_2	$x_2 \perp (x_3, x_1)$ and toward positive lon

Table 20: Notation from conversion from WGS 84 to ECEF coordinates.

F Conversion Between ECEF and ENZ Coordinates

We use $e \in \mathbf{R}^3$ to denote a point in East, North, and Down (ENZ) coordinates on the Earth relative to some origin on the surface of the WGS 84 ellipsoid. Both ENZ and ECEF coordinates are rectangular, so the transformation between them is equivalent to multiplication by a unitary matrix. We use U to denote the matrix that converts from ECEF to ENZ coordinates; i.e., $e = Ux$. It follows that the three rows of U are East, North, and Down in ECEF coordinates. Eq. 9 defines a mapping $X : \mathbf{R}^3 \mapsto \mathbf{R}^3$. Given an origin $\bar{w}$ we define the matrix

$$\bar{U} = \begin{pmatrix} \partial_{w(2)} X(\bar{w}) \\ \partial_{w(1)} X(\bar{w}) \\ -\partial_{w(3)} X(\bar{w}) \end{pmatrix}.$$

Note that we use $\partial_{w(2)} X(\bar{w})$ to denote the partial derivative of $X(w)$ with respect to w_2 and evaluated at $\bar{w}$. The rows of the U are the result of a Graham–Schmidt ortho-normalization of the rows of $\bar{U}$. For $i = 1, 2, 3$, we use use $U_i \in \mathbf{R}^3$ to denote the rows of $U \in \mathbf{R}^{3\times 3}$.

$$\begin{aligned} U_1 &= \bar{U}_1 / |\bar{U}_1| \\ U_2 &= \frac{\bar{U}_2 - (\bar{U}_2 U_1^{\mathrm{T}}) U_1}{|\bar{U}_2 - (\bar{U}_2 U_1^{\mathrm{T}}) U_1|} \\ U_3 &= \frac{\bar{U}_3 - (\bar{U}_3 U_1^{\mathrm{T}}) U_1 - (\bar{U}_3 U_2^{\mathrm{T}}) U_2}{|\bar{U}_3 - (\bar{U}_3 U_1^{\mathrm{T}}) U_1 - (\bar{U}_3 U_2^{\mathrm{T}}) U_2|.} \end{aligned}$$

We use $\bar{x} = X(\bar{w})$ to denote the ECEF coordinates corresponding to the origin. It follows that $e = U(x - \bar{x})$ transforms displacement $x - \bar{x}$ in ECEF coordinates to ENZ coordinates e [the origin in ENEZ corresponds to $(0, 0, 0)$]. It also follows that $x - \bar{x} = U^{\mathrm{T}} e$; i.e., U is unitary.

G Computing Ray Travel Time

We approximate the ocean sound speed as a function of depth only $c(z)$ and constant with respect to range r. Note that the function $c(z)$ is specified with respect to the surface of the water (surface depth) and not negative altitude with respect to the WGS 84 ellipsoid or down in ENZ coordinates. Here, z_0 is the ENZ down component of the tracking transducer. For our applications, the surface depth of the transducer is known either by the length of a cable (during the survey) or using an accurate pressure sensor (during tracking). We define Δz as the surface depth of the transducer minus the ENZ down component of the transducer. We restrict our attention to rays where down is monotonically increasing with respect to range; i.e., the initial angle of the sound ray with respect to the vertical θ is small enough so that the angle with respect to the vertical is always less than 90 degrees. The ray constant a is related to θ by [21, Eq. (3.106)]

$$a = \sin(\theta) c(z_0 + \Delta z)^{-1}.$$

We use $\tilde{c}(z)$ to denote a measured (and interpolated) profile of the sound velocity profile and allow for a constant shift between the measured values and our model for the sound speed; i.e., $c(z) = \tilde{c}(z) + \Delta c$. We define the slowness function $s : \mathbf{R}^2 \mapsto \mathbf{R}$ by

$$s(\Delta c, z) = \frac{1}{c(z + \Delta z)} = \frac{1}{\tilde{c}(z + \Delta z) + \Delta c}.$$

We have not represented the dependence on Δz because that value is explicitly measured. The range as a function of sound speed shift, down and initial angle is given by [21, Eq. (3.97)]

$$r(\Delta c, z, \theta) = \int_{z(0)}^{z} \frac{\sin(\theta) s(\Delta c, z_0)}{\sqrt{s(\Delta c, z')^2 - [\sin(\theta) s(\Delta c, z_0)]^2}} \, \mathbf{d} z'.$$

Note that we use $z(0)$ instead of z_0 when denoting integration limits. The corresponding travel time is given by [21, Eq. (3.101)] as

$$\tau(\Delta c, z, \theta) = \int_{z(0)}^{z} \frac{s(\Delta c, z')^2}{\sqrt{s(\Delta c, z')^2 - [\sin(\theta) s(\Delta c, z_0)]^2}} \, \mathbf{d} z'.$$

Let $u \in \mathbf{R}^3$ denote a location for the tracking transducer and $b \in \mathbf{R}^3$ a location for a seafloor transponder in ENZ coordinates. The initial angle θ satisfies the implicit equation

$$\begin{aligned} R(\Delta c, u, b, \theta) &= \int_{u(3)}^{b(3)} \frac{\sin(\theta) s(\Delta c, u_3)}{\sqrt{s(\Delta c, z')^2 - [\sin(\theta) s(\Delta c, u_3)]^2}} \, \mathbf{d} z'. \\ &= \sqrt{(b_1 - u_1)^2 + (b_2 - u_2)^2}. \end{aligned} \tag{10}$$

The straight line approximation for θ is

$$\tan(\theta_0) \approx \frac{\sqrt{(b_1 - u_1)^2 + (b_2 - u_2)^2}}{b_3 - u_3}.$$

We use Newton's method to solve for the initial angle starting at this approximation; i.e.,

$$\theta_{k+1} = \theta_k - \frac{R(\Delta c, u, b, \theta_k) - \sqrt{(b_1 - u_1)^2 + (b_2 - u_2)^2}}{\partial_\theta R(\Delta c, u, b, \theta_k)}.$$

Given an initial angle, we then compute the corresponding travel time using the equation for $\tau(z, \theta)$ above; i.e.,

$$T(\Delta c, u, b, \theta) = \int_{u(3)}^{b(3)} \frac{s(\Delta c, z')^2}{\sqrt{s(\Delta c, z')^2 - [\sin(\theta) s(\Delta c, u_3)]^2}} \, \mathbf{d}z'. \tag{11}$$

H Conversion From Bars to Depth

Given a latitude in degrees $\lambda \in \mathbf{R}$, and bars of mercury $p \in \mathbf{R}$ the following algorithm computes a depth $z \in \mathbf{R}$ relative to the surface of the ocean; see [22]:

```
P   =  10 * (p - 1)
gam = 2.226e-6
s   = sin( lambda * pi / 180 )
g   = 9.780318 * ( 1.0 + 5.2788e-3*s^2 + 2.36e-5*s^4 )
G   = g + P * gam / 2
d   = 9.72659*P - 2.2512e-5*P^2 + 2.279e-10*P^3 - 1.82e-15*P^4
z   = d / G ,
```

where `pi` denotes π the ratio of the circumference divided by the diameter of a circle and `lambda` denotes λ. We use this algorithm to define the function $D : \mathbf{R}^2 \mapsto \mathbf{R}$ by $D(\lambda, p) = z$.

I Multibeam Bathymetry

This section provides preliminary bathymetric plots for the SS500 — DVLA track, as acquired by the Kongsberg/Simrad EM122 multibeam system. The raw data files were processed using the open-source `MB-system` software [23]. No editing or cleaning has been performed on these files. Processing is modeled after that used by Zajaczkovski [24] with several variations. The commands used here are:

1. Make a list of all raw files:

   ```
   ls -1 *.all > list0
   ```

2. Edit the list to include only those files around the time and location of interest.

3. Make a datalist. Note that the raw file format is MBIO 58.

   ```
   mbdatalist -I list0 > list1
   ```

4. Generate ancillary data.

   ```
   mbdatalist -F-1 -I list1 -N -V
   ```

5. Make parameter files for each raw file:

   ```
   mbset -F-1 -I list1
   ```

6. Process the data list. This makes output files with new file endings. For example, processing `0007_20100511_200350_RV_Revelle.all` results in an output file with filename `0007_20100511_200350_RV_Revellep.mb58`.

   ```
   mbprocess -F-1 -I list1
   ```

7. Make a new list of processed files:

   ```
   ls -1 *.mb58 > list2
   ```

8. Grid the data. For the long track the command was

   ```
   mbgrid -I list2 -E0.001/0.001/degrees -R/125/131/18.5/22
   ```

Plots of the bathymetry along this section are shown in Figs. 51 and 52. The locations of the Seabird CTD casts are shown as + marks; the locations are those given in Table 19.

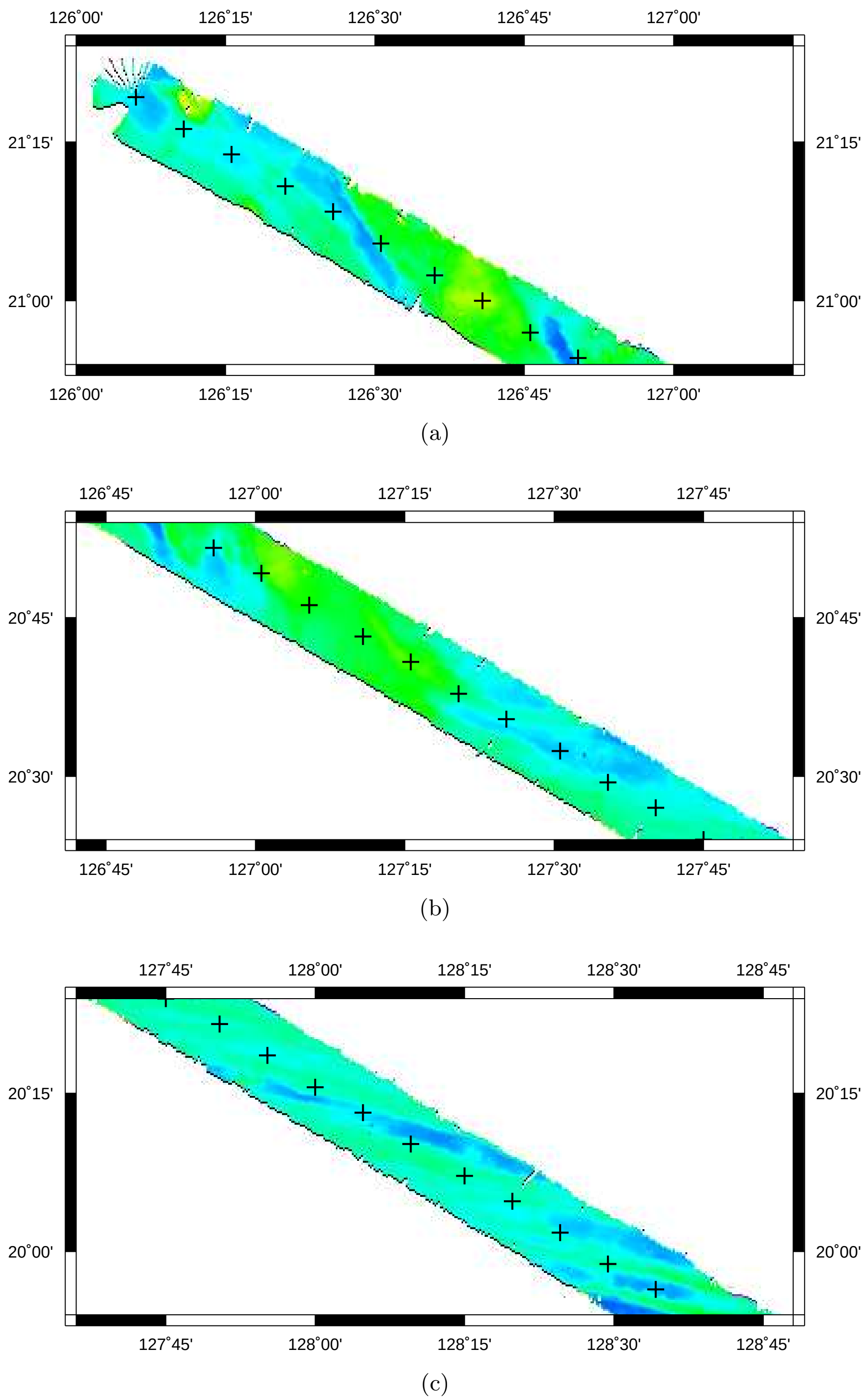

Figure 51: Multibeam bathymetry, transect from DVLA to SS500.

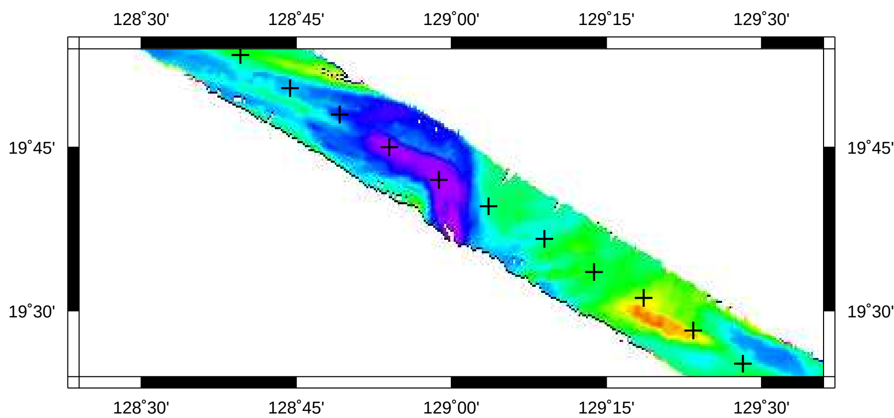

(a)

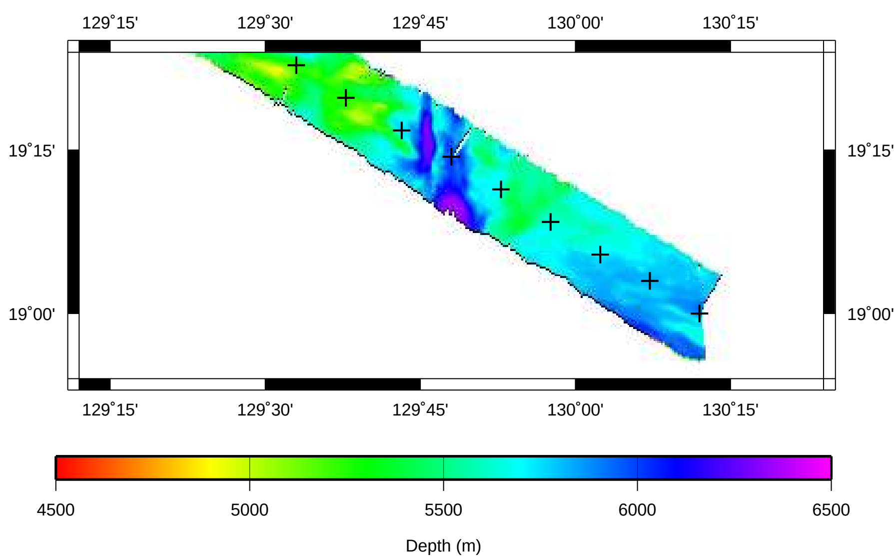

(b)

Figure 52: Multibeam bathymetry, transect from DVLA to SS500. (Continued from Fig. 51.)

REPORT DOCUMENTATION PAGE	*Form Approved* *OMB No. 0704-0188*

The public reporting burden for this collection of information is estimated to average 1 hour per response, including the time for reviewing instructions, searching existing data sources, gathering and maintaining the data needed, and completing and reviewing the collection of information. Send comments regarding this burden estimate or any other aspect of this collection of information, including suggestions for reducing the burden, to Department of Defense, Washington Headquarters Services, Directorate for Information Operations and Reports (0704-0188), 1215 Jefferson Davis Highway, Suite 1204, Arlington, VA 22202-4302. Respondents should be aware that notwithstanding any other provision of law, no person shall be subject to any penalty for failing to comply with a collection of information if it does not display a currently valid OMB control number.

PLEASE DO NOT RETURN YOUR FORM TO THE ABOVE ADDRESS.

1. REPORT DATE *(DD-MM-YYYY)*	2. REPORT TYPE	3. DATES COVERED *(From - To)*
28-10-2010	Technical Report	

4. TITLE AND SUBTITLE

PhilSea10 APL-UW Cruise Report: 5–29 May 2010

5a. CONTRACT NUMBER

5b. GRANT NUMBER

N00014-08-1-0843, N00014-07-1-0743, N00014-03-1-0181
N00014-08-1-0800, N00014-08-1-0797, N00014-08-1-0200

5c. PROGRAM ELEMENT NUMBER

6. AUTHOR(S)

Rex K. Andrew, James A. Mercer, Bradley M. Bell, Andrew A. Ganse, Linda Buck, Timothy Wen, and Timothy M. McGinnis

5d. PROJECT NUMBER

5e. TASK NUMBER

5f. WORK UNIT NUMBER

7. PERFORMING ORGANIZATION NAME(S) AND ADDRESS(ES)

Applied Physics Laboratory – University of Washington
1013 NE 40th Street
Seattle WA 98105

8. PERFORMING ORGANIZATION REPORT NUMBER

APL-UW TR 1001

9. SPONSORING/MONITORING AGENCY NAME(S) AND ADDRESS(ES)

Dr. Robert Headrick, Code 322OA
Office of Naval Research
One Liberty Center
875 North Randolph Street, Suite 4125
Arlington VA 22203

10. SPONSOR/MONITOR'S ACRONYM(S)

11. SPONSOR/MONITOR'S REPORT NUMBER(S)

12. DISTRIBUTION/AVAILABILITY STATEMENT

Approved for public release; distribution is unlimited

13. SUPPLEMENTARY NOTES

14. ABSTRACT

A team from the Applied Physics Laboratory of the University of Washington (APL-UW) conducted underwater sound propagation exercises from 5 to 29 May 2010 aboard the R/V Roger Revelle in the Philippine Sea. This research cruise was part of a larger multi-cruise, multi-institution effort, the PhilSea10 Experiment, sponsored by the Office of Naval Research, to investigate the deterministic and stochastic properties of long-range deep ocean sound propagation in a region of energetic oceanographic processes. The primary objective of the APL-UW cruise was to transmit acoustic signals from electro-acoustic transducers suspended from the R/V Roger Revelle to an autonomous distributed vertical line array (DVLA) deployed in March by a team from the Scripps Institution of Oceanography (SIO.) The DVLA will be recovered in March 2011. Two transmission events took place from a location designated SS500, approximately 509 km to the southeast of the DVLA: a 54-hr event using the HX554 transducer at 1000 m depth, and a 55-hr event using the MP200/TR1446 “multiport” transducer at 1000 m depth. A third event took place towing the HX554 at a

15. SUBJECT TERMS

underwater sound propagation, acoustic transducer, multiport source, ocean acoustical tomography, oceanographic instrumentation, PhilSea10, CTD Chain

16. SECURITY CLASSIFICATION OF: a. REPORT	b. ABSTRACT	c. THIS PAGE	17. LIMITATION OF ABSTRACT	18. NUMBER OF PAGES	19a. NAME OF RESPONSIBLE PERSON
Uncl.	Uncl.	Uncl.	Unlimited	115	Rex K. Andrew
					19b. TELEPHONE NUMBER *(Include area code)* 206 543 1250